

# Experimental Validation of a Structural Glass Window Design for In-plane Seismic Strengthening

Numerical predictions and experimental validation of unreinforced masonry structures in Groningen area



Final Version  
Master Thesis  
Mehmet Kisa  
03-08-2021



## Table of Contents

Preface .....	4
Summary .....	6
1. Introduction .....	9
1.1 Context.....	9
1.2 Main question .....	12
1.3 Sub questions.....	12
1.4 Methodology.....	13
PART I: LITERATURE STUDY .....	15
2. Literature study.....	16
2.1 Strengthening measurements 2.1.1 The Netherlands.....	17
2.1.2 Globally .....	19
2.2 Induced and tectonic earthquakes .....	23
2.3 Glass-timber strengthening .....	25
2.3.1 Glass.....	25
2.3.2 Glass timber composites.....	28
2.4 Developed system.....	30
PART II: NUMERICAL STUDY PRE-EXPERIMENT .....	32
3. Numerical study pre-experiment.....	33
3.1 Phase 0: Validation model .....	34
3.2 Phase 1: Initial models .....	40
3.2.1. Model 1 .....	40
3.2.2 Comparison initial models .....	46
3.3 Phase 2: Secondary models .....	49
3.4 Comparison models .....	52
3.4.1 Comparison of all models .....	54
3.5 Phase 3: Material model .....	56
3.5.1 Non-linear interface model.....	56
3.5.2 Coulomb friction model .....	58
3.5.3 Mooney-Rivlin.....	62
3.6 Several small studies.....	65
3.6.1. Mesh analysis.....	65
3.6.2. Bucklin analysis .....	67
PART III: EXPERIMENTAL STUDY .....	68
4. Experimental study .....	69
4.1 Introduction to the experiment.....	69

4.2 Before the experiment.....	72
4.2.1 Material properties Sikaflex and timber .....	72
4.3 Experimental results .....	74
4.3.1 Monotonic loading.....	74
4.3.2 Cyclic loading.....	78
PART IV: NUMERICAL STUDY POST-EXPERIMENT.....	84
5. Numerical model – Structural window frame.....	85
5.1 Numerical model after experimental research.....	85
6. Numerical masonry model.....	93
6.1 Validation numerical masonry model.....	93
6.2 Numerical masonry model.....	101
7. Strengthened numerical masonry model .....	104
7.1 Numerical model.....	104
7.2 Pushover calculation .....	110
PART V: DESIGN STUDY .....	116
8. Improved structural glass façade.....	117
8.1 Structural performance.....	117
8.2 Improvements.....	119
Discussion.....	126
Conclusion.....	129
Recommendations .....	131
References .....	133

## Preface

Before you lies the final report of my graduation research. This thesis is written to finalize the Master Building Engineering with the specialization in Structural Design at the Delft University of Technology. The topic of this research concerns the strengthening of a masonry wall due to the use of a structural window frame for seismic loadings. With this research, I had the opportunity to combine my interest in structural glass and seismic engineering. I learned a lot from this experience in both the office and in the laboratory. I'm very grateful for this experience and would like to thank everyone who helped me complete this research.

To begin with, I would like to thank my graduation committee from Delft University of Technology. I would like to thank Paul Korswagen for his guidance during the thesis. His help was very essential for the progress of the thesis. Especially the help with Diana was very important because I didn't know that much about it in the beginning stage. I would like to thank Chris Noteboom for his critical thinking and help during the thesis. When I needed extra help and a critical point of view, I could count on Chris. Furthermore, I would like to thank Jan Rots, the chairman of the committee. Even though we didn't have a lot of contact during the thesis, the contact moments we had were very valuable for the thesis. I would also like to thank Maria Belen Gaggero for her great teamwork during the thesis. Her input and collaboration were very essential for the thesis. We had a lot of contact during the process since she focused on the experiments and I focused on the numerical modelling.

In addition, I would like to thank the people of Pieters Bouwtechniek for their guidance during the thesis. I would like to thank Ycha van Diermen for his critical thinking and for allowing me to do my thesis at Pieters Bouwtechniek. I would like to thank Maik Odijk for his help with Diana, especially in the beginning stages his help was very useful. Furthermore, I would like to thank Marco Bosma for helping me by sharing his seismic knowledge with me during the thesis.

Furthermore, I would like to thank the Politecnico di Milano for supporting me during the thesis. The help of Enrico Sergio Mazzucchelli, Giacomo Scrinzi and Paolo Rigone was useful to me. During the thesis, we frequently had spar sessions online to get a different point of view about various topics. I especially appreciate that we could do presentations online to discuss the content and get critical feedback.

In conclusion, I would like to thank my family and friends for supporting me during the thesis. It was a long and difficult road and a lot of things happened in the meantime.

Looking back to the process of the thesis, it had its ups and downs. The pandemic had a large influence on the thesis. The testing campaign got delayed multiple times which resulted in changing the scope of the thesis. It also resulted in not participating in all lab-related activities. During the making of the structural window frame, it was not allowed to participate or observe the process. Furthermore, the contact which was made with the Politecnico di Milano was maintained online. The plan was to go to the campus of the Politecnico di Milano and work together offline, due to the pandemic this was not possible anymore.

Although all these downfalls good outcomes still resulted. All the activity in the lab was well communicated, therefore all obtained results were within reach. This included the process of the making of the façade. The contact between the Politecnico di Milano remained online, which was still an effective approach to communicate. The contact with the supervisors of the TU Delft also remained online, which was an effective approach. In the first half of the thesis, the contact with

Pieters Bouwtechniek remained in the office. The one day per week appointments in the office were really helpful to get the thesis started and to get an idea of the working situation of Pieters Bouwtechniek. In the second half of the thesis, the contact remained mainly online. All in all, the process and communication between all parties went well.

In the end, the master was an unforgettable journey and I would like to thank everyone who made this happen.

*M.Kisa*

*Delft, August 2021*

## Summary

Since the sixties, The Netherlands is pumping natural gas from the bottom of the northern part of The Netherlands. These gas extractions are responsible for mostly all earthquakes in the Groningen area. Since the nineties, the number and intensity of induced earthquakes rapidly increased, which led to damage of houses and buildings and issues regarding safety. This has a big impact on house owners and inhabitants. In 2019 the government decided to stop gas extraction by 2022. However, earthquakes are still expected to occur. Furthermore, the structural condition of 26.000 houses needs to be measured and strengthened if necessary. Current strengthening measurements are mostly very visible. However, this can change by using the window frame as part of the structure, particularly interesting for Dutch houses characterized by large window openings.

Previous research was carried out at TU Delft on the influence of a structural window frame on the in-plane seismic performance of unreinforced masonry structures in the Groningen area. The structural window frame is made of a timber frame, an adhesive and a double-glazing unit. The numerical predictions from previous research were promising since they showed a significant increase of the in-plane seismic performance of the masonry and a reduction of the expected cracking damage. This was possible while having no significant influence on the aesthetic appealing of the residential building. In this thesis, the focus is on the validation of the numerical model based on experimental testing. From this, the main research question was formulated as “How can the structural window frame be modelled to agree with the experimental results, in order to assess the seismic performance for unreinforced masonry structures?”.

The design of the structural window frame is thought out carefully. The timber frame consists of an outer part, which is made from Meranti hardwood, and an inner part, which is made from Okoume plywood. The timber frame is connected to the glass panel with a structural adhesive called Sikaflex-252. The hardwood increases the overall stiffness of the window frame, whereas the plywood prevents peak stresses inside the glass panel on the occasion of contact between the glass panel and the timber frame.

The thesis is divided into five parts: 1. the literature study, 2. numerical study pre-experiments, 3. experimental study, 4. numerical study post-experiment and 5. the design study. The *numerical study pre-experiment* functions to provide the loading protocol for the experimental study. The *numerical study pre-experiment* is divided into phases. Non-linear finite element analyses have been conducted using DIANA FEA 10.4 in order to investigate the behaviour of the structural window frame. To begin with, the model is validated against previous experiments. In addition, various models are made with different parameters to understand the effect of different assumptions on the structural behaviour of the structural window frame. Different assumptions are made for the boundary conditions, stiffness of the connections and material models. The results included the displacement curve and stresses within the glass panel. It is concluded that a specific non-linear elastic interface model for the adhesive is the best suitable model since it has well adjustable features so the contact between glass and timber is well controllable. The results of the numerical models give a broad perspective of how the structural window could behave, although it does not include the cyclic behaviour.

The third part of the thesis is the *experimental study*. The structural window frames have been built and tested in the Stevin-II laboratory at the Delft University of Technology. Six window frames are built to be tested individually and six frames are going to be tested in combination with a masonry wall. The window frames are being tested for a monotonic and cyclic load. The experiments measure

the in-plane shear force with the displacement jack. The results showed that the structural window frame was behaving plastically since the shear force was stabilizing at a certain point. The first experiment showed that the structural window frame needed to be strengthened with screws to prevent cracking of the timber frame. The cyclic experiments showed that there was almost linear behaviour for small displacements. However for larger displacements, the stiffness was reduced significantly. For all experiments, the glass panels and the Meranti hardwood did not show any form of damage. The Okoume plywood, which is the inner bar, is pinched only for the upper and bottom part, while the Okoume plywood on the side are not influenced at all. This is due to the geometry of the window frame. The plywood and Sikaflex are also tested individually to verify the material properties. This is used as input for the numerical models.

The fourth part of the thesis is about the *numerical study post-experiment*. The numerical model needs to be adjusted in order to suit the experiments. The displacement curve deviates at the moment of contact between the glass panel and the timber frame. Whereas the numerical model predicts an increase of stiffness and strength due to contact, in practice the glass panel pinches inside the timber frame which does not increase the stiffness and strength as much as predicted and even stabilizes at a later point. Since the pre-experimental models did not include this pinching behaviour, the numerical model was subsequently improved by adding a serial spring system. Both the adhesive and the timber are modelled as a non-linear spring to replicate the pinching behaviour. One equivalent spring is modelled in DIANA of which the stiffness is based on the two underlying springs in series. Experimental results were used for the material properties of the plywood and Sikaflex. After all modifications to the numerical model, the numerical results suited the experimental results better.

Subsequently, the post-experiment numerical study was extended to include the masonry in addition to the structural window frame. In particular, comparisons were made between the original masonry wall and the strengthened masonry wall including the structural window frame, to analyse the effectiveness of the strengthening method. The masonry wall consists of solid clay bricks. The so-called Engineering Masonry model in DIANA was adopted, which is a commonly known and used engineering model for masonry. The numerical masonry model is validated by comparing it with experiments with similar properties that have been done before. The graph of the displacement curve showed similar results. Displacement-controlled nonlinear pushover analyses were performed. The masonry model including the structural window frame showed an increase of 15% for the in-plane shear force capacity and a decrease of 23% for the crack width for a displacement of 4 mm, compared to the unstrengthened masonry wall. This demonstrates the effectiveness of the strengthening method, both with regard to the ultimate limit state, which includes the in-plane shear force, and regarding the lower damage state, which includes the crack width.

The computed pushover capacity curves were subsequently evaluated against the seismic demand for the case of Appingedam by making a pushover analysis. The pushover calculation showed that both the unstrengthened and strengthened masonry wall are able to withstand the seismic loads in Appingedam. Although according to the assumptions, the structural window frame results in an increase of the shear force capacity of 47% for larger displacements. An evaluation was done according to Annex G NPR 9998, by comparing the capacity curves against the damped ADRS demand curves. The ductility of the structure can be increased by increasing the effective mass to 15000 kg. Since the calculation is only valid for the assumed values, these results should not be taken too strictly.

The fifth part is the *design study*. The design study focuses on the improvement of the design of the structural window frame. The study focuses on three aspects: a stiffer timber frame, a thinner adhesive and a more sustainable design. Using a frame that is twice as stiff and strong has resulted in a significant change in the structural behaviour. The initial behaviour is the same since the behaviour of the adhesive is more dominant in the beginning. The maximum shear force is higher since the stiffer timber frame is able to withstand higher loads. Furthermore, the stabilisation of the in-plane shear force occurs later. The standard thickness of the adhesive is 5 mm. Using an adhesive thinner than 5 mm results in a change of structural behaviour. The contact between the glass panel and timber frame occurs sooner, the stiffness increases but the maximum in-plane shear force remains similar. Numerical modelling for a thinner adhesive did not show any significant increase of the shear stiffness or decrease of the crack width. In addition, it is difficult to precisely apply the correct thickness of the adhesive. Therefore, using a thinner adhesive than 5 mm does not result in more beneficial results. The last studied design improvement is about the sustainability of the design by a design approach and not by numerical modelling. The structural window frame is tested on the principles of a circular economy. Making only screwed connections could inspire to use the window frame after its life span increasing its lifespan. Maintaining the structural window frame frequently could increase the lifespan of the structural window frame as well.

Finally, recommendations for further research are given. Additional experimental research on masonry walls including the structural window frames and further comparisons with the numerical results are recommended, as the effectivity of the window frame within the masonry wall is expected to increase for larger sizes of the structural window frame. Regarding the design, the thickness of the adhesive calls for further research, as does the use of screwed connections instead of glued connections to increase the sustainability of the window frame. Regarding the numerical model, it is recommended to investigate the cyclic unloading/reloading behaviour by coding or making use of a different finite element program in order to include the pinching effect. This should also be done for the numerical masonry model including the structural window frame. Furthermore, it is recommended to investigate whether the structural window frame has potential for seismic applications abroad and for non-seismic oriented functions such as stabilizing glass facades.

# 1. Introduction

## 1.1 Context

Since the sixties, The Netherlands are pumping natural gas from the bottom of the northern part of The Netherlands. These gas extractions are responsible for mostly all earthquakes in the northern part of the Netherlands. The first earthquake happened on 26 December 1986 in Assen (KNMI, 2019).

Since then, the number of earthquakes increased. The number of earthquakes differs per year, at Figure 1 the total number of earthquakes in the Groningen gas field of a period from 1991 until 2019 is given. It is seen, that most of the earthquakes have a magnitude smaller than 1.5. In Figure 2 the earthquakes which have a magnitude higher than 1.5 are given (KNMI, 2019).

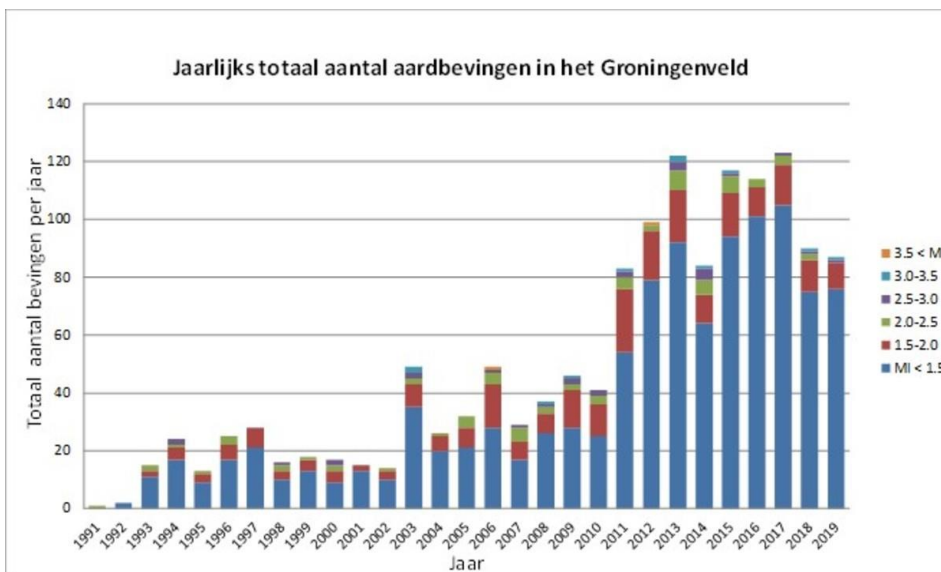


Figure 1: Total number of earthquakes in the Groningen gas field, from 1991 until 2019. ©KNMI

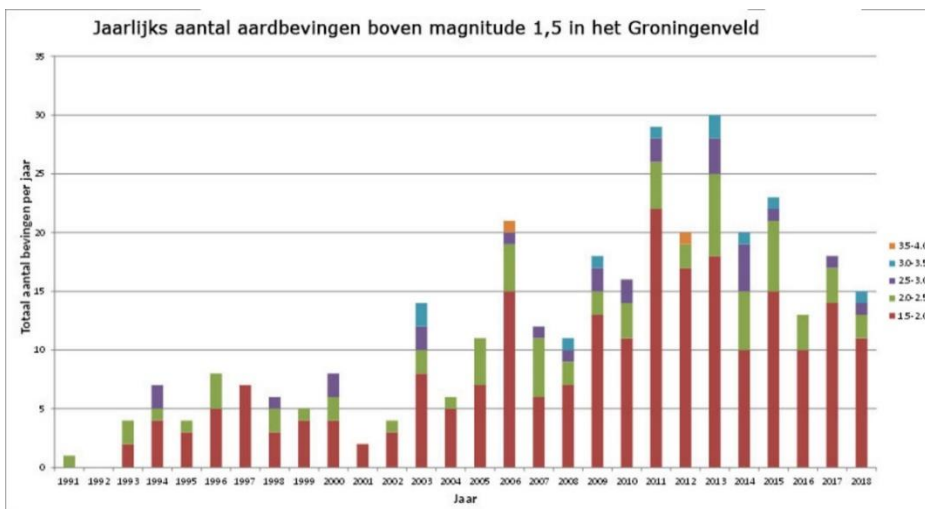


Figure 2: Total number of earthquakes in the Groningen gas field, from 1991 until 2019. ©KNMI

## Reducing gas extraction

In 2018 the government announced that the gas extraction from Groningen will be ended. By stating that the only way to guarantee the safety and safety experience in Groningen is to remove the origin of the earthquakes. Therefore, the government decided to decrease the gas extraction to under 12 billion Nm<sup>3</sup> by 2020 and zero by 2030.

However, in 2019 the government decided to speed this process up, by completely stopping the gas extraction by mid-2022 in the ideal situation. However, earthquakes are still expected to occur and, although their intensity will decrease, still light damage can occur in the future and still the most fragile houses have to be strengthened in order to make them sufficiently safe. The structural condition of 26.000 houses needs to be measured and strengthened if necessary. The speed in stopping the gas extraction is dependent on the weather, the gas usage and the speed at which foreign countries and large consumers are changing to other energy resources. Furthermore, the government made use of nitrogen. Nitrogen is added to gas, by doing so less gas from Groningen is necessary (Rijksoverheid, 2019).

The earthquakes cause damage to houses and buildings, which leads to uncertainties for inhabitants. Strengthening measurements are taken to repair the damaged buildings and strengthen them. However, these measurements have a big impact on the reputation of the province Groningen. Typical strengthening options like using a steel frame are very visible and often aesthetically unappealing. Concluding, a sustainable long-term solution has to be found to compensate the inhabitants of Groningen and the province itself (Rijksoverheid, 2018).

On the 20<sup>th</sup> of March 2021, a trip was done to the Groningen area to inspect the situation. In Loppersum the locals talked about the situation concerning the induced earthquakes. They mentioned that it was difficult for the inhabitants since they weren't heard for a long time by the government, see Figure 3. Therefore besides the structural damage, they also had a lot of psychological damage as well. They mentioned that most of the damage was not directly visible however, it was on the inside of the buildings. Occasionally, some buildings also had visible damage on the outside of the masonry wall, see Figure 4. In Loppersum the resistance against the policy of the government for the area of Groningen is very visible. The people are frustrated, but they work hard to repair their homes.

Various strengthening techniques have been proposed in the past, ranging from improved connections to strengthening the masonry via reinforcement. However, recently also innovative techniques have been proposed. One of them is the inclusion of structural glass in windows, particularly interesting for Dutch houses characterized by large window openings.



*Figure 3: Local of Loppersum showing the damage of masonry wall*



*Figure 4: A repaired masonry wall*

## Prototype

Delft University of Technology is working on a prototype of a glass timber composite facade for masonry buildings in the area of Groningen. Previous research (de Groot, 2019) has been done on the influence of a structural window frame on the in-plane seismic performance of unreinforced masonry structures. The results showed that a structural window improved the in-plane seismic performance of the masonry and reduces the expected damage, while having no significant influence on the aesthetic appealing of the masonry housing.

The focus of that thesis was specifically on a masonry wall and a residential terraced house. The structural window design aims to increase the in-plane seismic force capacity on an existing masonry structure. The window is made of a timber frame, a semi-rigid adhesive and a double-glazing unit.

The numerical predictions are promising however, research still needs to be done to understand its practical behaviour. Therefore, this master thesis will analyse this prototype further. Numerical strengthening predictions will be validated with an experimental testing campaign. Based on these results the structural façade will be improved and further suggestions and usages will be explored.

## 1.2 Main question

How can the structural window frame be modelled to agree with the experimental results, in order to assess the seismic performance for unreinforced masonry structures?

## 1.3 Sub questions

### **Part 1: Literature study**

- What is the current situation of the induced seismic activity in Groningen and what are the strengthening measurements?
- How are buildings reinforced for tectonic seismic activities in other countries?
- What is the difference between tectonic and human-induced earthquakes and strengthening measurements?
- What are the benefits of using a glass timber composite structure for seismic loadings?
- What has been done in the previous research related to this topic?

### **Part 2: Numerical study: pre-experiment**

- How can the numerical model be improved in order to establish the loading protocol for the experimentation?

### **Part 3: Experimental study**

- What is the set-up of the experimentation?
- What are the results of the experimental research?
- What are the damages due to the experimentation?

### **Part 4: Numerical study: post-experiment**

- Do the results of the experiments correspond with the results of the numerical analysis?
- If not, how can the numerical model be adjusted to be similar to the experimental results?
- What is the behaviour of the masonry wall including the structural glass façade?

### **Part 5: Design study**

- How can the design of the structural glass window be improved for better structural behaviour of the masonry wall?
- How can the design of the structural glass window be improved to be more sustainable?

## 1.4 Methodology

This research consists of 5 parts:

- Part 1: Literature study
- Part 2: Numerical study – pre-experiment
- Part 3: Experimental study
- Part 4: Numerical study – post-experiment
- Part 5: Design study

### **Part1: Literature study**

The current situation of Groningen involving seismic activity is addressed in the Introduction. To get an overview of the current knowledge and practical solutions, the current strengthening strategies for masonry buildings in Groningen and abroad will be investigated. Since earthquakes happen all over the world, it is interesting to investigate if the usage of a structural window would have any potential for a tectonic earthquake. To understand whether it would be logical to use a structural glass frame for the strengthening of a masonry wall, the differences and similarities of a human-induced and tectonic earthquake should be investigated.

The current knowledge of a glass timber composite should be made clear to argue why it could function as a solution for seismic strengthening of masonry structures. The benefits and disadvantages should be made clear.

This research is a continuation of three research. To start from the last point, the results of the previous research should be gathered.

### **Part 2: Numerical study – pre-experiment**

Secondly, the numerical model of the previous research, made by A.F.de Groot, should be made to have the same starting point. From there the model should be more elaborated. The model should be similar to the experiments that are going to be performed on the structural glass window. This includes different loading scheme's as monotonic and cyclic loading, as well as different material models for the adhesive. Therefore, the numerical model could be validated by the results of the experiments and predictions could be made in the future of similar cases. The goal is to establish the loading protocol for the experimentation.

### **Part 3: Experimental study**

#### *Structural glass window*

The structural glass window frame will be tested on its in-plane behaviour. There are two different measurements for the glass window, one for the masonry wall and one for the calcium silicate wall. Each type will have one test with a monotonic loading and two tests for cyclic loading. Therefore, in total 6 experiments will be done to investigate the in-plane behaviour.

#### *Structural glass in masonry*

Secondly, the structural glass window frame will be put in a masonry wall of clay bricks and calcium silicate brick. At least 2 experiments will be done with the masonry wall with clay bricks and 2

experiments with the wall with calcium silicate bricks. However, due to the pandemic experiments are delayed and this aspect is kept out of the focus of the master thesis.

#### **Part 4: Numerical study – post-experiment**

The results of the experimentation and the numerical model should be compared with each other. The numerical model of the structural window frame will be adjusted to agree with the experimental results.

A numerical model should be made from the masonry wall including and excluding the structural façade to understand its structural behaviour. The results should also function to predict the experimentations made in the future. Based on these results a pushover calculation will be made. The analysis of these masonry wall experiments is beyond the scope of this thesis.

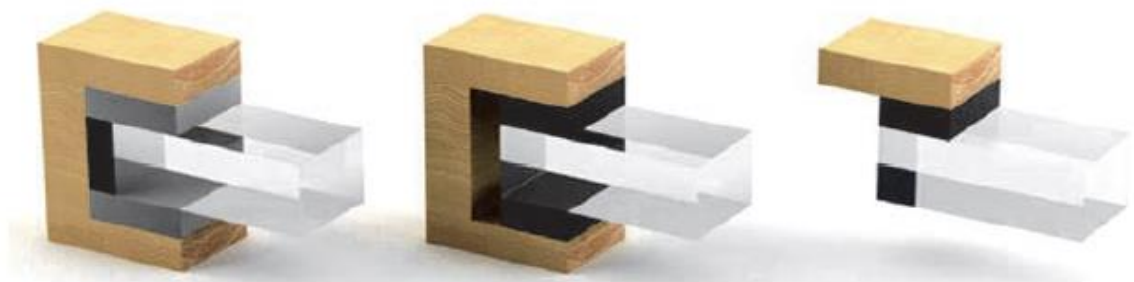
#### **Part 5: Design study**

The chosen adhesive and glass are of importance for the structural behaviour and ductility of the façade. Therefore, it is important to investigate how the design of the structural window can be optimised according to the results of the experiments. The façade should be made in a certain way, which is interesting from a structural and sustainable point of view.

## **Planning**

See the attachment for the initial planning. However, this planning changed due to the circumstances of the pandemic.

## PART I: LITERATURE STUDY



## 2. Literature study

In the literature study, certain background information is being discussed to understand the context of the thesis.

Current strengthening measurements are being discussed to understand what is currently being used to strengthen buildings. Furthermore, a basic understanding of seismic activity and the difference between tectonic and induced seismic activity is important to understand the relevance of this master thesis. By doing so it can be discussed whether a structural façade would be a realistic solution in a broader perspective.

Using a glass-timber composite structure is not something new, therefore the relevance and importance of these composite structures are being discussed in this chapter.

This master thesis is a continuation of previous research, therefore it is important to understand what is already been done. The wheel should not be invented again furthermore, this thesis should use the conclusions and findings made by previous research as input for this master thesis.

## 2.1 Strengthening measurements

### 2.1.1 The Netherlands

The damage to the houses and buildings, which are caused due to the gas extractions, are being settled by the “Tijdelijke Commissie Mijnbouwschade Groningen” (TCGM) since 19 March 2018. By doing so, the claim settlement is organized and independent of the NAM and the government. The NAM (Nederlandse Aardolie Maatschappij) is responsible for the gas extractions in Groningen. The TCGM takes care of the claim settlements which are submitted since 31 March 2017, until the “Instituut Mijnbouwschade Groningen” takes over (Rijksoverheid, 2018).

It is important to know what strengthening options for seismic loadings are possible and being used in the Netherlands. A view examples will be discussed in this paragraph. According to (Bouwen met Staal, 2014) there are six strengthening options:

1. Mitigation measures for higher risk building elements
2. Tying of floors and walls
3. Stiffening of flexible diaphragms
4. Strengthening of existing walls
5. Replacement and addition of walls
6. Foundation strengthening

This thesis focuses on the strengthening of a masonry wall for in-plane behaviour. Only option 4: Strengthening of existing walls will be discussed here. When the first 3 levels are assured, a tied building with stiff diaphragms will distribute the seismic forces to the walls in a favourable manner. This is in the in-plane direction, if the capacity of the unreinforced masonry is exceeded, the strength of the wall needs to be increased. One solution is to use carbon fibre-reinforced polymer (CFRP), which is connected to the masonry, see Figure 5.

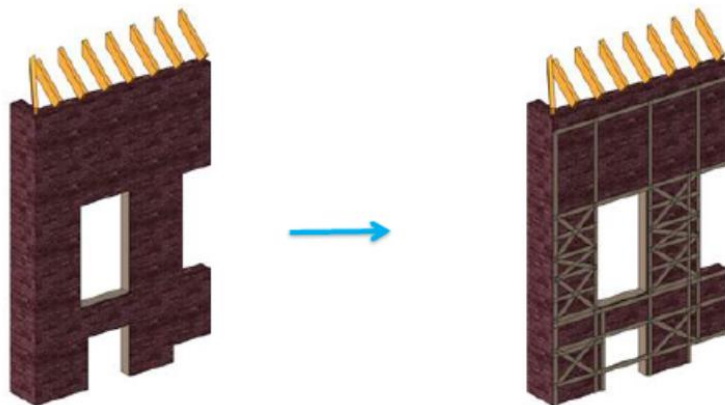


Figure 5: Increasing the strength of masonry wall by adding material (Bouwen met Staal, 2014)

This applies to internal and external walls, which increases the bending and shear capacity of masonry piers and spandrels. The benefit of CFRP is that it has both high strength and low mass. However, wall strengthening in this manner requires access to both inside and outside the building. Therefore, temporary relocation of inhabitants and furniture and readjustment of the wall finishing needs to be considered. These drastic measures will change the appearance of the building.

Another option is to use shotcrete or concrete overlays to supplement both the in-plane and out-of-plane strength. However, this is mostly used in utility buildings, since the intervention can be carried

out from the outside of the building, see Figure 6. Alternatively, a system of internal mullions could be used, to provide the capability to span out-of-plane. This is mostly used for agricultural buildings, since interior aesthetics are assumed less important here, see Figure 7.

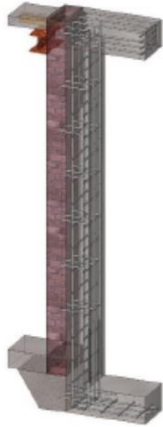


Figure 6: Reinforced concrete overlay (Bouwen met Staal, 2014)

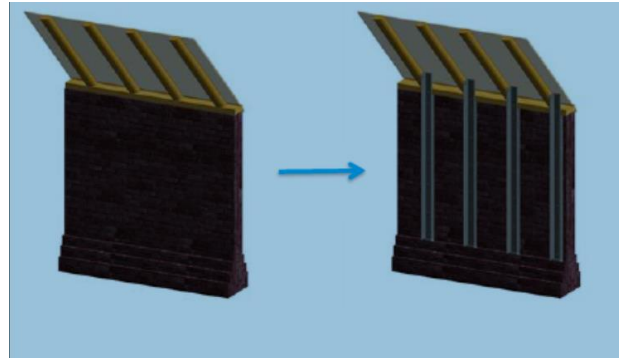


Figure 7: Addition of structural elements (Bouwen met Staal, 2014)

According to (Roijsackers et al., 2017) there is a similar approach. The strengthening measurements are divided into four topics. Foundation, side wall, long wall, end wall and roof. For the foundations, it is necessary that the horizontal forces can be taken by the foundation. Most shallow foundations can be strengthened if necessary. The side walls are mostly not governing in-plane but could be governing in the out-of-plane direction. Adding a wooden or steel wall will strengthen the out-of-plane behaviour. The end walls are most vulnerable. This could be dealt with by making the roof floor stiff and make a good connection between the end wall and the roof floor.

However, the side walls have the most problems and are the most interesting for this thesis, see Figure 8. From experience, it is noted that using steel trusses is a good solution. The steel trusses are used individually per household. It is important to have enough adjustment settings since the dimensions could give problems. The best result would be to use isolated façade elements with integrated steel trusses. The connections with the existing floor would be crucial here. Since the floors are mostly thin, connections are hard to make. Console connection seems to be the solution here, see Figure 9. Dependent on the foundation the inhabitants could choose for removal or maintaining the outer façade. Another important factor here is whether the inhabitants are willing to leave their house during the renovation or not.



Figure 8: 3D View of a house (Roijsackers et al., 2017)

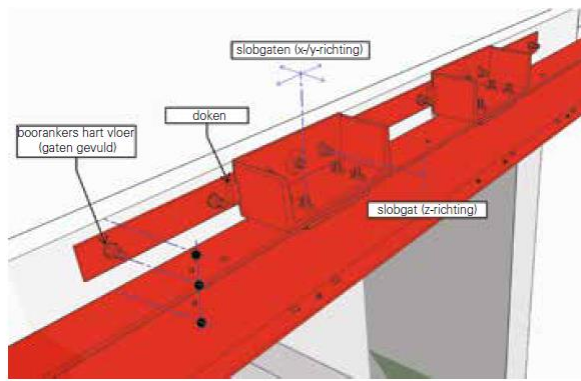


Figure 9: Connection of the floor edge and the console (Rojakkers et al., 2017)

### 2.1.2 Globally

In other countries such as Italy, they have more experience concerning earthquake resisting structures. In (Modena et al., 2009) the following interventions to increase the seismic improvement are discussed: improving structural connections, reducing horizontal diaphragm deformability and increasing masonry strength.

An important aspect to be taken into account for the seismic behaviour of existing masonry buildings are good connections between structural elements. In order to allow preferable global behaviour, it is important to improve the connections between masonry walls, walls and floors and walls and roofs. This could be done by inserting ties, confining rings and using tie-beams at the top of the building. By doing so, a better load redistribution is applied and overturning of the walls is prevented.

Increasing the masonry strength improves the performance and restores the original mechanical properties. The local rebuilding methodology 'scuci-cuci' aims to restore the wall continuity along crack lines. It also aims to recover heavily damaged parts of masonry walls, see Figure 10.



Figure 10: Example of "scuci-cuci" intervention (Modena et al., 2002)

Another method to increase the masonry strength is to use non-cement-based mortar grouting. However, this injection doesn't significantly change the stiffness of walls, see Figure 11.



Figure 11: Mortar grouting  
(Vintzileou and Tassios, 1995)



Figure 12: Positioning of stainless-steel threaded bars as ties

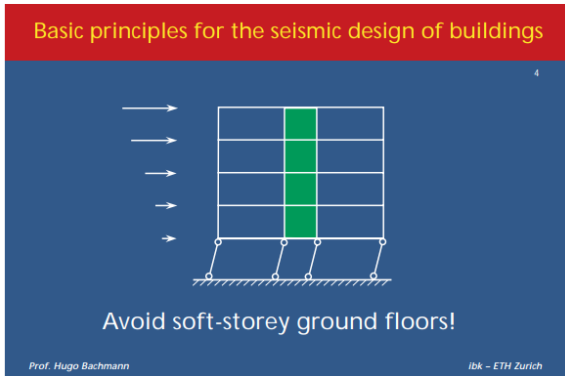
To reduce transversal deformations, local problems of out-of-plane buckling or overturning due to lack of connections, small-sized tie beams across the wall can be used. This will supply a connective function between the wall leaves. This is a supplemental solution for injections, see Figure 12. The combination of injection and tie beams can provide a larger increase of the overall strength of the wall (Valuzzi et al., 2004).

Another important intervention is increasing the in-plane stiffness of the floors. It must be evaluated carefully since it influences the redistribution of seismic action to the walls. Ideally, the seismic behaviour should be transferred from the floors to the walls parallel to the earthquake direction. There are various ways to increase the stiffness of floors, such as using rotated double planking or using steel diagonals. However, this would be out of the scope of the thesis.

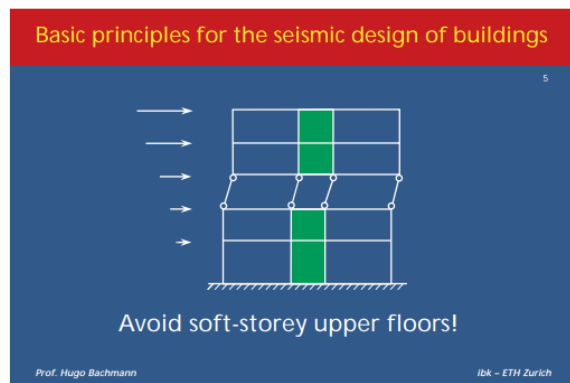
## Design phase

A better solution would be to make changes to a building in the design phase before it is built. Collaboration between the architect and civil engineer in the earliest planning stage could prevent serious consequences and additional costs caused by seismic activity (Bachman, 2003). By doing so, both parties can contribute with different expertise. The traditional so-called “serial design” is inefficient. In this work method, the structure needs to be “fixed” to be resistant to earthquakes, which results in expensive and unsatisfactory patchwork. A so-called “parallel design” is much more efficient and economical. By doing so aesthetics, functional, economical and structural requirements are better integrated.

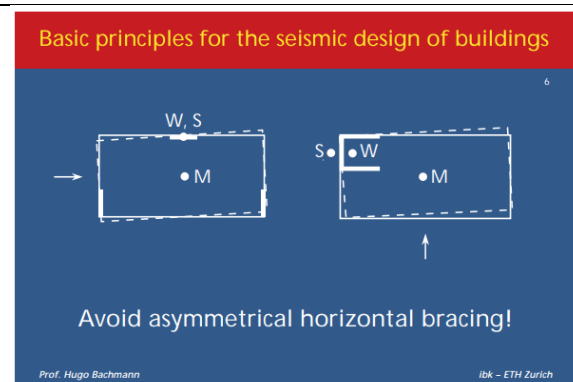
Integrating basic principles in buildings could prevent seismic failure. A few guidelines and measurements from (Bachman, 2003) are shown in Table 1.



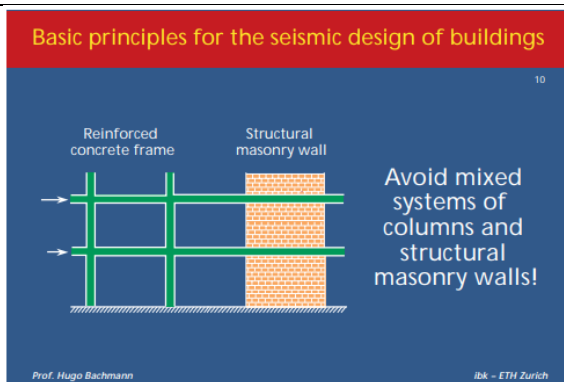
1. Avoid soft-storey ground floors:  
 - Make sure that the ground floor is stiff in the horizontal directions



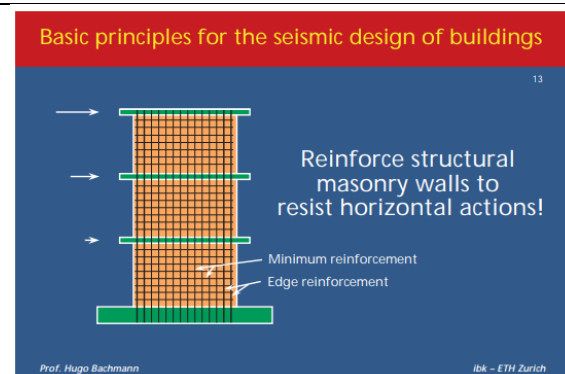
2. Avoid soft-storey upper floors:  
 - Make sure upper floors are as stiff as the other floors to avoid a sway mechanism



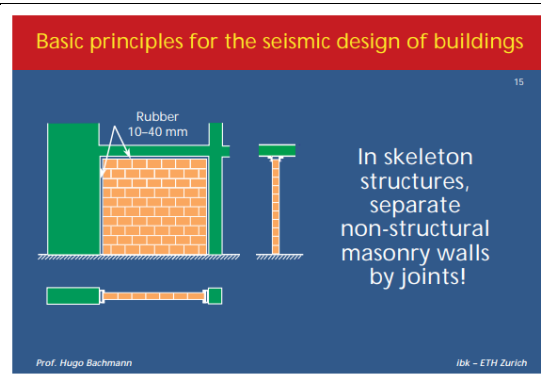
3. Avoid asymmetric bracing:  
 - Use symmetrical bracings along the edges of the building as far away from the centre of mass.



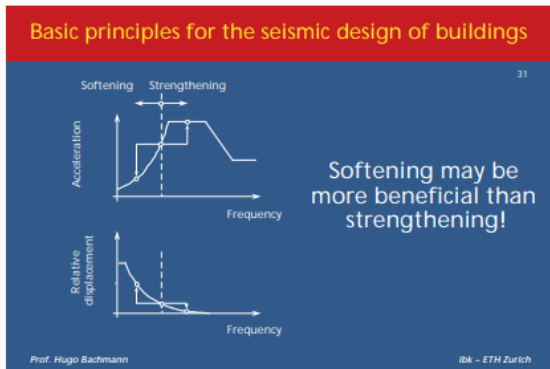
4. Avoid mixed systems with columns and structural masonry walls:  
 - Mixed systems prove to be unfavourable because of their lack of flexibility with building modifications. The masonry walls have less seismic resistance, due to the inertia forces from their own and the columns.



5. Reinforce structural masonry to resist horizontal actions:  
 - Stiffen them in the longitudinal direction to be more sustainable against seismic action.



6. In skeleton structures, separate non-structural masonry walls by joints:  
 - Damage due to weak earthquakes could be prevented by flexible joints



7. Softening may be more beneficial than strengthening:

- Under certain conditions, it may improve to soften rather than strengthen the structure. By softening it reduces the eigen frequency, based on the eigen frequency it could reduce the acceleration and thus the seismic force. However, softening also increases the relative displacement.

Table 1: Overview of basic principles to prevent seismic failure (Bachman, 2003)

Whether to stiffen or soften a structure depends on certain conditions. For the Groningen area, it is more beneficial to stiffen the structure since softening will increase the displacement and thus increase the cracks in the relative thin masonry wall. In Italy for example they have more thick masonry walls since the seismic design is integrated into their buildings. For these conditions, it would be more beneficial to soften the structure and use dampers to decrease the acceleration.

## Conclusion

In short, there are a lot of different techniques to strengthen buildings for seismic activities. These techniques could be used in the design phase or after construction, although it would be more efficient and cheaper to make adjustments in the design phase. After construction, these measurements are mostly very visible. Therefore, creating a solution that is useable and less visible after the construction phase would be interesting.

## 2.2 Induced and tectonic earthquakes

In an earthquake, seismic waves arise from sudden movements in the earth's crust. The ground moves rapidly in all directions, mainly horizontally, but also vertically. If the ground moves rapidly back and forth, the foundations follow these movements. This causes strong vibrations in the structure, which can lead to damages to the building. These seismic effects are determined by three ground motion parameters: ground acceleration, velocity and displacement. These parameters depend on numerous factors like the distance, depth of the epicentre and the local soil. Buildings must therefore be designed to cover considerable uncertainties and variations (Bachman, 2003).

Comparing seismic events to each other is a difficult task since they are complex geophysical events affected by many parameters. The comparison of seismic records for the same seismic event at different locations is not straightforward. Furthermore, comparing natural and induced seismicity, which are not at a similar location is an extremely difficult task. One reason is the availability of data, the limited number of regions have induced seismic records and they cover a very short period of observation. Furthermore, relatively small natural earthquakes need to be compared to induced earthquakes. But these seismic events are not always kept in regions where high seismic activity takes place.

According to (Bal et al., 2018) there are no significant differences between the induced seismicity and natural seismicity.

In this study, strong motion waveforms were compared between induced seismicity and natural seismicity. The waveforms for the induced events were from the Groningen earthquake. No clear differences between the records were detected.

The selected records were applied on a simple wall structure by doing laboratory experiments and SDOF analysis. The wall is a typical calcium-silicate unreinforced masonry wall that can be found in the Groningen region. It was found that the difference between induced and natural seismicity in respect of the damage on the wall is not significant.

It could be discussed that there is still a different important difference. The regions where natural earthquakes take place are used to these events. So, they implement this in the design of buildings. Regions where the induced seismic activity takes place, are not used to these events. Thus, these buildings are also not designed for these loads. See Figure 13 for an overview of the European Seismic Hazard Map.

A quick conclusion between induced seismicity and natural seismicity is that they are different. This statement is however the result of a misconception of comparing the results of large seismic events and the results of induced seismicity. This is because the comparison is made using non-comparable quantities. However, it should be noted that this research had a limited database. So, a firm conclusion was not made.

Another research stated that there were significant differences between induced and tectonic seismic activity. Induced seismicity is shown to have: higher rate of background effects, faster temporal offspring decay, a higher rate of repeating events, a larger proportion of small clusters and larger spatial separation between parent and offspring, compared to tectonic activity (Zaliapin, 2016). Although this research was about induced and tectonic seismic activity in California and South Africa.

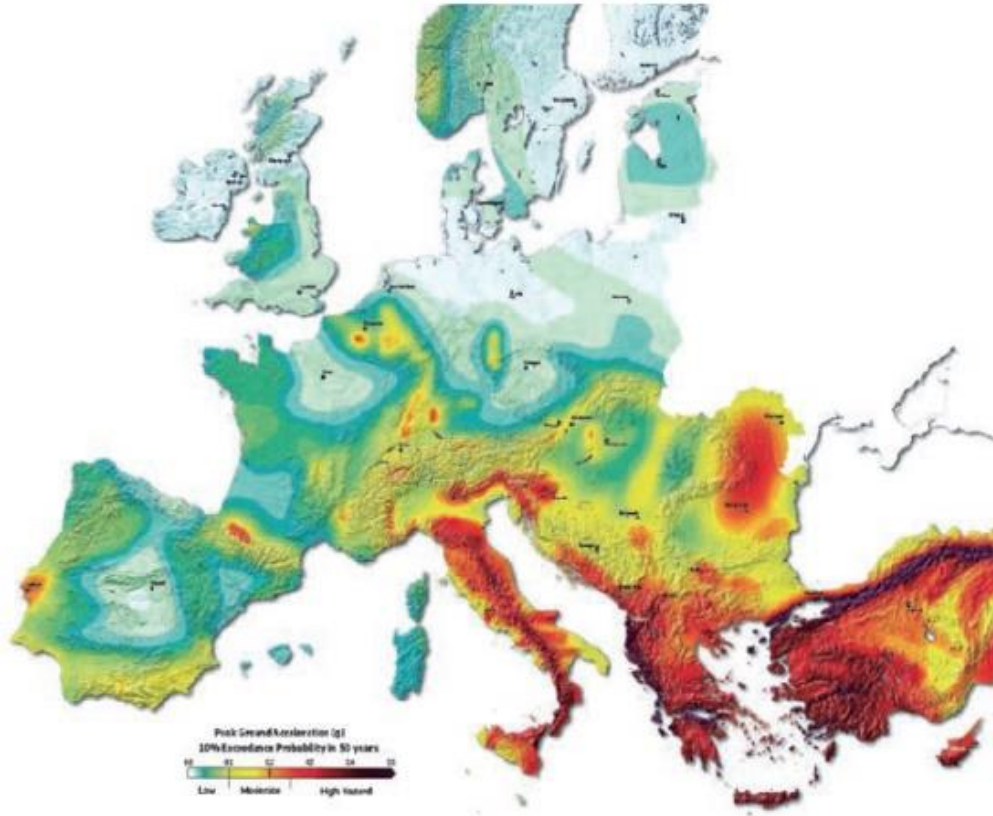


Figure 13: European Seismic Hazard Map

## Conclusion

It is difficult to compare induced seismic activity with each other, since they are complex geophysical events affected by many parameters. Comparing natural and induced seismicity, which are not at a similar location is an extremely difficult task. According to (Bal et al., 2018) there are no significant differences between the induced seismicity and natural seismicity and according to (Zaliapin, 2016) there are differences. What is important though is that the regions where natural earthquakes take place are used to these events. Therefore, they implement this in the design of buildings. Regions where induced seismic activity takes place, are not used to these events and the buildings there are not designed to withstand seismic activity.

## 2.3 Glass-timber strengthening

### 2.3.1 Glass

The introduction and strengthening methods about glass are written based on the information in the Glass Construction Manual. (Schittich et al., 2007)

Glass is a uniform material where the molecules are in random order and do not form a crystal lattice. This is the reason why glass is transparent. Glass has an amorphous isotropy, which means that the properties are not dependent on the direction. Glass which is commonly used in buildings is soda-lime-silica glass. This glass type is generally resistant to acids and alkaline solutions.

Float glass is the most used type of glass. High-quality glass clear glass is possible to produce by the industrial process. See Table 2 for an overview of the glass properties.

Properties	Symbol	Values	Unit
Density	$\rho$	2500	$kg/m^3$
Modulus of elasticity	E	70,000	$N/mm^2$
Poisson's ratio	$\nu$	0.4	-

Table 2: Glass properties (Schittich et al., 2007)

Designing with glass is complex, due to its strong but brittle behaviour. It behaves elastically without any plasticity. The maximum allowable stress is determined by local peak stresses, which occur due to local flaws, chipped edges or cracks. Damage to the microstructure of glass occurs as well that increase the peak stresses. Unfortunately, surface flaws can't be avoided around edges or drilled holes. Therefore, the usable strength should be understood as a statistical variable. The resistance of glass to pressure is significantly higher. Therefore, the glass strength is calculated based on tensile strength or bending strength. See Figure 14 for the relation between surface flaws and glass strength. It is shown that the normal distribution of strength for new glass has an average of 45 MPa. Damaged glass has a lower average strength.

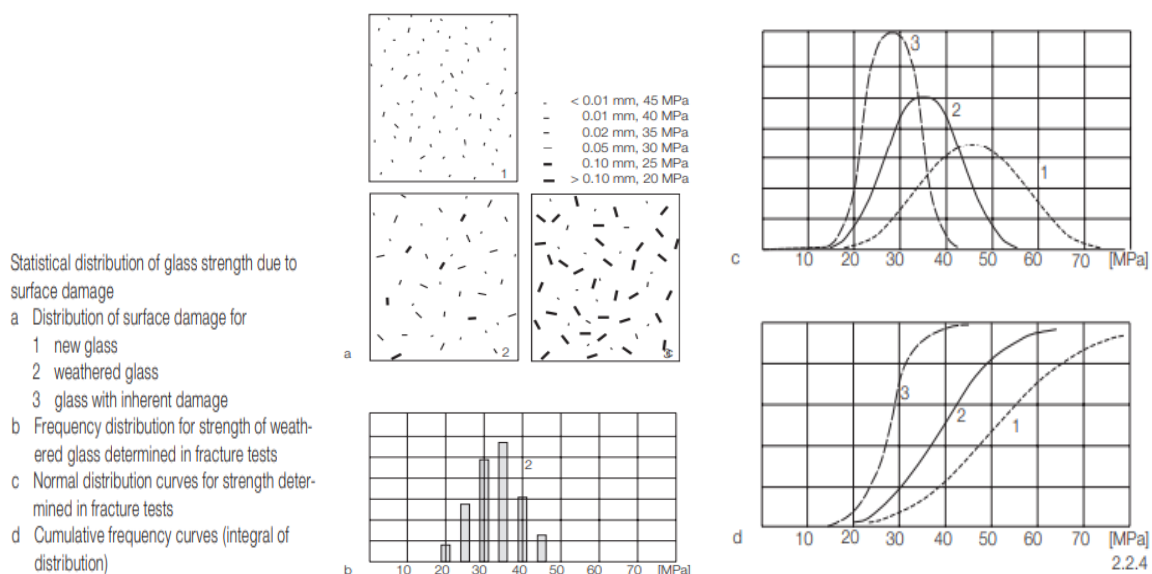


Figure 14: Statistical distribution of glass strength due to surface damage (Schittich et al., 2007)

## Strengthening methods glass

Annealed glass can be strengthened by making it thermally toughened glass. This is done by first heating it up and then suddenly cooled down by blasting cold air. As a result, the surfaces cool down faster than the core. This creates additional compressive stresses in the surface and tension forces in the middle. By doing this the glass gets prestressed, see Figure 15.

The surface of thermally toughened glass can withstand high tensile forces due to prestress. When it is overloaded, it breaks into numerous small blunt pieces. Similar to toughened glass, there is heat-strengthened glass. However, there are some differences. The cooling of the heated glass takes longer, therefore the built-up of the compressive forces are lower than toughened glass. By doing this the fracture pattern also differs. The fracture patterns are larger than toughened glass and the failure mechanism is less brittle, see Figure 16. It is important that any edge working must be done before the strengthening procedure for both techniques. In other words, how more you strengthen glass, the more brittle it behaves and the smaller fracture patterns occur at breakage.

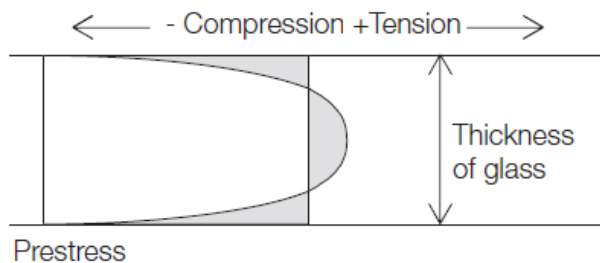


Figure 15: Stress distribution of thermally toughened glass (Schittich et al., 2007)

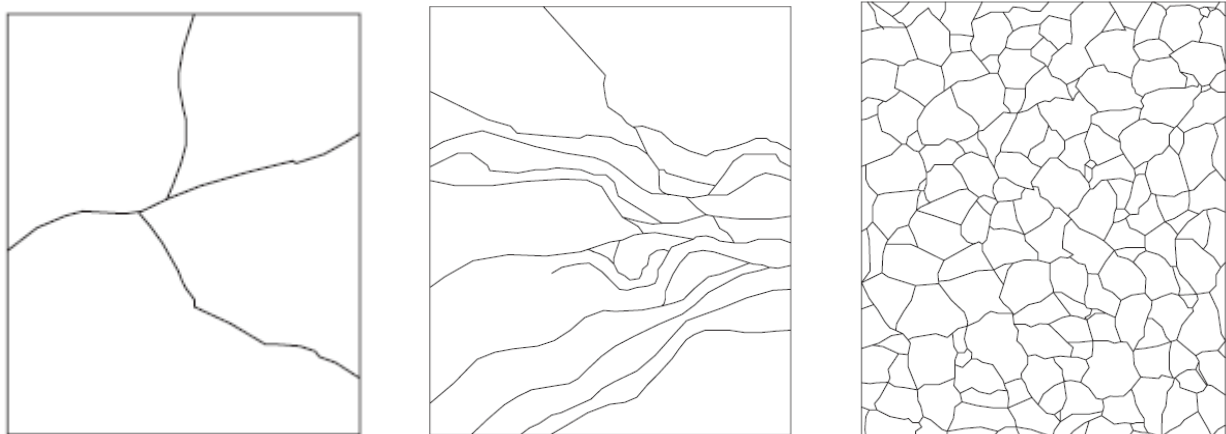


Figure 16: Fracture patterns of, from left to right: annealed, heat strengthened and thermally toughened glass. (Schittich et al., 2007)

## Laminated glass

Laminated glass is a unit of glass that has two or more glass panes with an intermediate layer. This intermediate layer bonds the glass panes with each other during the manufacturing process. This layer has varieties in material, thickness, colour and transparency. Laminated glass avoids crack propagation, thus it has structural advantages over a monolithic section. This is especially the case in the post-breaking phase. The function of the interlayer is to distribute impact forces around the glass sheet, limit the size of the cracks, retain the glass fragments, create residual resistance and reduce the risk of deep injuries in case of breakage. Furthermore, the interlayer is capable of having plastic deformation during impact and static loads after impact (Castori & Speranzini, 2017). Some examples of interlayers are Polyvinyl Butyral (PVB), Sentry Glass Plus (SGP), Ethylene Vinyl Acetate (EVA) and Polyethylene terephthalate (PET). See Table 3, it is shown that SGP has a relatively high elastic and shear modulus compared to the other interlayers.

Property	PVB	SGP	EVA	PET
Thickness ( $mm$ )	0.760	0.760	0.760	0.760
Weight density ( $kg/m^3$ )	1070	950	970	1270
Tensile strength ( $N/mm^2$ )	20.0	34.5	26.0	53.0
Elastic Modulus ( $N/mm^2$ )	24	612	18	2200
Shear Modulus ( $N/mm^2$ )	8	211	7	-
Ultimate strain (%)	300	400	350	$\geq 200$

Table 3: Overview of mean mechanical properties of interlayers at room temperature (Castori & Speranzini, 2017)

Another advantage of using an interlayer is that the stresses and deflections are less than two panels that are not connected. The amount of reduction is based on the amount of shear resistance. With a shear resistant connection, the stresses reduce by half and the deformation by a factor of four, see Figure 17.

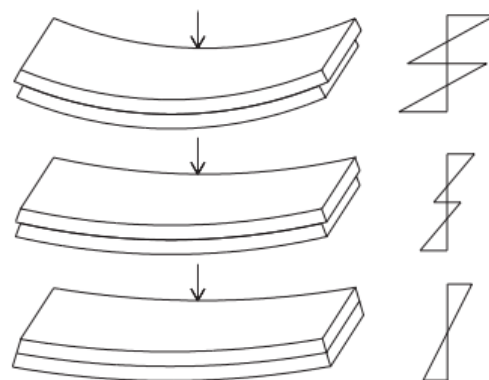


Figure 17: Deformation behaviour and stress distribution. From top to bottom: panels not connected, elastically bonded laminated safety glass, rigidly bonded or monolithic panels.

## Conclusion

There are a lot of possibilities of modern glass in civil engineering. The strength of glass doesn't have an absolute value, because of the microscopic and macroscopic defects of the glass surface. As it behaves elastically and has no reserves for plastic behaviour.

However, laminating glass increases the residual resistance, avoids crack propagation and reduces stresses and deflection. Furthermore, glass can be strengthened due to thermal strengthening methods in a safe manner. However laminated annealed glass has a higher residual capacity when failure occurs of one panel than thermally toughened glass. In addition, glass has a high compression strength. Therefore, glass can be an useful structural material for strengthening the walls when applied properly.

### 2.3.2 Glass timber composites

This paragraph is written based on the information of (Stepinac et al., 2016). The combination of structural glass and a timber frame results in a composite system that has good behaviour during an earthquake. The composite system is energy-efficient, cost-effective, aesthetical and has good load-bearing characteristics.

The deformability of a timber frame and the tensile stress distribution in glass depends on the geometry of the composite system and the type of adhesive. Niedermaier distinguished three different timber-structural glass composite systems. These are: a composite system with polyurethane and silicone adhesives, a double-sided composite system with epoxy adhesives, and a single-sided composite system with epoxy adhesives, see Figure 19. These glass elements were monolithic glass elements. The deformability of the timber frame and the tensile stress distribution depends on the geometry of the composite system and the type of adhesive.

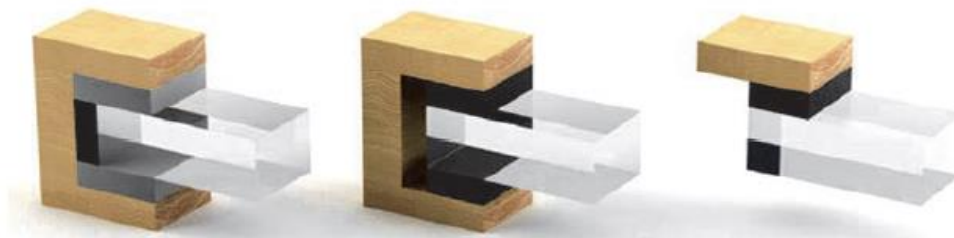


Figure 19: Several composite systems, from left to right: polyurethane and silicone adhesives, a double-sided composite system with epoxy adhesives, and a single-sided composite system with epoxy adhesives (Stepinac et al., 2016)

Glass elements contribute significantly to the transfer of vertical load and the increase of stiffness (Cruz et al., 2010). Environmentally speaking, composite timber-glass facades generate up to 16 times less CO<sub>2</sub> than the aluminium made façade. Nonetheless, it also exhibits a greater energy efficiency (Rosliakova, 2014). This is a great asset since the market for “eco-friendly” products has grown over the years.

Glass is often used in energy-efficient buildings and placed on the south side for residential buildings. Often stabilizing glass would be neglected out of the calculation for the stability. This would lead to a conclusion that the rigidity centre and centre of mass are not located at the same place, see Figure 18. Therefore, a significant increase of the torsional deformation for buildings in an earthquake environment would be determined. However in reality, the glass would have a significant positive effect on the horizontal stiffness. Countries located in the south and southeast of Europe are often affected by earthquakes. However, the use of glass in a structural way is limited in these regions because of a lack of research and regulations. Furthermore, in Eurocode 8 glass is disregarded as a structural element to lateral seismic loading.

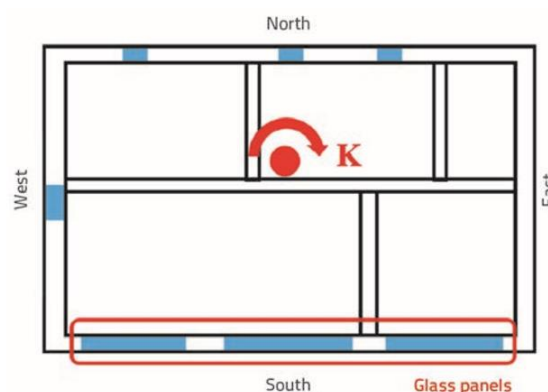


Figure 18: Residential building with glazed south side, rigidity centre shifted northward (Stepinac et al., 2016)

The advantage of using glass as a structural element is that it can replace visible diagonal elements and secure stability.

Several articles referred to in (Stepinac et al., 2016) are published on earthquake-resistant timber-glass composite systems. Samples were tested and demonstrated a high bearing capacity but had a low ductility. The required ductility could be achieved by using mechanical fasteners or using a polyurethane adhesive. Timber and glass separation occurred relatively quickly for the adhesive alternative, resulting in no loadbearing capacity. Most composite systems fail at the contact between timber and glass due to adhesive failure.

Experimental tests (Stepinac et al., 2016) were made on a timber-structural glass composite system, without using steel fasteners and adhesives. Steel fasteners weren't used, due to its brittle behaviour when used with glass. By not using adhesives friction due to the adhesive would not occur. It was concluded that it behaved very well in dynamic and cyclic conditions. Several variations were made, glued in rods had a great ductility and bearing capacity. The timber frame protects the glass and as a composite system, it can resist a considerable earthquake. While it maintains its vertical bearing capacity.

In the study of (Huvener, 2009) the structural behaviour for a composite structure is researched. This composite structure exists of a steel frame and glass panel which are connected through a structural adhesive. In paragraph 3.1 this research is more elaborated.

## Concluding

Composite timber glass systems behave well in earthquake environments. The composite system is energy-efficient, cost-effective, aesthetical and has good load-bearing characteristics. Glass timber frame behave well in earthquake surroundings since it can increase the in-plane stiffness of the structure and can have sufficient ductility when using mechanical fasteners or polyurethane. Attention should be paid to the bond between timber and structural glass. Timber-structural glass composite is an innovative solution for the market and there is room for further improvement and research.

## 2.4 Developed system

Delft University of Technology is working on a prototype of a glass timber composite for the area of Groningen. Since in this area, the masonry structures are being damaged by human-induced earthquakes. A previous master thesis has been done on the influence of a structural window on the in-plane seismic performance of unreinforced masonry structures (Groot, 2019).

The focus of the thesis was specifically on a masonry wall and a residential terraced house. The structural window design aims to increase the in-plane seismic force capacity on an existing masonry structure. The window is made of a timber frame, a semi-rigid adhesive and a double-glazing unit, see Figure 20.

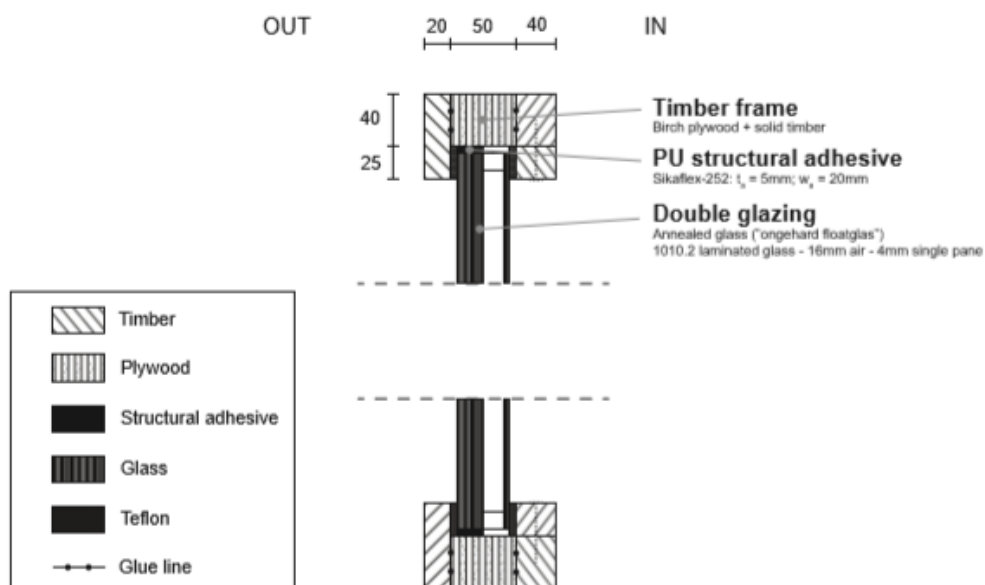


Figure 20: Cross-section structural glass window frame (de Groot, 2019)

The structural adhesive used is called Sikaflex-252 and had a thickness of 5 mm. See paragraph 3.1 Phase 0 for the properties of Sikaflex-252. The structural glazing unit exists of two laminated glass panels of each 10 mm. The structural glass frame is connected to the existing structure by an injection mortar joint.

The structural window was investigated using DIANA FEA 10.2. Numerical studies have been done for validation studies and seismic strengthening. Moreover, the influence of the window size and its influence is being addressed, see Figure 21 for the overview of the numerical studies.

The capacity curve of the structure is determined by a monotonic pushover loading scheme. The city of Groningen and Appingedam are selected as locations.

The seismic performance of the unstrengthened and strengthened masonry structure is assessed by the seismic force capacity, a capacity check and damage evaluation. The seismic force capacity is the maximum in-plane shear force resulted from a certain displacement load.

The results showed that a structural window improved the in-plane seismic performance of the masonry and reduces the expected damage. The seismic force capacity of the strengthened masonry walls reaches 137%, 300% and 367% compared to an unstrengthened wall, depending on the

window size. The larger the window size, the more effect it has. Moreover, the influence of a strengthened wall is limited while it is larger for unstrengthened walls.

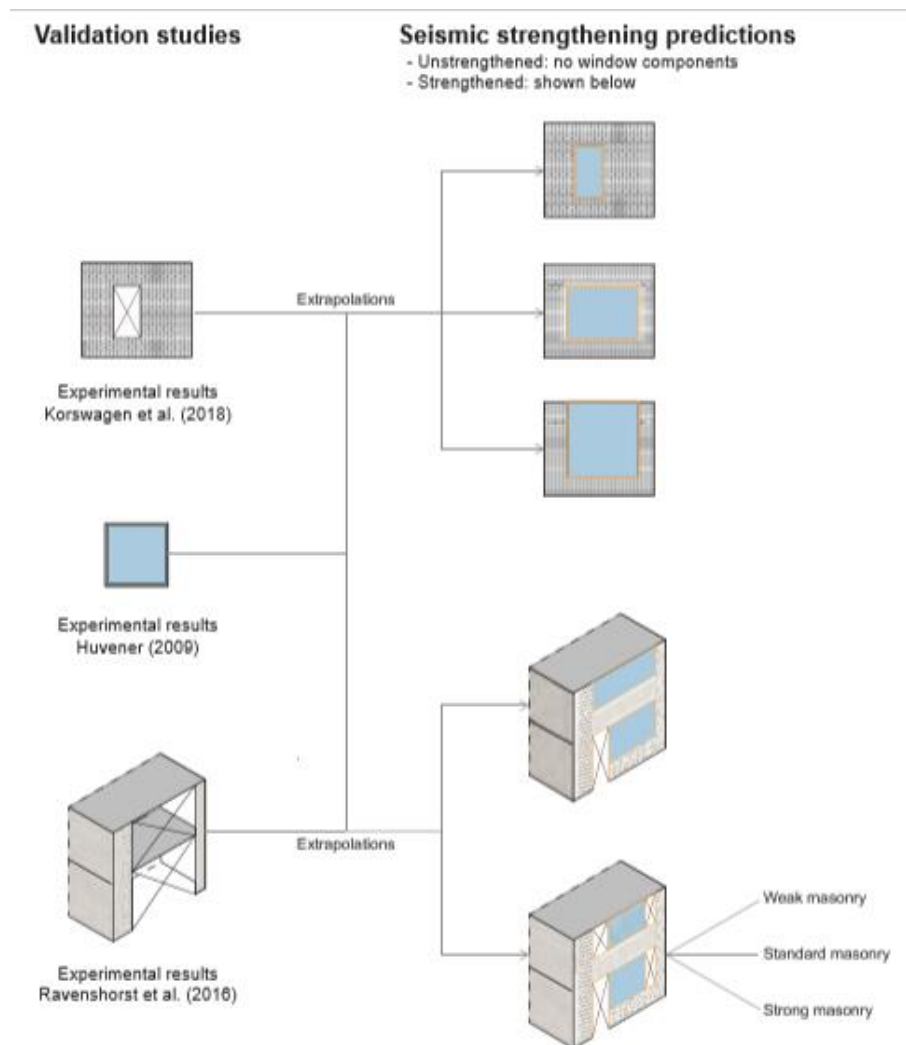


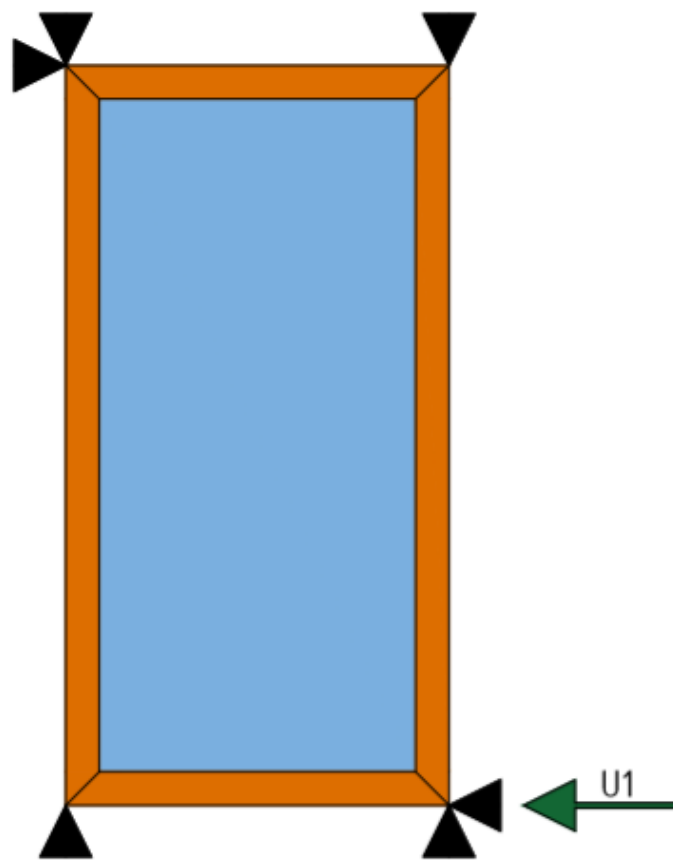
Figure 21: Overview numerical studies (de Groot, 2019)

## Conclusion

The numerical predictions are promising however, research still needs to be done to understand its practical behaviour. Therefore, this master thesis will analyse this prototype further. Numerical strengthening predictions will be validated with an experimental testing campaign. Based on these results the structural façade will be optimised and further suggestions and usages will be explored.

In part 1 all subquestions which are mentioned in paragraph 1.2 for part 1 are answered.

## PART II: NUMERICAL STUDY PRE-EXPERIMENT



### 3. Numerical study pre-experiment

In this chapter, the numerical study is being described. Various numerical models are made to predict the behaviour of the structural glass window. The structural behaviour is being described step wise to verify the results and keep the model as simple as possible.

Firstly, the properties of the numerical model should be verified with Huvener's experimental results (Huvener, 2009). From these results, the dimensions and material will be adjusted to the structural glass façade which will be tested. This will be a simple model, where the timber frame is modelled as a line element and the glass window as a 2D element. Secondly, the timber façade will be modelled as a 2D plane element in order to get more detailed results about the stresses in the frame. Furthermore, the influence of the supports and the mesh size will be investigated.

The most critical part of the model is the adhesive. The behaviour of the adhesive has a big role in the distribution of the forces and structural behaviour of the structural glass façade. Therefore, the adhesive will be modelled with various material models to verify which model suits the material behaviour the best. This will be researched for mono-tonic and quasi-static loadings.

All these models will be compared with each other and with the experimental results to verify their structural behaviour. Phase 0 is to verify the first numerical model with the experimental results of Huvener. Phase 1 model is to model the structural façade as simple as possible, to reduce any complex calculation. The complex models are made to see the influence of a more detailed numerical model in Phase 2. Furthermore, several material models are compared to model the loading/unloading behaviour of the structural façade in Phase 3.

Finally, several small studies have been done. A Mesh analysis has been done to determine the correct mesh size. Furthermore, a buckling analysis has been done to calculate the sensitivity of out of plane buckling.

The following models and analysis are described in this chapter:

- Phase 0: Validation model
- Phase 1: Initial models
- Phase 2: Secondary models
- Phase 3: Material models
- Mesh Analysis
- Buckling analysis

### 3.1 Phase 0: Validation model

The properties of the numerical model for the structural window frame should be verified. Therefore, the results of the numerical model are compared to the results of Huvener's experiment (Huvener, 2009). This experiment is done to verify the properties of the Sikaflex adhesive and obtain the displacement curve. To model the window frame DIANA FEA 10.4 is used. An in-plane monotonic load is applied to obtain the capacity curve.

In the study of (Huvener, 2009) the structural behaviour for a composite structure is researched. This composite structure consists of a steel frame and glass panel which are connected through a structural adhesive. This adhesive is called Sikaflex-252 and is commonly used for cyclic behaviour.

#### Huvener

Huvener researched a square steel frame with a glass panel. He changed the interface and compared the structural behaviour. In Figure 23 and Figure 24 the results of the experiments are further explained and shown. In the research of Huvener some conclusions have been made which are also important for the design of the structural window frame. The results of the Huvener experiment had the following conclusions:

- The relation between the displacement and the in-plane load has two stages for square glass panels and three stages for rectangular glass panels
- Normal and shear stiffness of the adhesive determines the in-plane stiffness
- Glass panel starts cracking at glass-steel contact
- At glass-steel contact, the in-plane load is mostly transferred through the compression diagonal in the glass
- The adhesive bond is pushed away from the compression zone and torn off at the tension zone
- The residual capacity is good due to the properties of annealed float glass
- Square glass panels have one contact moment where in-plane load increases
- Rectangular glass panels have two contact moments where in-plane load increases
- The members of the steel frame are subjected to bending at the contact of the glass and steel

These findings will be taken into account for the design and results of the structural window frame.

## Model Geometry

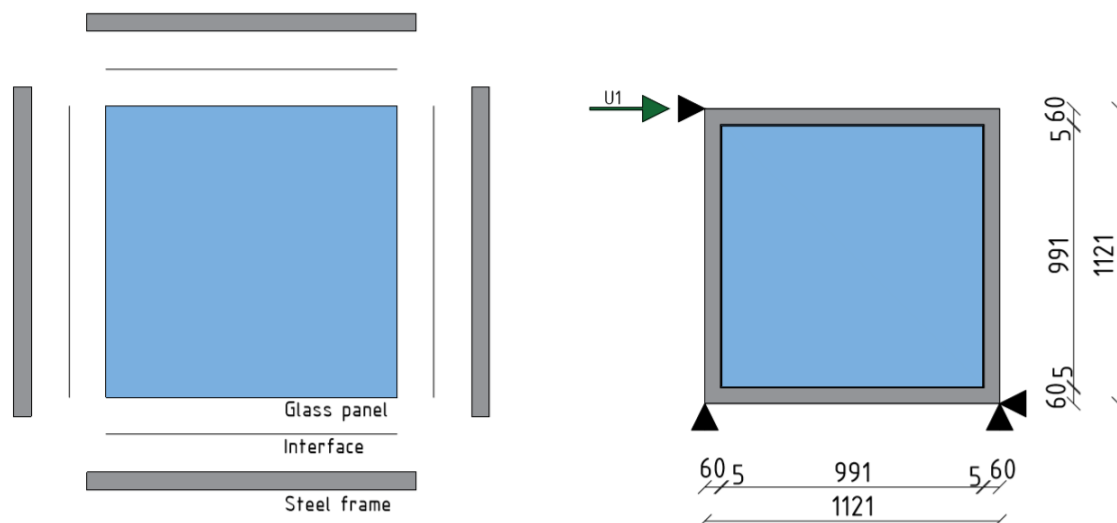


Figure 22: Computational model for the glass window

The model exists of a glass panel of 12 mm thick, which is surrounded with an adhesive of 5 mm thick called Sikaflex-252. The adhesive bonds the glass panel and the steel frame to each other. The steel frame consists of 4 beams which are connected as hinges. The displacement load  $U_1$  of 40 mm is put on the top support, see Figure 22.

## Discretization

The glass panel is modelled with quadrilateral plane stress elements, since out of plane failure is not expected. To simplify the model, the steel frame is modelled as a line with class-III beam elements. The steel frame and the glass panel are both modelled with linear elastic properties. The PU adhesive is modelled with nonlinear properties. It is modelled with nonlinear 2D line interface elements, see Table 4. The nonlinear behaviour is taken into account with diagrams, such as tearing of the joint, see Figure 23. The in-plane thickness of the joint is 5 mm and the out-of-plane thickness is 12 mm.

	Glass pane	Steel frame	PU adhesive
Material model	Linear elastic isotropic	Linear elastic isotropic	Nonlinear elasticity
Element class	Regular Plane Stress (CQ16M)	Class-III beams 2D (CL9BE)	2D line interface (CL12I)
DOFs	$u_x, u_y$	$u_x, u_y, \theta_z$	$u_x, u_y$
Integration scheme	2x2	2-point Gauss	3-point Newton-Cotes
Mesh size (mm)	50	50	50
Thickness (mm)	12	-	12
Cross-section ( $mm^2$ )	-	7200 (120 x 60)	-
NLE properties input	-	-	Diagrams

Table 4: Discretization into elements for the numerical model

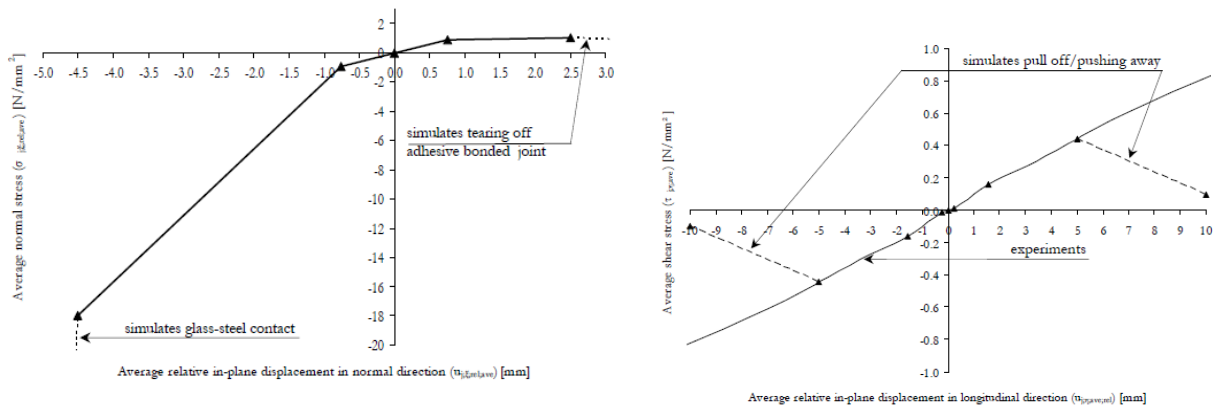
## Material Properties

As mentioned, the glass panel and the steel frame are modelled with linear elastic isotropic properties, see Table 5.

Parameter	Symbol	Unit	Glass panel	Steel frame
Young's Modulus	E	MPa	70,000	210,000
Poisson's ratio	$\nu$	-	0.23	0.2
Mass density	$\rho$	kg/m <sup>3</sup>	2400	7,800

Table 5: Material properties

The PU Adhesive, Sikaflex 252, is modelled with nonlinear 2D line interface elements. The linear elastic properties of the interface are  $k_n = 1.2 \text{ N/mm}^3$  and  $k_s = 0.1 \text{ N/mm}^3$ . Tearing of the adhesive joint occurs at a normal displacement of +2.5 mm or a transverse displacement of -5 mm and +5 mm. Furthermore, the glass panel and the steel frame have contact at a normal displacement of -5 mm, which increases the stiffness of the joint dramatically. See Figure 23 for the relative displacement-traction diagram of the adhesive.



[-7.5 1,800,00; -5 -18; -0.75 -0.9; 0 0; 0.75 0.9; 2.5 1; 25 0.001]

[-50 -0.0005; -5 -0.5; 0 0; 5 0.5; 50 0.0005]

Figure 23: Initial diagrams PU adhesive- Sikaflex 252 (Huveners, 2009)

## Analysis Method

An overview of the analysis method is shown in Table 6.

Load	Load name	Monotonic load
	Load	40 mm
	Load step	0.01 (100)
Iterative procedure	Procedure	Regular Newton-Raphson
	Max. number of iterations	50
	Line search	No
Convergence criterium	Norm	Force & Displacement
	Tolerance	0.01
	No convergence	Terminate

Table 6: Analysis method

## Capacity curve

In

Figure 24 the obtained capacity curve of the experiment of (Huveners, 2009) is shown. The graph is divided into two stages. In the first stage no cracks occur. At the moment of contact between the glass and the steel frame, the second stage starts and cracking of the glass initiates. The model also reacts stiffer in stage 2, due to the contact of the steel frame and glass. This is around 22 mm for the experiment. All the experiments had a maximum deformation of 40 mm since this was the limit of the jack. The residual capacity of the system is good. In the first stage, the system warns by a large horizontal deformation. In the second stage, the system warns by cracking of the glass together with an increase of the in-plane load. In this stage the plasticity occurs due to cracking of the glass. The interlocking of the glass panel and the steel frame creates a certain increase of shear and a residual capacity. The experiment was stopped at 40 mm due to the maximum displacement of the jack and not of failure of the glass. However you would prefer to have plasticity somewhere else because of the brittle failure pattern of non-laminated glass. For seismic design the plastic behaviour is of essence since you would like to prevent brittle failure of the structure due to the displacements and acceleration of an earthquake. In practice, the criterion is the limitation of the horizontal in-plane displacement.

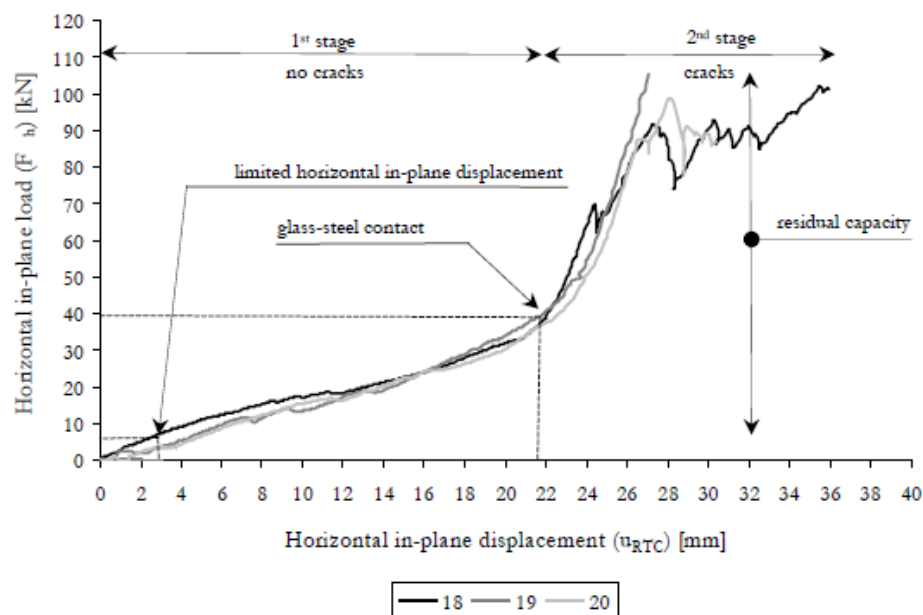


Figure 24: Displacement curve of experiments (Huveners, 2009)

In Figure 25 the capacity curve of the experiment and the numerical model are shown. In phase 1, which is the pre-activation stage, the capacity curves match well. In stage 2, which is the post-activation stage, the numerical model reacts stiffer than the experiments. Due to the linear elastic properties of the glass in the second stage, the numerical model reacts stiffer than the experiment and failure does not occur.

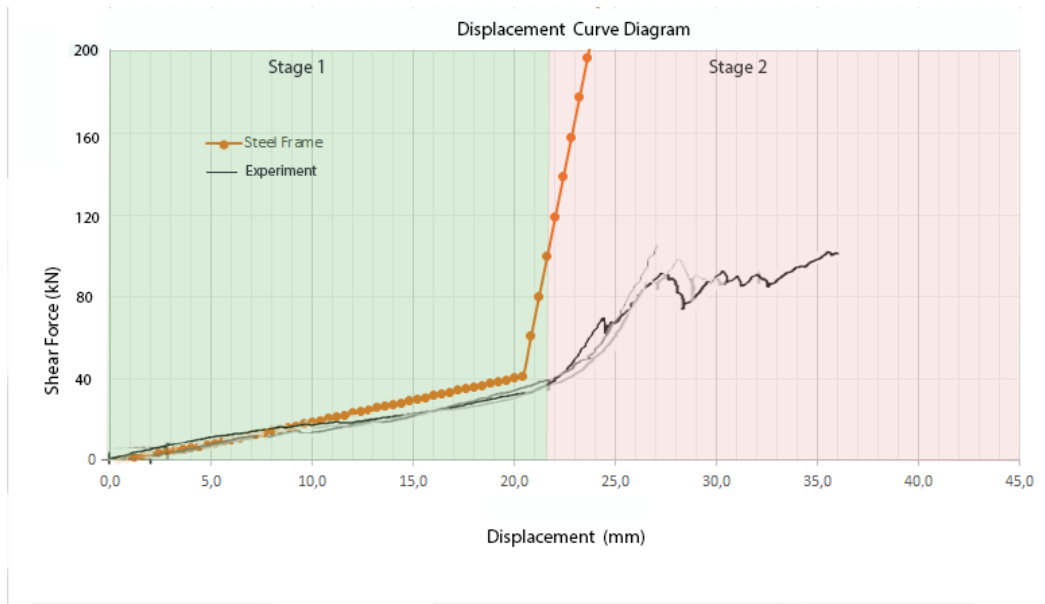
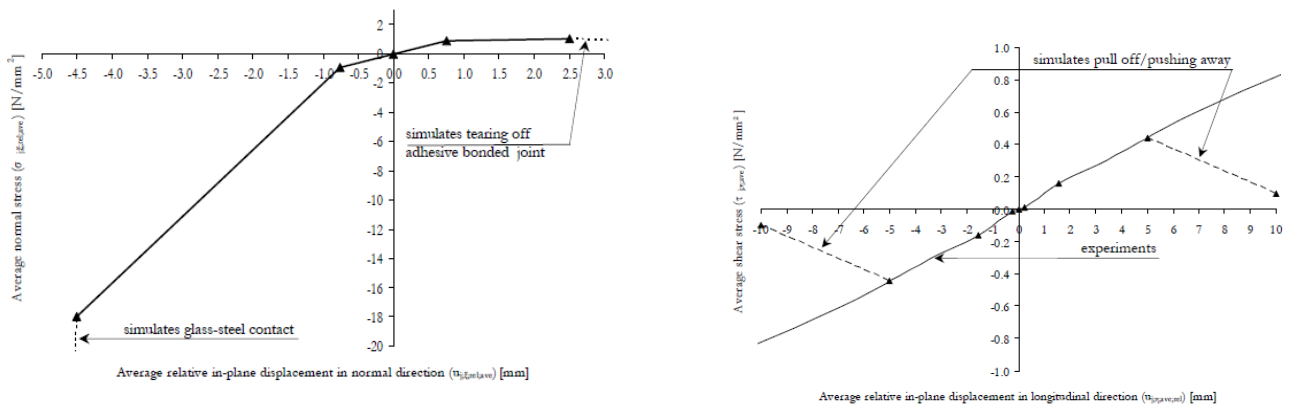


Figure 25: Displacement curve of experiment and self-made numerical model

## Calibration of results

To improve the post-activation behaviour of the structural glass façade, the numerical model is adjusted. Therefore, the stiffness of the structural interface beyond -5 mm is reduced.



[-10 -1200; -5.5 -50; -5 -18; -0.75 -0.9; 0 0; 0.75 0.9; 2.5 1; 25 0.001]

[-50 -0.0005; -5 -0.5; 0 0; 5 0.5; 50 0.0005]

Figure 26: Improved diagrams PU adhesive

In Figure 27 a comparison is shown between the experimental results, the initial numerical model and the improved numerical model. The improved model shows similar results in both stage 1 and the beginning of stage 2.

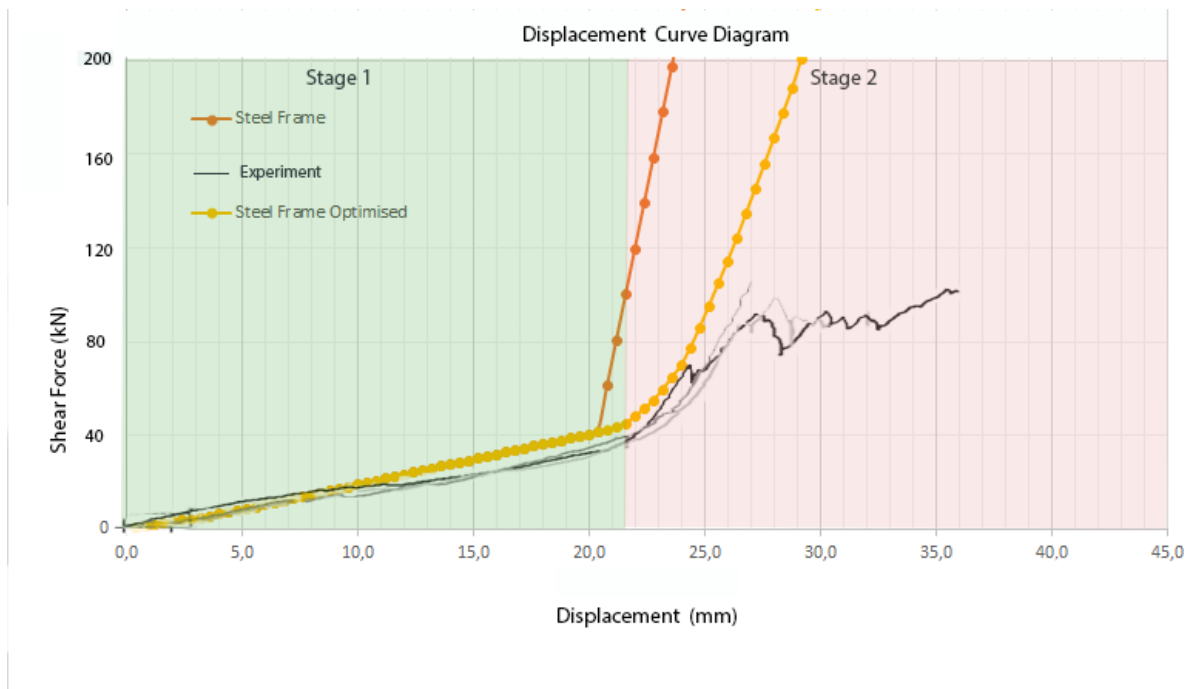


Figure 27: Displacement curve of experiment and all numerical models

## Conclusion

In this paragraph, the experimental results of (Huveners, 2009) are compared with a numerical model to verify the numerical results. In the initial numerical model the results are similar to the experiments in stage one, in the second stage the numerical model reacts stiffer. Due to the linear elastic properties of the glass in the second stage, the numerical model reacts stiffer than the experiment and failure does not occur. Therefore, the properties of the structural adhesive are adjusted. The displacement curve of the improved model shown in Figure 27 has similar results with the experiments for both stage 1 and stage 2. From this, it can be concluded that the numerical model behaves similarly to the experiments in both stages. The cracking of the glass is difficult to fully model with linear elastic properties. This model however indicates the behaviour just after the pinching of the glass into the steel frame.

## 3.2 Phase 1: Initial models

### 3.2.1. Model 1

In the previous paragraph, the numerical model was verified with the experiments of (Huvener, 2009). In this paragraph the numerical model will be adjusted to the measurements, load and materials of the upcoming experimentation of the structural glass façade, see Chapter 4. The displacement curve and the stresses at crucial points will be shown and discussed.

### Model Geometry

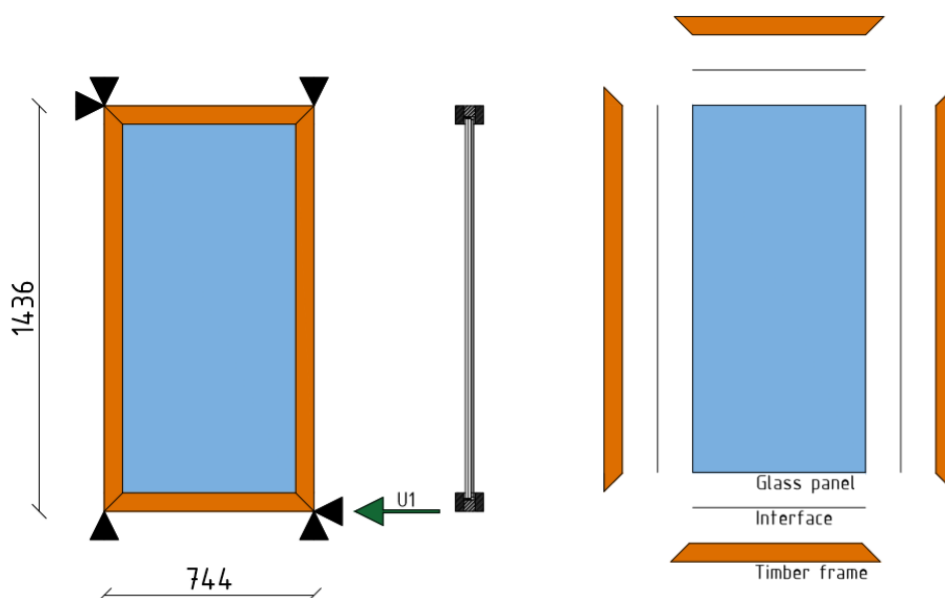


Figure 28: Geometry of the structural glass façade for a calcium silicate masonry wall

In Figure 28 the geometry of the structural glass façade is shown. Since two different masonry walls will be tested, there are two facades with different measurements. The calcium silicate masonry wall has a glass panel of 654 x 1346 mm, the solid clay masonry wall has a glass panel of 640 x 1370 mm. The timber frame has the same measurements for each facade. For the numerical model, the measurements of the calcium silicate are taken. It is not expected that there is a significant difference between the two facades since the measurements are similar.

See Appendix E.1 for the drawings with the exact dimensions for the calcium silicate version. The connections between the bars of the timber frame were assumed to be hinges. The load is placed on the right bottom since this will be the case for the experiment. In Figure 29 a detail is shown of the edge of the frame. The timber frame exists of a composite structure of Okoume Plywood and Meranti Hardwood. Okoume Plywood is used around the glass panel. Since plywood has a low stiffness in both x and y direction it results in low peak stresses of the glass pane. To increase the stiffness of the timber frame Meranti Hardwood is used, this type of wood is good in stiffness. Therefore, the timber frame causes low peak stresses in the glass while remaining a stiff frame. The timber elements inside the timber frame are connected through a glued connection. Between the

Okoume Plywood and the glass panel, the Sikaflex-252 is used as the structural adhesive. To clamp the glass panels Teflon foils are used at the sides. The 4 mm glass panel is of non-structural purpose, see Figure 29.

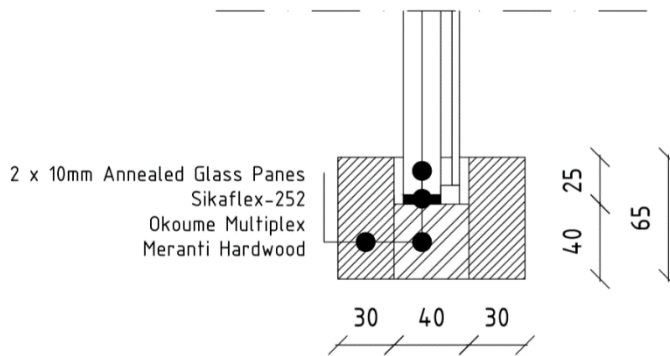


Figure 29: Detail of the timber frame

## Discretization

To discretize the model a few assumptions are made. The timber frame is modelled as a frame of 65 mm x 100 mm with an average stiffness of 15 000 N/mm<sup>2</sup>. See Appendix B.1 for the calculation of the stiffness and the density. The glass panels of each 10 mm are modelled as one glass panel of 20 mm. The adhesive is modelled the same as in the previous paragraph. See Table 7 for the discretization of the numerical model.

	Glass pane	Timber frame	PU adhesive
Material model	Linear elastic isotropic	Linear elastic isotropic	Nonlinear elasticity
Element class	Regular Plane Stress	Class-III beams 2D	2D line interface
DOFs	$u_x, u_y$	$u_x, u_y, \theta_z$	$u_x, u_y$
Integration scheme	2x2	2-point Gauss	3-point Newton-Cotes
Mesh size (mm)	50	50	50
Thickness (mm)	20	-	5
Cross-section (mm <sup>2</sup> )	-	6500 (100 x 65)	-
NLE properties input	-	-	Diagrams

Table 7: Discretization into elements for the numerical model

## Material Properties

See Table 8 for the material properties.

	Symbol	Unit	Glass pane	Timber frame
Young's Modulus	E	MPa	70,000	15,000
Poisson's ratio	$\nu$	-	0.23	0.4
Mass density	$\rho$	kg/m <sup>3</sup>	2500	565

Table 8: Material properties

## Analysis Method

See Table 9 for the analysis method. The monotonic load is a displacement load of 60 mm, which is monitored in 100 load steps.

Load	Load name	Monotonic load
	Load	60 mm
	Load step	0.01(100)
Iterative procedure	Procedure	Regular Newton-Raphson
	Max. number of iterations	50
	Line search	No
Convergence criterium	Norm	Force & Displacement
	Tolerance	0.01
	No convergence	Continue

Table 9: Analysis method

## Results

The stages which are discussed in the previous paragraph for the displacement curve, can be divided in a total of four subphases. In Figure 30 the numerical results are shown for the displacement curve and in Figure 31 the exaugerated deformations and behaviour of the structural window is shown for the subphases. The springs in black are unloaded, in red are in compression and in green are in tension. Phase 1a is the linear elastic phase, this is where the adhesive behaves elastically. Phase 1b is the adhesive tearing, this is where the normal relative interface displacement reaches beyond + 2.5 mm. The model gives this value at 13.2 mm. Phase 2 is when the timber frame and the glass pane intersect with each other. This is when the relative interface displacement is 5 mm. According to the model this is around a displacement of 25.8 mm. At a displacement of 33 mm the tensile peak stresses reach over 45 N/mm<sup>2</sup>, which is the limit of annealed glass. This is the phase when the glass will crack, glass could technically crack at the beginning of phase 2. However peak stresses are complicated to measure in a numerical model since cracks are dependent on imperfections in glass. Therefore, the experimentation will finally confirm when the glass starts to crack. In the displacement curve 2 kinks are visible, the first kink is the first contact between the glass and the bottom and upper timber frame. The second kink is due to the contact of the glass and the side timber bar, which is around 37.2 mm.



Figure 30: Displacement curve of Model 1

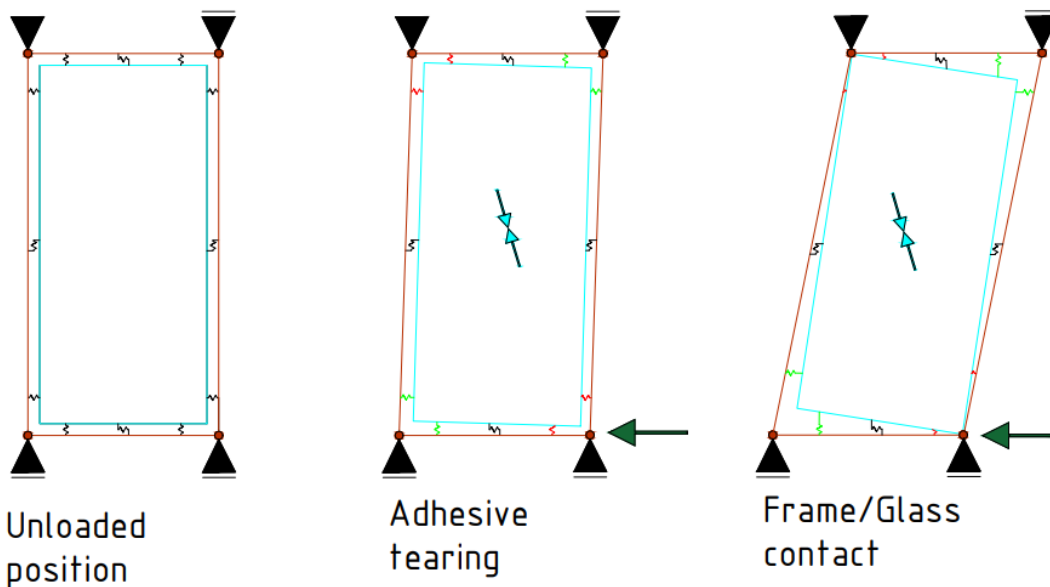
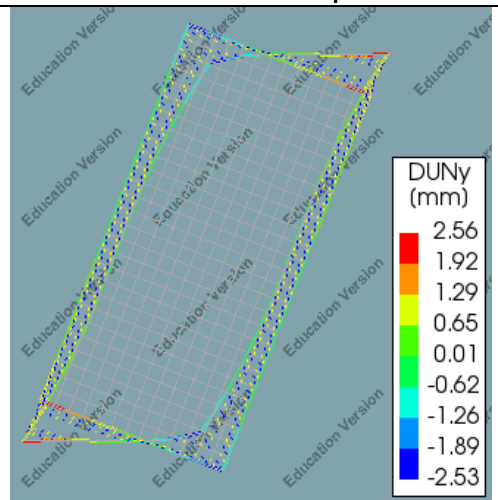


Figure 31: Behaviour of the structural window during different phases

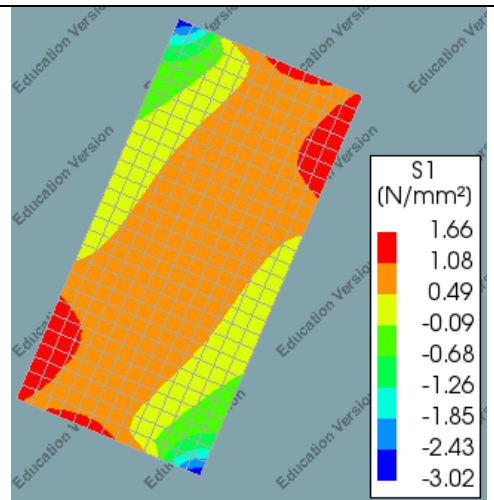
## Glass

The adhesive starts tearing when relative interface displacement reaches beyond + 2.5 mm. The total displacement is then around 13.2 mm. At a displacement of 25.8 mm, there is an intersection between the glass and the timber frame. This is because the relative interface displacement is over 5 mm. You can also see a kink in the force-displacement diagram. The peak stresses are the highest in the corners and decrease as you go further away from the corners. At a displacement of 33 mm, the maximum tensile stress is  $45\text{N/mm}^2$ . This means that the tensile limit of  $45\text{N/mm}^2$  of annealed glass is reached. According to the numerical model, breakage will occur in the corners. See Table 10 for the numerical results

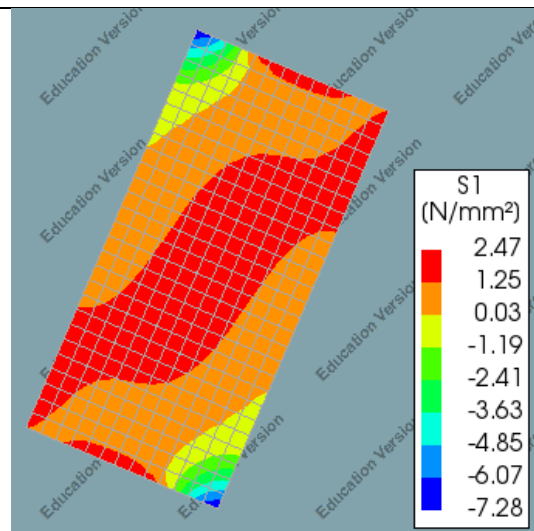
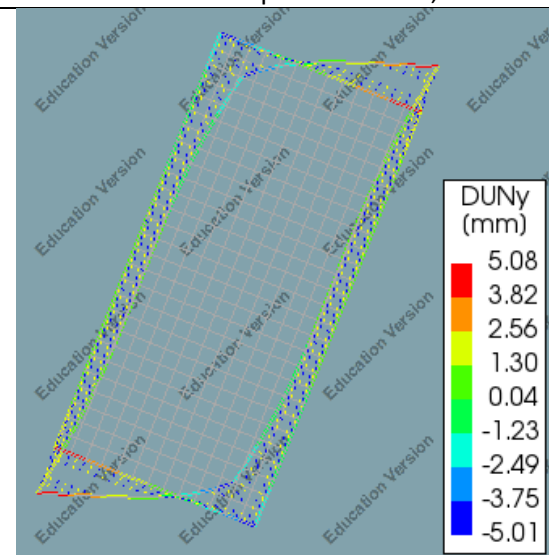
Relative Interface Displacement



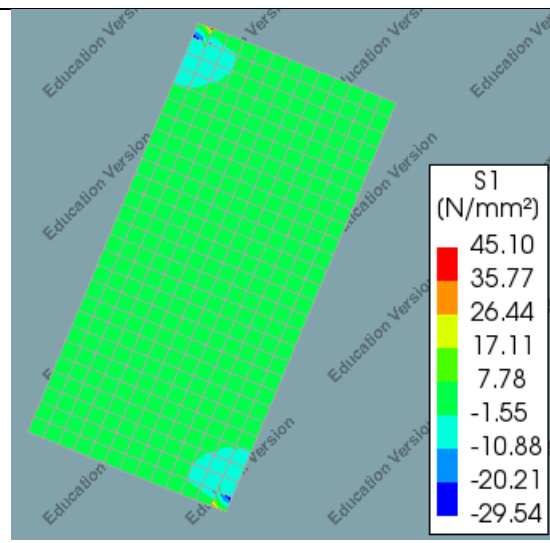
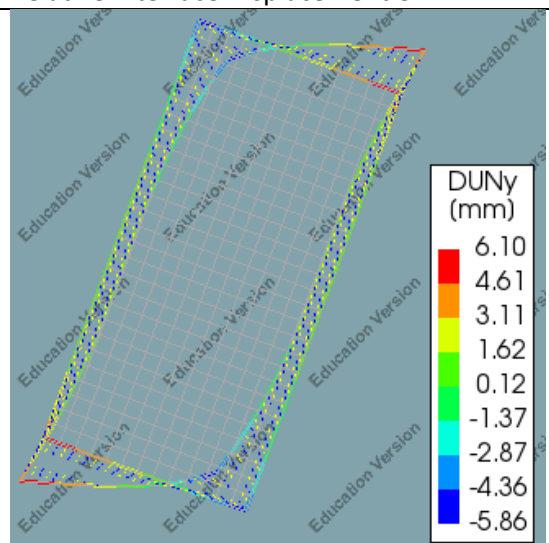
Maximum Stress Glass



Total Displacement: 13.2 mm  
Relative Interface displacement: +2,5 mm



Total Displacement: 25.8 mm  
Relative Interface Displacement-5 mm



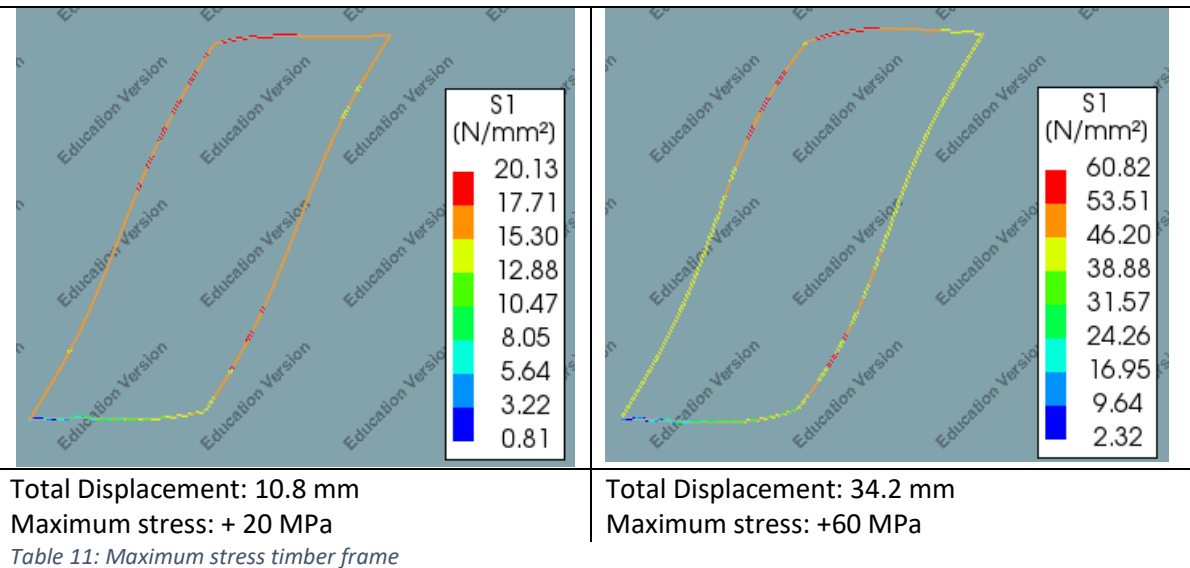
Total Displacement: 33 mm  
Maximum stress: +45 MPa

Table 10: Relative interface displacement vs the maximum stress

## Timber

It is complicated to confirm the failure of the timber frame since the timber frame is modelled as a line element. The plywood has a low stiffness modulus and thus has a low resistance strength, this is neglected in this model. The timber frame elements consist of plywood and hardwood. The plywood has approximately a resistance of 20 MPa. See chapter 4.2.2. where the resistance is being researched. The timber frame reached 20 MPa around 13.2 mm according to the numerical model. The hardwood has approximately a bending resistance of 60 MPa since the strength class is around D60. The timber frame reached 60 MPa around 34.2 mm according to the numerical model. See Table 11 for the numerical results.

### Maximum stress timber frame



## Conclusion

The calculation of the numerical model of the structural window frame is made. The displacement curve can be divided into 4 phases. According to the numerical model, glass timber collision will occur around 25.8 mm and cracking of the glass will occur around 33 mm. However, cracking of the plywood already occurs at 10.8 mm. Based on these findings it may seem that the structural window frame cannot have large displacements. However, the non-linear behaviour of the timber and the glass is not included in this model. The glass frame is laminated and still has residual loadbearing capacity left after cracking. Failure of the structural glass façade is assumed when the in-plane force is no longer available.

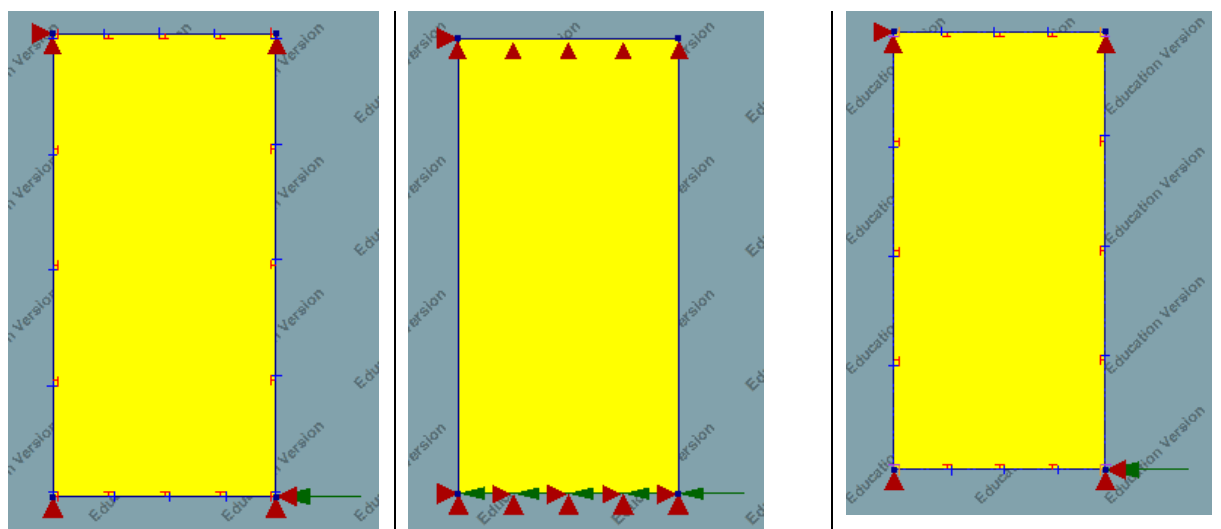
All these findings are based on a basic model with basic assumptions. To understand the behaviour of the numerical model better different assumptions will be made on the numerical model. These alternative assumptions are discussed in paragraph 3.2.2.

### 3.2.2 Comparison initial models

Since there are a lot of variables within the numerical model a few alternative assumptions are compared with each other. The supports in the previous paragraph are assumed as only hinged connections at the corners. However, in the experiment the bottom and upper bar are enabled to bent to the outside. Since the timber frame is connected with hinges in the previous paragraph, plastic hinges are possible to occur in the timber frame. However, at the beginning of the experiment it will still have some rotational stiffness. The load can also vary from a point load or a line load since the frame will be clamped and pushed on the bottom part of the frame. To include the varying complex behaviour of the structural window frame several assumptions are made. The following alternative models are made:

- Model 1: Only supports at the corners
- Model 2: Supports at the bottom and upper bar + distributed load
- Model 3: Only supports at the corners + rigid connections within the timber frame

Model 1 is already explored in paragraph 3.2. Model 2 has line supports and a distributed load. In this model, the timber bar is not able to bend outside, just like for the experiment. The influence of a distributed load is also taken in this model. Model 3 is similar to model 1 however, the corner



Model 1

Model 2

Model 3

connections of the timber frame are rigidly connected. See Table 12 for an overview of the models.

Table 12: Overview of the numerical models

The material properties, discretization and displacement load are the same for every model. See the previous paragraph for the properties.

## Results

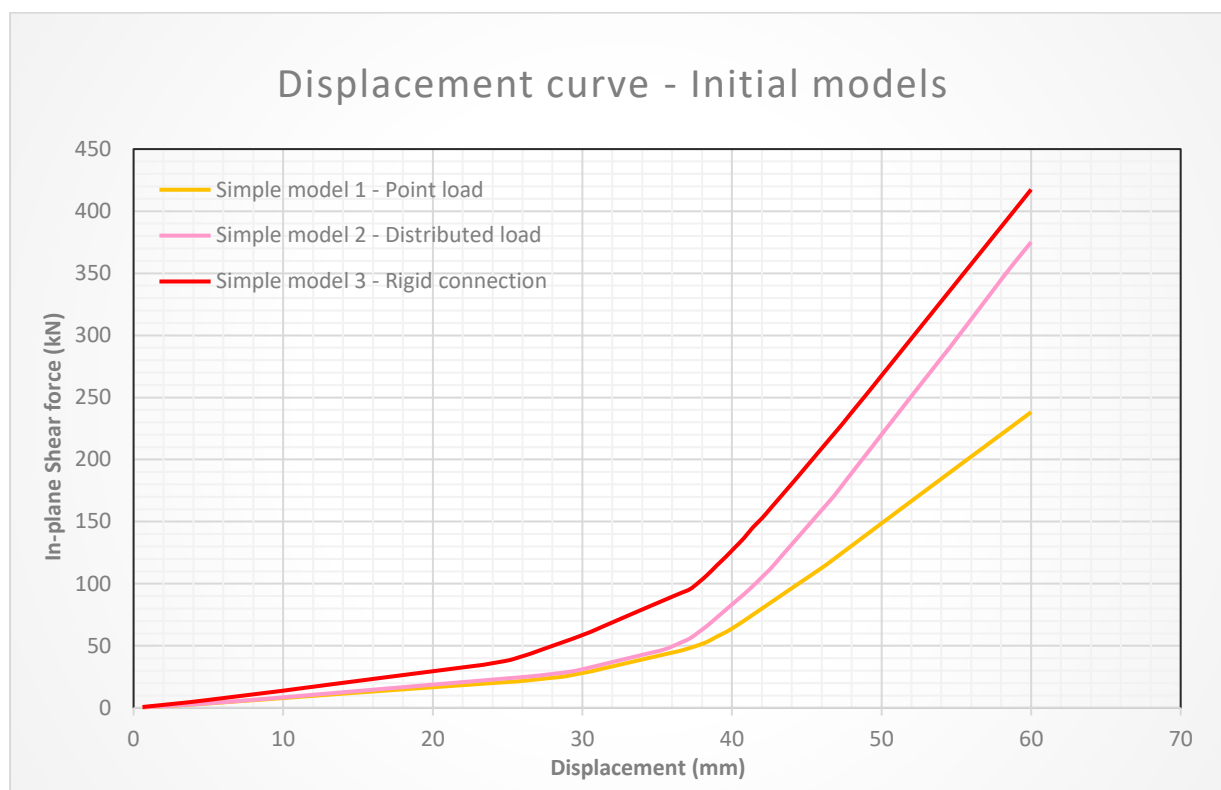


Figure 32: Comparison between models

	Model 1	Model 2	Model 3
Phase 1b (mm)	13.2	13.2	12
Phase 2 (mm)	25.8	27	23.4
Phase 2b (mm)	33	-	39

Table 13: Overview phases

The models have similar points where the phases change, see Figure 32 and Table 13. Model 1 and 2 have a similar behaviour until 35 mm or so. This is where the glass is in contact with both the bottom/upper bar and the side bar. After this displacement, model 2 starts to behave stiffer due to the line supports. The distributed load does not affect the in-plane shear behaviour. Model 3 behaves stiffer in all phases. This is because the rigid connection affects the stiffness through the whole displacement load. What is noticeable is that model 2 and 3 have the same increase in stiffness after around 37 mm. This could mean that the supports and a rigid connection have a similar effect on the stiffness at the clamping of the glass between the timber bottom/upper and side bar. In appendix A.1 an overview of the stresses is given. Similar to model 1, the stresses in the glass panel are relatively low until the collision between the glass and the timber frame occurs. After contact, the peak stresses increase rapidly. It is questionable whether this will happen in practice as well since the timber frame will behave plastically. This plastic behaviour is not included in the numerical model.

## Conclusion

The numerical models showed interesting initial results. Model 1 has the lowest shear force capacity and model 3 has the highest shear force capacity over the entire displacement. Model 1 and 2 have a similar behaviour until 35 mm or so. This is where the glass is in contact with both the bottom/upper bar and the side bar. After this displacement, model 2 starts to behave stiffer due to the line supports. The distributed load does not affect the in-plane shear behaviour. Model 3 behaves stiffer in all phases. This is because the rigid connection affects the stiffness through the whole displacement load.

These displacement curves will be used for the initial loading protocol of the experimentation of the structural window frame. However, it is not possible to verify which model is the most realistic since the results are not compared to the experiments yet.

The next step is to make a more detailed numerical model. The timber frame is expected to behave plastically and stresses of the timber frame are as important as the stresses inside the glass panel. Therefore, the timber frame is modelled as regular plane stress elements instead of beam elements. This is further explained in paragraph 3.3.

### 3.3 Phase 2: Secondary models

In the previous paragraph, the timber frame is modelled as a line model to reduce complexity. However in reality, the timber frame has a certain volume and should be modelled as such. Furthermore, the stresses in the line model are not reliable. Therefore, the timber frame is modelled with regular plane stress elements in this paragraph.

The geometry of the model is the same as model 1. However, the timber frame is modelled as a 2D element. The model is called model 4, see Figure 33. For the exact dimensions of the structural window frame for the calcium silicate masonry wall see attachment E.1.

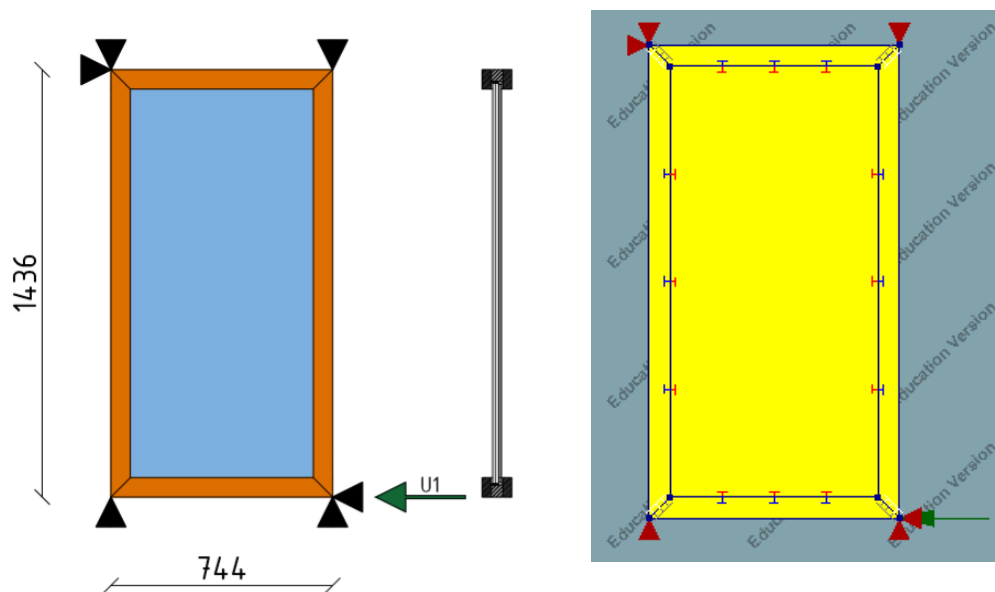


Figure 33: Left: Geometry of the structural window frame, Right: Numerical model in DIANA

#### Discretization

To discretize the model a few assumptions are made. The timber frame is modelled as a frame of 65 mm x 100 mm with an average stiffness of 15 000 N/mm<sup>2</sup>. See Appendix B.1 for the calculation of the stiffness and the density. Later in the research, this value seemed to be smaller however, at the time this was the value based on the calculations. There was no reason to change this value since all models had assumed this value and the main point was to compare the different models. The glass panels of each 10 mm are modelled as one glass panel of 20 mm. The adhesive is modelled the same as in the previous paragraph. See Table 14 for the discretization of the numerical model.

	Glass pane	Timber frame	PU adhesive
Material model	Linear elastic isotropic	Linear elastic isotropic	Nonlinear elasticity
Element class	Regular Plane Stress	Regular Plane Stress	2D line interface
DOFs	$u_x, u_y$	$u_x, u_y$	$u_x, u_y$
Integration scheme	2x2	2x2	3-point Newton-Cotes
Mesh size (mm)	50	50	50
Thickness (mm)	20	-	5
Cross-section ( $mm^2$ )	-	6500 (100 x 65)	-
NLE properties input	-	-	Diagrams

Table 14: Discretization into elements for the numerical model

## Material Properties

See Table 15 for the material properties. The Young's Modulus of the timber frame is calculated here with the initial results for the experiments on the timber frame. In chapter 4 and 5, it is explained that the actual value is lower. However, since the essence of the analysis is to compare the results, the same Young's Modulus is maintained in all models for Chapter 3.

	Symbol	Unit	Glass pane	Timber frame
Young's Modulus	E	MPa	70,000	15,000
Poisson's ratio	$\nu$	-	0.23	0.4
Mass density	$\rho$	$kg/m^3$	2500	565

Table 15: Material properties

## Analysis Method

See Table 16 for the analysis method. The monotonic load is a displacement load of 60 mm, which is monitored in 100 load steps.

Load	Load name	Monotonic load
	Load	60 mm
	Load step	0.01(100)
Iterative procedure	Procedure	Regular Newton-Raphson
	Max. number of iterations	50
	Line search	No
Convergence criterium	Norm	Force & Displacement
	Tolerance	0.01
	No convergence	Terminate

Table 16: Analysis method

## Results

It is important to set the limit when the structural glass window is considered as failure. The failure could be by cracking of the glass or failure of the timber frame. For the initial results, it is assumed that failure of the structural window frame occurs when the in-plane force is no longer available.

In general, it is noticeable that the in-plane behaviour behaves stiffer than model 1, see paragraph 3.2.1. This is because the timber frame is modelled with rigid connections, it is not possible to fully model it as a hinge in a 2D plane. Phase 1b, which is when the adhesive starts tearing, starts at 11,4 mm. Phase 2, when frame/glass contact occurs, starts at 23,4mm. Furthermore, phase 2b is around 24,6 mm, this is when the glass starts cracking according to the numerical model. The deflection of phase 1 and 2 are quite similar to model 1. However, phase 2b is very close to phase 2. The peak stresses in the model increase dramatically fast when the first glass contact occurs. This is not realistically and should be taken into consideration. Two kinks occurred in the graph, this is due to the geometry of the façade and also occurred in the simple model. The first kink is the first contact between the glass and the timber frame, which is at 23,4 mm. The second kink is at 34,2 mm, which is due to contact between the glass and both the upper/lower bar and the sidebar.

The experimentation will finally confirm if and/or when the glass starts to crack.

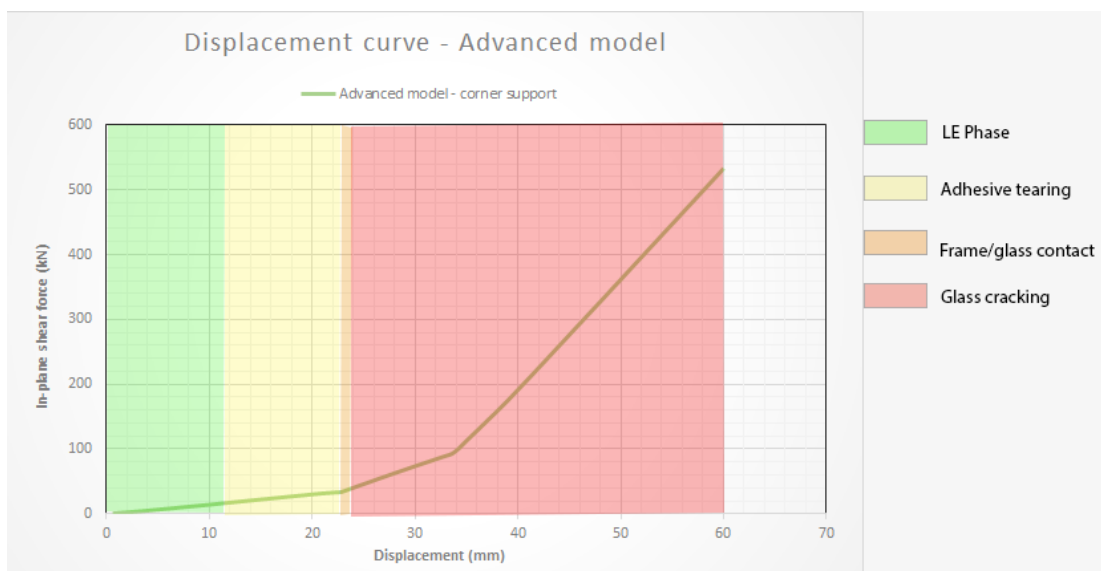
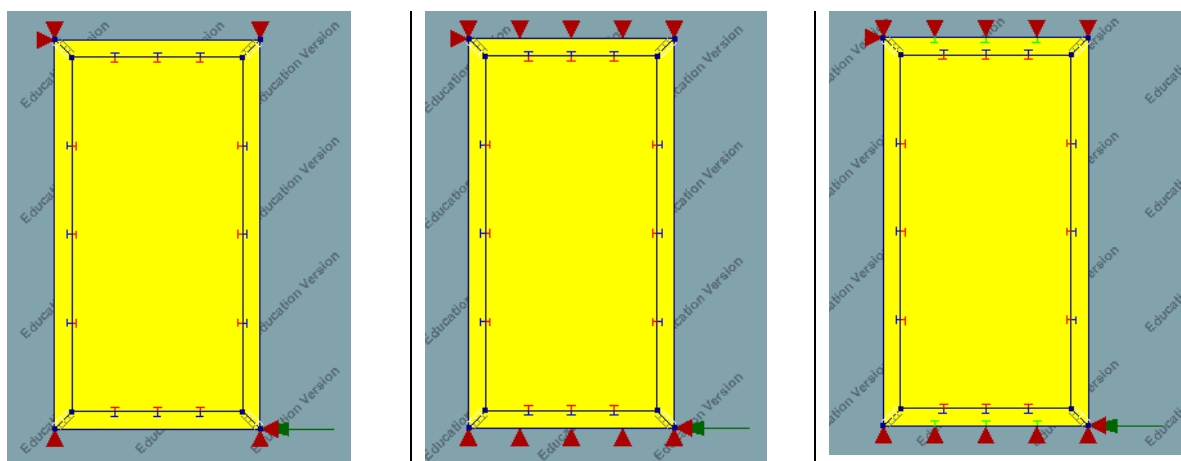


Figure 34: Displacement curve of model 4

### 3.4 Comparison models

In the secondary numerical models, there are a lot of variables such as the supports and support connections. The supports in the previous paragraph are assumed as only hinged connections at the corners. However, in the experiment the bottom and upper bar is enabled to bent to the outside. Therefore, line supports have been placed over the bottom and upper bar as well. In addition to this is, the upper and lower bar can bend or deform inwards. Therefore, a boundary interface is modelled that makes sure it can only take pressure forces to make sure only inward bending of the timber bar is possible. This boundary interface is included only in model 6. A regular support would prevent both inwards and outwards bending. The load is not varied, since this did not affect the structural façade. Model 4 is already researched in paragraph 3.3. Model 5 and 6 are identical to model 4, the material properties, discretization and displacement load are the same for every model. See paragraph 3.3 for the properties. However, the supports are different for model 5 and 6. The following alternative models are made:

- Model 4: Only supports at the corners
- Model 5: Line supports at the bottom and upper bar
- Model 6: Line supports at the bottom and upper bar including boundary interfaces



Model 4

Model 5

Model 6

See Table 17 for an overview of the models.

Table 17: Overview of the numerical models

## Results

From Figure 35 and Table 18 it can be concluded that the models are very close to each other. Model 5 and 6 behave the same, that's why it is difficult to see both lines. This would mean that it does not matter whether the support has a boundary interface or not. Model 4 deviates from the other models at the point of the second kink of the displacement curve, this is around 35 mm. The second kink illustrates the moment when the glass panel is in contact with both the upper/bottom bar and the sidebars. Placing line supports for the upper and bottom support, like in model 5 and 6, creates a higher stiffness since bending of the timber bottom and upper bar is prevented. This effect is also seen in the difference between model 1 and model 2 in paragraph 3.2.2.

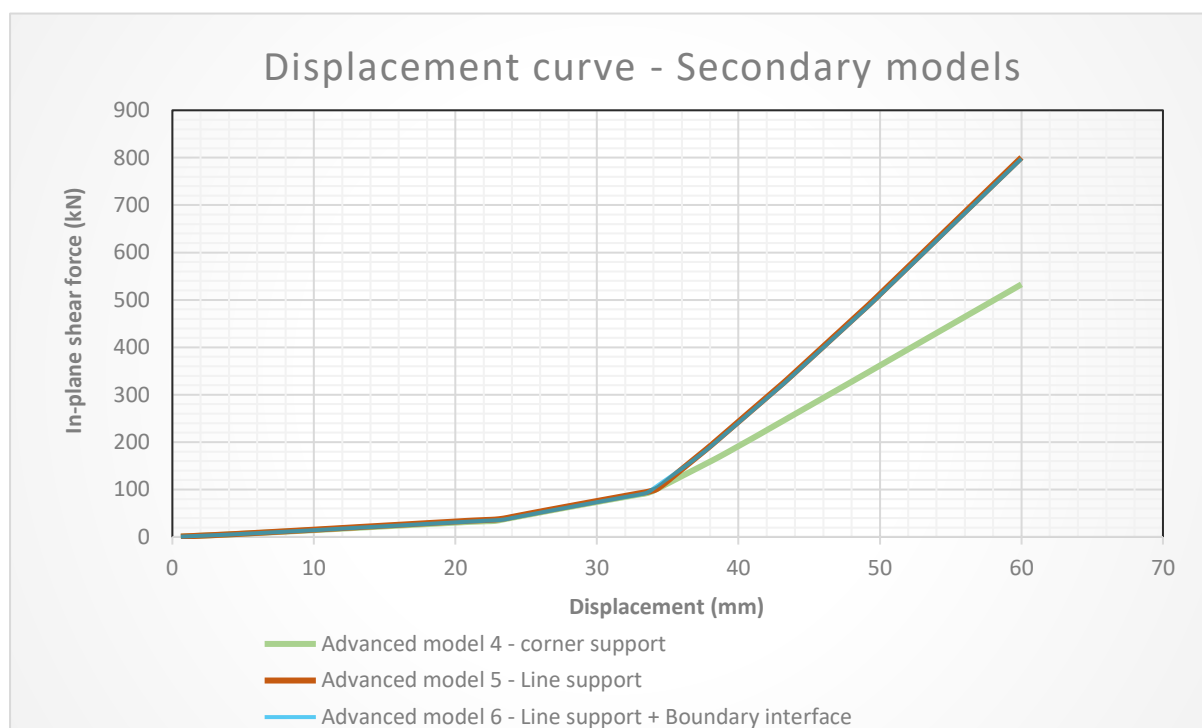


Figure 35: Comparison between models

In Table 18 an overview of the phases of the numerical models is given. The phases are close to each other. What is noticeable is that phase 2 and phase 2b are significantly close to each other. This means that peak stresses in the glass increase significantly after contact between the frame and glass panel according to the numerical model. However, it is doubtful whether the peak stresses would increase like this. It would depend on the pinching behaviour of the timber frame since this behaviour is not included in the numerical model.

	Model 4	Model 5	Model 6
Phase 1b (mm)	11,4	11,4	12,6
Phase 2 (mm)	23,4	23,4	23,4
Phase 2b (mm)	24,6	24,6	25,2

Table 18: Overview phases

### 3.4.1 Comparison of all models

In Figure 36 all displacement curves are shown. It can be seen that the secondary models react stiffer than the initial models. In phase 1 the secondary models react similarly to model 3. This is because both models assume rigid connections of the timber frame. Model 3 and model 4 are also close to each other since both models only have supports at the corners. However, model 4 still reacts stiffer. This is due to that the timber frame behaves differently during phase 2 at the initial model. The second kink occurs later for the initial models, which means that the increase of shear force occurs later as well. This is due to the geometry of the timberframe, which has a surface for the secondary models and is a line in the initial models.

Model 2, model 5 and model 6 all have line supports. It is seen that these models with line support react stiffer compared to the numerical models with no line supports with similar conditions. Model 5 and model 6 react the stiffest thus is the upper boundary, model 1 is the least stiff and thus is the lower boundary.

It should be noted that all these values are theoretical values. Similarly to the experiment in (Huvener, 2009) it could be expected that when cracks occur the stiffness will not increase. Instead, the stiffness will stabilize or zig-zag at a certain displacement and eventually decrease to zero when it fails.

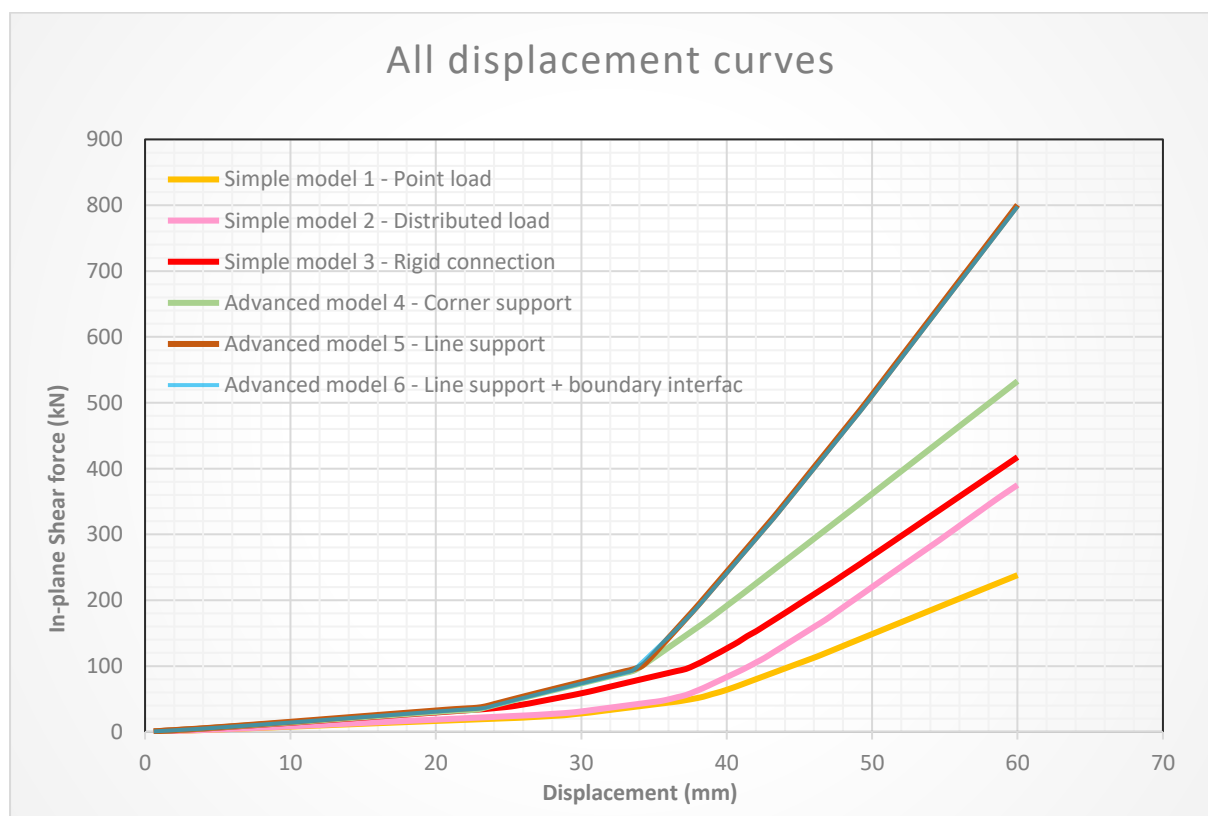


Figure 36: All displacement curves

## Conclusion

All numerical models behave differently due to the assumptions that have been made. Model 5 and model 6 react the stiffest thus is the upper boundary, model 1 is the least stiff and thus is the lower boundary. From the experiment it could be verified which model is the most realistic.

Since the structural window frame will be used for seismic loadings, the seismic behaviour should be looked into as well. This will be discussed in the next paragraph. Several material models are discussed here.

### 3.5 Phase 3: Material model

The structural glass façade will be loaded, during the experimentation, for a monotonic load and a cyclic load. The cyclic behaviour of a structural glass façade is of importance for a seismic environment. In the previous paragraph, a monotonic loading was applied only. Therefore, in this paragraph the focus will be on applying a cyclic loading. A quasi-static loading is a cyclic loading that is applied very slowly. In other words, time and inertial force are irrelevant.

In the previous paragraph, the adhesive is modelled with non-linear interface elements. This is practical for a monotonic load since you can describe its behaviour very well. However, for cyclic loading it just follows the same in-plane behaviour as for the monotonic load. Thus, there is no stiffness or strength reduction inside the numerical model. Also, there is no energy being absorbed by the numerical model. In practice, there should be a strength reduction since the adhesive will start to tear at some point. Therefore, several material models are made to model the behaviour of the structural adhesive and include this strength reduction behaviour. The following material models are compared with each other:

- Non-linear interface model
- Coulomb Friction model
- Mooney-Rivlin model

The Coulomb Friction model and Mooney-Rivlin model are tested on two blocks with an interface to model its behaviour. When the models are working correctly the interface is used for the actual model. Hereby numerical model 5 is chosen as a standard for every numerical model since it is the most detailed numerical model. Hereby only the adhesive will change depending on the material model. Model 5 and 6 have the same numerical results, but model 5 is less complex due to excluding the boundary supports.

#### 3.5.1 Non-linear interface model

The non-linear interface model is the same model which is described in the previous paragraphs. It makes use of 2D non-linear interface elements to model the behaviour of the structural adhesive. The same discretization and material properties as used as mentioned in the previous paragraph for the advanced model. The only difference is the Analysis method, see Table 19.

The cyclic load is a displacement load of 60 mm. This displacement load behaves cyclically with 100 load steps.

Load	Load name	Monotonic load
	Load	60 mm
	Load step	0.01(100) -0.01(100) 0.01(100) -0.01(100)
Iterative procedure	Procedure	Regular Newton-Raphson
	Max. number of iterations	50
	Line search	No
Convergence criterium	Norm	Force & Displacement
	Tolerance	0.01
	No convergence	Terminate

Table 19: Analysis method

## Results

The displacement curve for using non-linear interface elements for a cyclic loading doesn't differ from the displacement curve for the monotonic loading. The material model doesn't take strength reduction into account. Therefore, the unloading and second displacement loading is just an exact copy of the first displacement load. However, the main benefit of using this model is that the structural behaviour of the interface is controllable. See Figure 37 for the displacement curve.

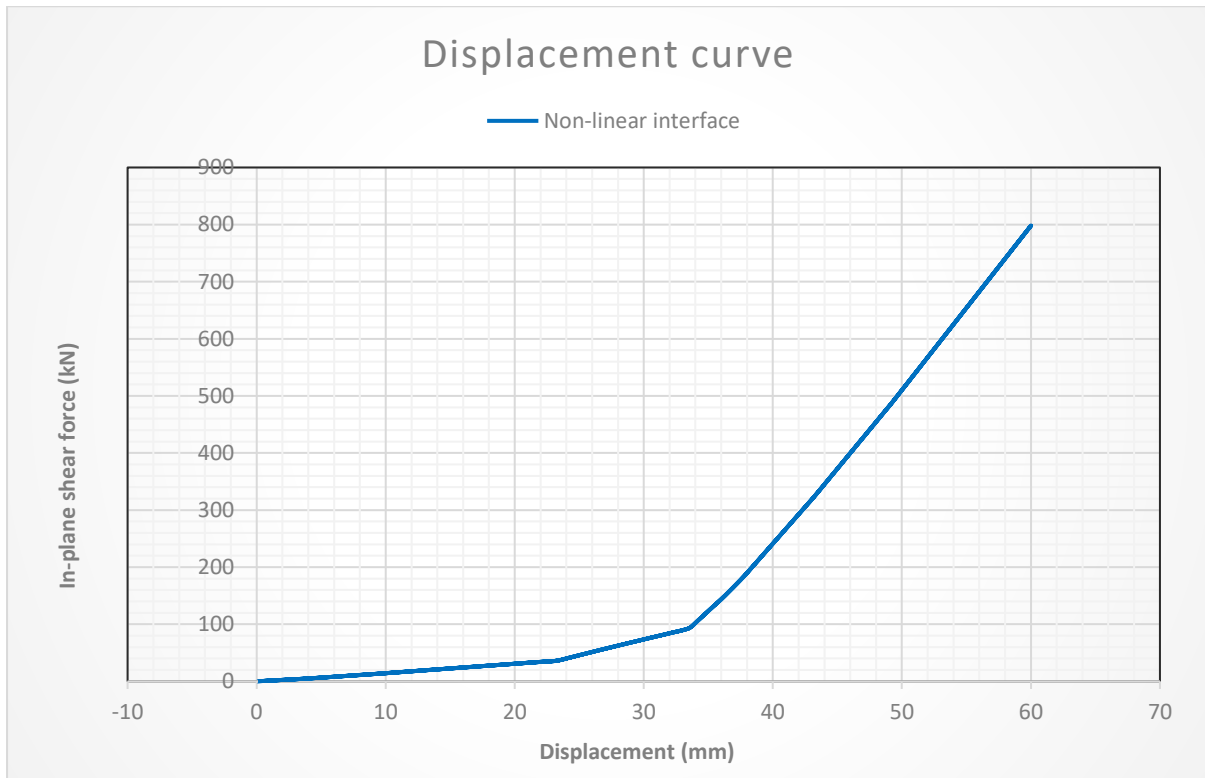


Figure 37: Displacement curve Non-linear interface

### 3.5.2 Coulomb friction model

The Coulomb friction model is an alternative model to the original model. In general, the interface between two parts of a structure is determined by frictional behaviour. This behaviour can be modelled with the Coulomb friction model, which is similar to the Mohr-Coulomb plasticity model.

In Figure 38 a figure of the coulomb friction is shown.  $C$  stands for cohesion,  $\phi$  is the friction angle.  $t_n$  stands for traction in the normal direction and  $t_t$  stands for the traction in the tangential direction (DIANA, 2017).

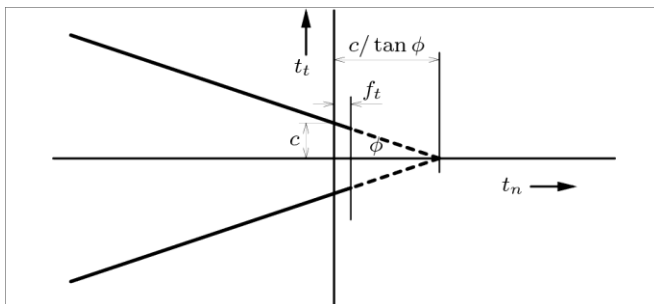


Figure 38: Coulomb friction (DIANA, 2017)

For a Coulomb friction model, there are different interface opening options. This interface opening is crucial for the behaviour of the interface and thus of the overall structural model. These interface openings are a gapping model with constant shear retention and non-linear soil bedding. For a gapping model, it is possible to indicate the tension stress in which tearing occurs of the adhesive, thus it is possible to indicate when the shear stiffness reduces. A non-linear soil bedding model is more frequently used for soil calculations however, it is still interesting to look into since the maximum stress can be indicated in the model.

To see the influence of these interface openings options several numerical models have been tested on different loads.

In Appendix A.2 the modelling of the test model is being shown. In this model, the interface is modelled for a simple model with two blocks. This is done to understand the material model better.

From these models, the following can be concluded. Tearing of the adhesive is visible in the model and decreases the strength when the maximum shear stress is reached. However, there is no increase in stiffness due to contact between the two blocks visible in the models. This would be a problem in the window frame model since the contact between the glass panel and the timber frame is crucial.

Using the material models for the structural window frame will conclude whether the Coulomb friction model is a suitable material model to use for cyclic loading for the structural window frame.

## Structural window frame model

For the structural window frame model, the gapping model and the nonlinear soil bedding model will be used. The same geometry as for initial model 2 is used. The only difference is a point load is used instead of a line load, see Figure 39. The material properties need to be adjusted to the correct values. These values are determined in paragraph 4.2 by the experiments and by the supplier. According to the supplier of the Sikaflex adhesive, the tear resistance is  $7 \text{ N/mm}^2$  and the strain when breakage is expected is 400% of the original thickness (Sika Nederland B.V., 2012). The shear resistance is determined by experiments which are illustrated in paragraph 4.2. The shear resistance is determined to be around 2 MPa. The friction angle is assumed 17 Degrees since this is the same angle as for a glass steel connection. The model for gap appearance is noted as brittle since the maximum shear stress of 2 MPa is not reached. Thus, it didn't matter that the gap appearance was brittle or shear retention. For the Coulomb model 6 the same material properties are assumed, see Table 20.

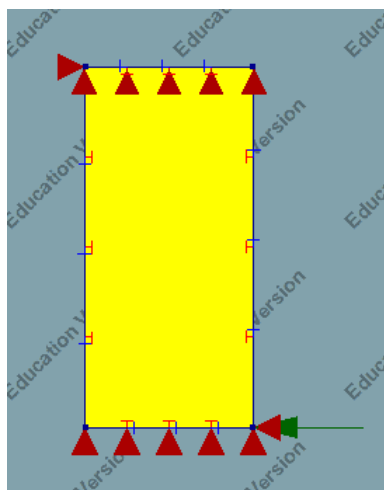


Figure 39: Numerical model for Coulomb model 5 and 6

	Coulomb Model 5	Coulomb Model 6
Cohesion ( $\text{N/mm}^2$ )	2	2
Friction angle ( $^\circ$ )	17	17
Dilatancy angle ( $^\circ$ )	0	0
Interface opening	Gapping model	Nonlinear soil bedding
Tensile strength ( $\text{N/mm}^2$ )	7	-
Model for gap appearance	Brittle	-
Reduced shear stiffness ( $\text{N/mm}^3$ )	-	-
Unloading-reloading normal stiffness ( $\text{N/mm}^3$ )	-	100
Maximum compressive stress ( $\text{N/mm}^2$ )	-	20

Table 20: Material properties Coulomb model 5 & 6

## Analysis

The analysis method is similar to the previous analysis method. However, the load step involves Unloading as well as re-loading.

		Coulomb Model 5: Gapping model	Coulomb Model 6: Soil bedding
Load	Load name	Cyclic load	Cyclic load
	Load	100 mm	100 mm
	Load step	0.01(100) -0.01(100) 0.01(100)-0.01(100)	0.01(100) -0.01(100) 0.01(100) -0.01(100)
Iterative procedure	Procedure	Regular Newton-Raphson	Regular Newton-Raphson
	Max. number of iterations	50	50
	Line search	No	No
Convergence criterium	Norm	Force & Displacement	Force & Displacement
	Tolerance	0.01	0.01
	No convergence	Terminate	Terminate

Table 21: Analysis method of the coulomb model 5 & 6

## Results

For Coulomb model 5 the adhesive starts tearing around 30 mm however, the shear stress does not reach its maximum of 2 MPa , therefor the plastic behaviour due to shearing does not occur. See Figure 40 for the tearing of the adhesive due to high tensile stresses and see Figure 41 for the maximum shear stresses in the adhesive. The important aspect is that the model does not react to the intersection between the glass panel and the timber frame. This aspect already showed in the test model. Furthermore, the unloading line is a straight line, which means that there is no plastic behaviour for unloading in the numerical model.

The Coulomb model 6, where nonlinear soil bedding is used, behaves differently. The unloading behaviour is visible for the first cycle. However, the second cycle behaves very unpredictably. Furthermore, this model also does not react to the intersection between the glass panel and the timber frame. See Figure 42 for the displacement curve of both models.

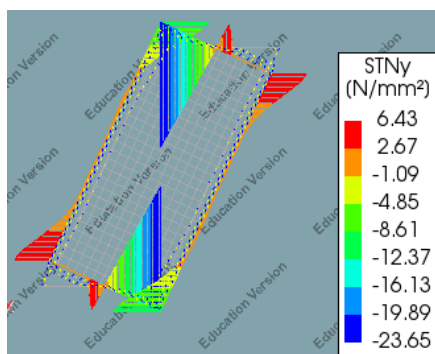


Figure 40: Normal stress at maximum displacement

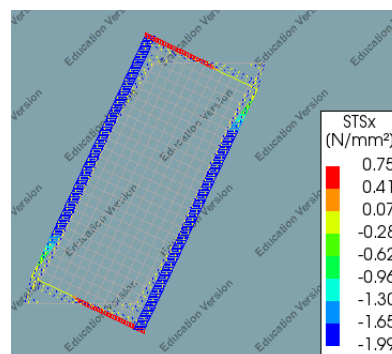


Figure 41: Shear stress at maximum displacement

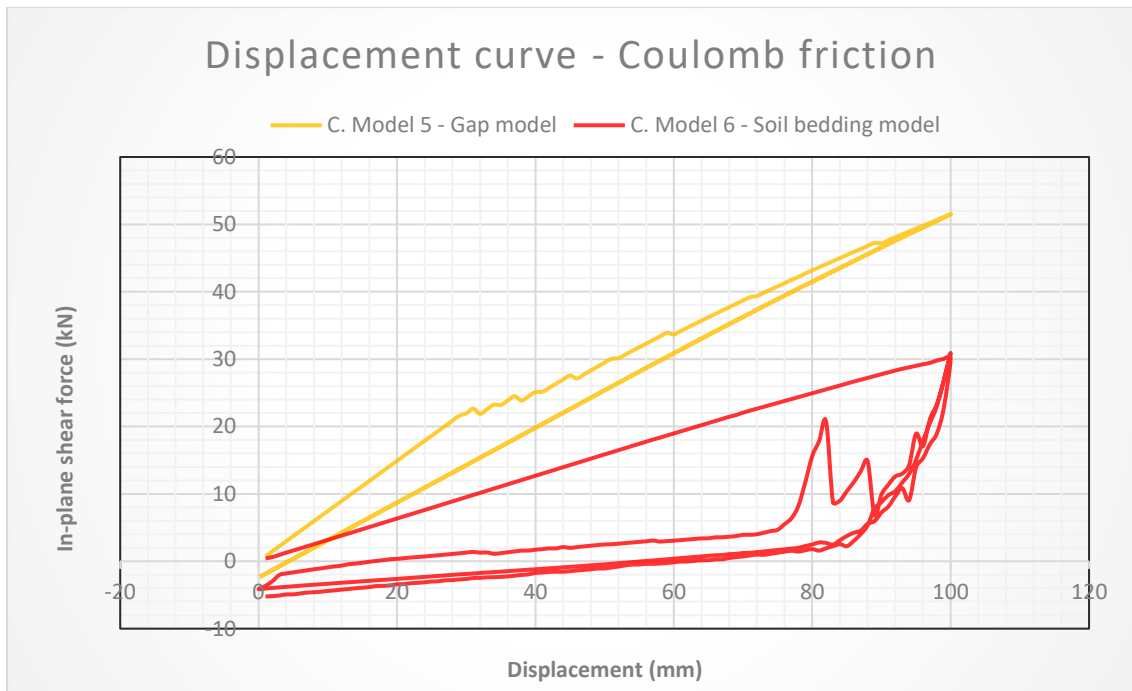


Figure 42: Displacement curve for the Coulomb friction model for model 5 & model 6

## Conclusion

Both models seem promising due to the strength reduction and unloading behaviour. However, due to no interaction between the glass panel and the timber frame, the model does not represent the structural window frame very well. Furthermore, both models react not predictable and sufficient enough to represent the complex behaviour of the window frame.

### 3.5.3 Mooney-Rivlin

A different approach to model the structural adhesive is to make use of hyperelasticity. Rubbery material can be modelled with this method. This method uses material description based on strain energy density, instead of stress-strain-like description. Hyperelasticity models are based on the Total Lagrange description. A well-known, way to construct a strain energy density function is the Mooney-Rivlin model.

Research (Amstutz et al., 2018) shows that the mechanical behaviour of a Sikaflex elastic PU adhesive has been investigated under quasi-static and monotonic increasing loading. Several hyperelastic material models have been made to compare with the experimental results. The results concluded that the Mooney-Rivlin with five parameters showed the best potential. Accurate predictions were also provided by the Mooney-Rivlin with two parameters. Diana only has the option to model a Mooney-Rivlin model with two parameters.

In another study (Noteboom et al., 2020), structural silicone is modelled with a Mooney Rivlin model with  $C1 = 0.33$  MPa and  $C2 = 0.005$  MPa. Therefore, these values are used for the numerical model.

Similarly, to the Coulomb Friction model, the Mooney-Rivlin model is also modelled with only two timber blocks. The model is made using plane strain elements since this is required for the Mooney-Rivlin model. See Appendix A.2

The results show a linear behaviour for the shearing of the adhesive. There is no tearing of the adhesive or plastic behaviour visible. Using this adhesive for the structural window frame would conclude whether this material model is usable.

### Structural Window Frame

In Figure 43 the geometry of the structural window frame for Mooney-Rivlin is shown. The same material properties are used as for the test model. The geometry of the structural window frame is the same as mentioned in paragraph 3.2. The adhesive has an in-plane thickness of 5 mm. The model is made with plane strain elements since Mooney-Rivlin is only useable using plane strain elements. The displacement load is one cycle of 60 mm. The analysis method is similar to the previous analysis method of the coulomb friction. However, the load step is one cycle instead of two cycles and the type of geometrical nonlinearity is Total La grange.

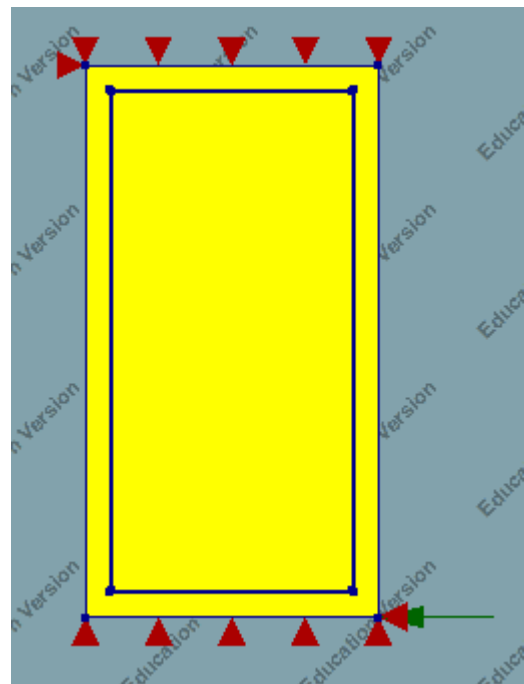


Figure 43: Structural window frame for Mooney Rivlin

## Results

The results show that the interface has a rubberlike behaviour, see Figure 44. However, it is difficult to verify the stiffness of the interface. For the initial results, the input parameters, which are based on previous research (Noteboom et al., 2020), are taken for the test model and the actual model.

In Figure 44 the displacement curve for the Mooney-Rivlin model is shown of the structural window frame. In this model, a clear increase of stiffness is seen around 30 mm. This means that the contact between the glass and the timber frame is taken into account in this model. However, the In-plane shear force is lower than for the non-linear interface model. This could be due to the input parameters that were assumed by previous research. Furthermore, two parameters are not sufficient enough to represent the complex behaviour of the model

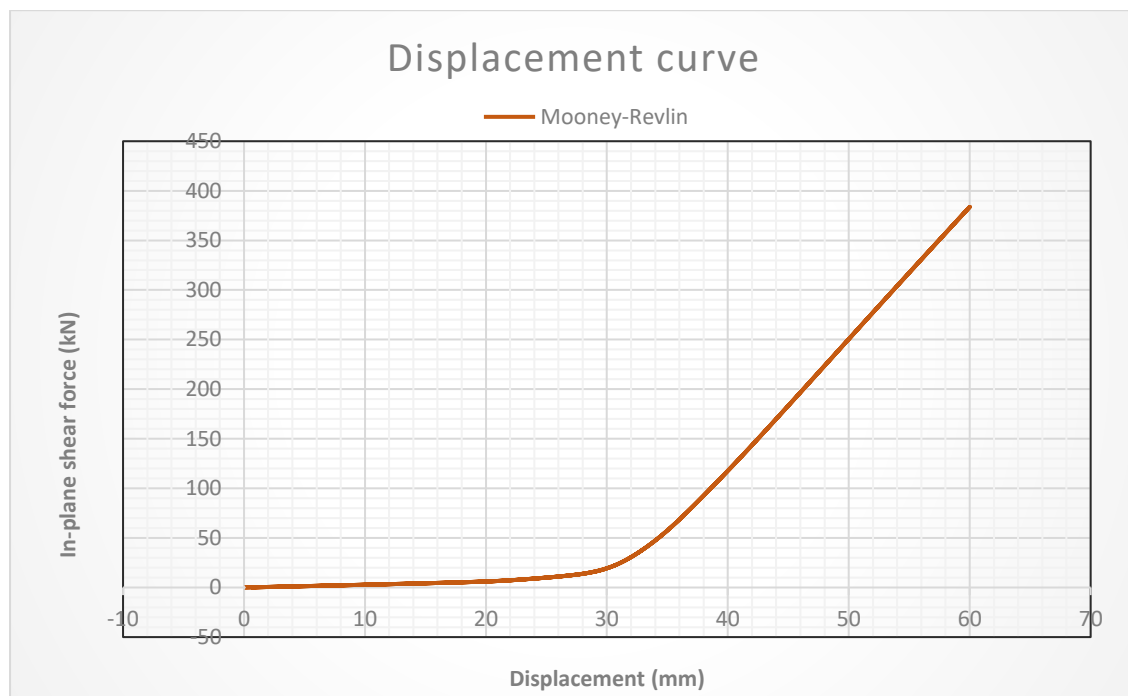


Figure 44: Displacement curve Mooney-Rivlin

## Conclusion

Although Mooney Rivlin is frequently used for rubbery materials, it is questionable whether it is suitable for the structural window frame. The structural behaviour is determined by two parameters, which are not sufficient enough to determine the complex behaviour of the window frame. A benefit compared to the Coulomb friction model is that the model does recognize an intersection between the glass panel and the timber frame. However, strength reduction is not included in the model.

## Final conclusion

Based on the findings, the non-linear interface gives the best result to simulate the complex behaviour of the window frame. Therefore, it is used in the following chapters of the thesis. Non-linear interface elements are able to control the complex behaviour of the structural window frame. Unfortunately, strength reduction or plasticity is not taken in this model. However, the other models also don't show a good alternative. Coulomb friction doesn't include the intersection between glass and timber and the Mooney Rivlin model is very unpredictable. Furthermore, the existing material models in Diana are not suitable yet for the plastic behaviour of the adhesive or timber frame in this context. Therefore, non-linear interface elements are the best suitable for the structural window frame, even though it is just useable for monotonic loading. In chapter 5 the reasoning for using non-linear interface elements is more elaborately explained.

### 3.6 Several small studies

In this paragraph, several small studies will be summarised and discussed. These investigations are made to have a better understanding of the model and to verify crucial steps of the modelling process. In Appendix A.3 and A.4 these studies are explained more elaborately. The following studies have been made:

- Mesh analysis
- Buckling analysis

#### 3.6.1. Mesh analysis

For every computational model, the mesh size is very crucial. The mesh size is a determinant for the accuracy of the computational model. How smaller the mesh size, how more accurate the model. However, a smaller mesh size also results in a higher computational calculation time. Therefore, an optimum mesh size should be found.

In Appendix A.3 a mesh analysis has done for model 1 to calculate the optimum mesh size, which takes into account accuracy and calculation time. The mesh consists of quadratic elements. Three different mesh sizes were compared: 25 mm, 50 mm and 100 mm. For the analysis, three different displacements of the structural façade are compared. These are the transition phases between phase 1a-1b, 1b-2a and 2a-2b. The corresponding displacements are 12.6 mm, 25.8 mm and 33 mm.

The stresses in the glass were similar for all mesh size for small displacements. However, for large deformations, the stresses were different for different mesh sizes. These high stresses are not reliable, since these high stresses will not occur during the experiment. This is because the softness of the multiplex is not included in the computational model. The stresses in the timber beam are also not reliable since the frame is made out of beam elements.

For the behaviour of the structural façade, the displacement curve is the most crucial. In Figure 45 the displacement curves of the models are shown with different mesh sizes. It is seen that a mesh size of 100 mm is different from a certain distance. Since the curve for the mesh size of 25 mm and 50 mm are very close to each other, the mesh size of 50 mm is preferred. This has to do that a mesh size of 25 mm takes more computational time to calculate.

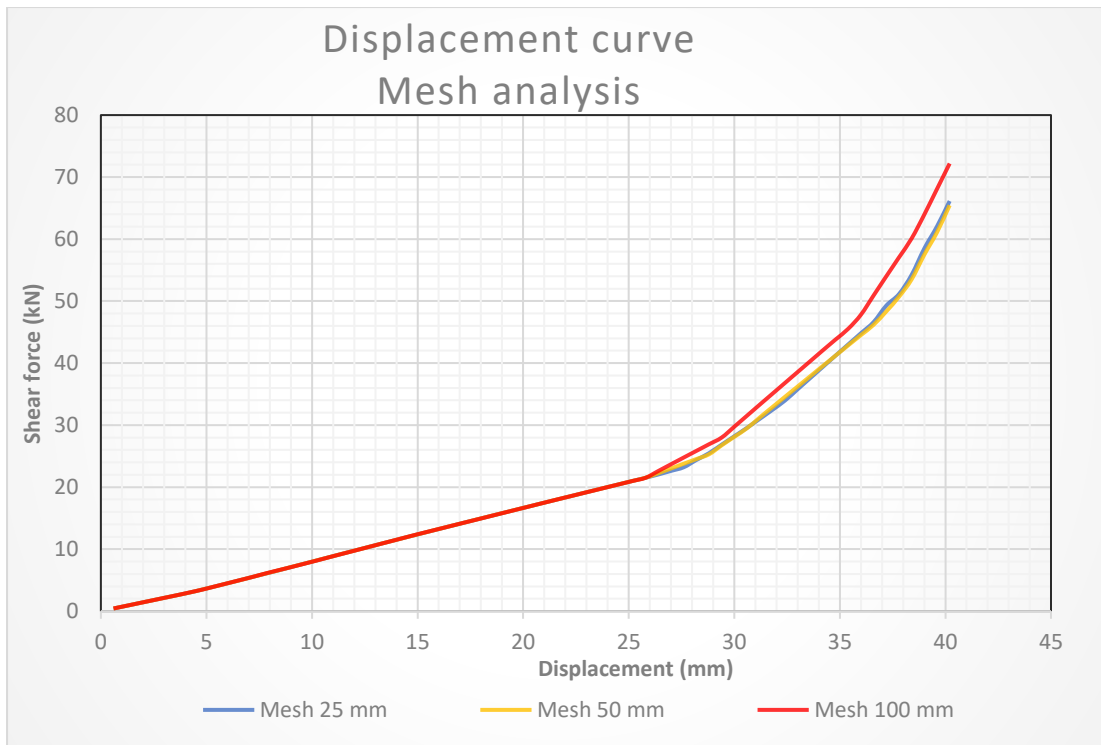


Figure 45: Displacement curve mesh analysis

### 3.6.2. Bucklin analysis

The shear buckling behaviour is analysed as an isotropic glass plate that is supported along four edges. A distinction is made for a hinged and clamped connection along the edges to determine the lower and upper limit. These calculations are based on (Amadio & Bedon, 2015).

To calculate the Shear Buckling resistance, the equivalent thickness of the glass panel needs to be calculated. See Appendix A.4 for the calculation.

The shear resistance is 405.3 kN for a hinged and a rigid connection since the  $\chi$  value will be one for both assumptions. It is unlikely that the glass panel will have a design force beyond the shear buckling resistance. It is more likely that the glass will penetrate in the multiplex and the timber frame will fail than that the glass element will fail by shear buckling. This is because the timber is less stiff than the glass panel. Concluding, shear buckling is not assumed to be crucial for the structural window frame.

By making all these analyses an answer is given to the sub-question mentioned in paragraph 1.2 for part 2.

### PART III: EXPERIMENTAL STUDY



## 4. Experimental study

The experiments are of significant importance for the aim of this thesis. It will illustrate the structural behaviour of the structural window frame. Furthermore, the numerical modelling part should resemble the results of the experimentations.

In this part and chapter, the experimental research of the structural glass façade is being introduced and discussed. Firstly, the experimentation of the structural window frame itself is being introduced. Secondly, the experiments on the timber frame and the adhesive are being illustrated and discussed. Finally, the experimentation on the structural window frame is being shown and discussed. This includes the loading protocol, the results for the monotonic and cyclic loading and a visual inspection of the damage.

In Chapter 5 the results of the experimentations are being compared to the results of the numerical model.

### 4.1 Introduction to the experiment

In this paragraph, a short introduction is given about the experimentation of the structural glass façade.

In total 12 prototypes will be made of the structural glass window. Six for the experiment of the structural window on its own and six for the experiments including the masonry walls. There are two different window sizes since two different masonry walls are going to be tested including the structural glass façade. Namely, a calcium silicate masonry wall and a solid clay masonry wall, see Table 22. The drawing of the structural window frame including the dimensions and built-up are shown in Attachment E.

Sample name	Unit type and size (mm)	Boundary conditions
CS-X	Calcium Silicate Brick Masonry (1436x744x100)	Double clamped
Clay-X	Solid Clay Brick Masonry (1460x730x100)	Double clamped

Table 22: Specification testing

## Testing protocol

A DIC measuring system is used to measure crack initiation and propagation and displacement for the glass and timber frame. DIC stands for digital image correlation and tracking, it is an optical method that uses image registration techniques for accurate measurements of changes in images. It is often used to measure strains and deformations. To verify the DIC, LVDT's sensors will be placed as well, which measures the displacement. LVDT stands for Linear Variable Differential Transformers, it can be used to detect very small displacements. With special software, named GOM Correlate, the DIC will be analysed.

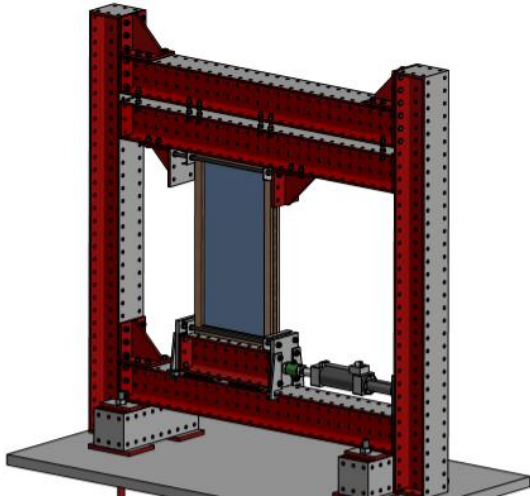


Figure 46: Test set-up (Gaggero)

## Loading scheme

In Figure 46 the Test set-up is shown. The structural glass window rests on the structure, so only the horizontal displacement will be applied to the structure. Before the test, a wooden frame will be placed instead of the window, see Figure 49. This pre-test is performed to check if the sensors work properly. Furthermore, the timber which is used for the frame will be tested separately to calculate the density and the E-modulus. The timber frame consists of meranti hardwood and Okoumé plywood. The results can be used to determine the E-modulus of the timber. The polyurethane adhesive will also be tested before the actual test. The bondage of the glass/adhesive and adhesive/timber will be tested to see its behaviour.

Each window will be tested in-plane with a minimum of one monotonic loading. After the monotonic loading two cyclic loadings will be done for each window.

## Instrumentation

The measurement system has been designed to:

- Record the global horizontal and vertical deformations of the window
- Record the evolution of the crack pattern by DIC
- To produce time-displacement, time-force and force-displacement diagrams
- Measure the deformation of the adhesive

The DIC measurement system will measure the deformations for the glass panel and the timber frame. By doing this the relative interface deformation can also be calculated. The LVDT's sensors will be placed to verify the measurements of the DIC system. The window will be painted white with black dots on the inside of the window, see Figure 47. In this picture, the LVDT sensors are also visible. It is noticeable that the structural façade is being clamped at the bottom and upper part. This prevents the rotation of the timber frame. On the other side of the façade the sensors for the timber frame are placed, see Figure 48 . In this picture, a sketch is visible which shows the location of all sensors. The regular sensors are being placed at the corners and go diagonally. The glass panel of 4 mm won't be removed, in order to verify its influence.



Figure 47: Structural glass façade during testing

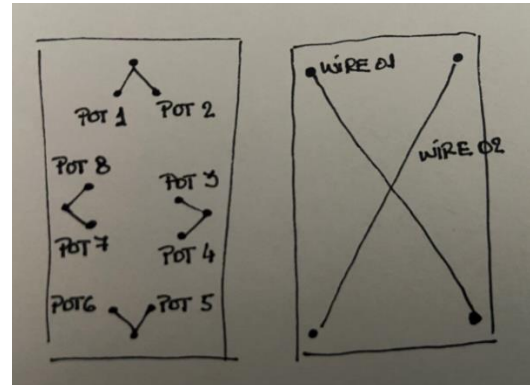


Figure 48: Upper: Sketch of sensors  
Lower: Sensor's timber frame

## 4.2 Before the experiment

A wooden frame is being used to test the setup. It is seen that the bottom and upper part are being clamped by a steel u-profile, See Figure 49. This is to make sure that the wooden frame will be pushed evenly. The bottom part will be pushed by the jack.



Figure 49: Experimental set-up of the wooden frame

See (M.B.Gaggero & P.Korswagen, 2020) for an explanation of how the structural glass façade is constructed.

### 4.2.1 Material properties Sikaflex and timber

In Appendix B.2 the experiments for determining the bond properties of Sikaflex-252 are discussed. According to the results the black and white Sikaflex behave differently. However due to the low number of experiments and advise from the manufacturer an initial shear stress of 2 MPa is assumed. See Table 23 for an overview of the properties. See (Gaggero,2020) for more detailed information about the experiment.

Specimen name	$f_p$ (MPa)	$f_v$ (MPa)	$f_{v,res}$ (MPa)	$G_{II}$ (N/mm)
ST1	0.50	<b>2.08</b>	0.07	26.81
ST2	1.00	<b>2.10</b>	-	30.50
ST3	1.00	<b>1.19</b>	0.18	12.09
ST4	0.5	<b>1.29</b>	0.08	14.26

Table 23: Overview of the evaluated properties (Gaggero,2020)

In Appendix B.2 the experiments for determining the material properties of the timber frame are shown elaborately. Firstly, a non-destructive resonance test was done in order to determine the material properties. These are shown in Table 24.

	(A) Okoumé Multiplex Y-Direction	(B) Okoumé Multiplex X-Direction	(D) Meranti elements
<b><math>p</math> (<math>kg/mm^3</math>)</b>	<b>473.4</b>	<b>484.9</b>	<b>601.9</b>
<b>E (GPa)</b>	<b>5.7</b>	<b>5.3</b>	<b>16.0</b>

Table 24: Overview results (Gaggero, 2020)

According to the experiment the average stiffness is 5.5 GPa however, the supplier mentioned a bending stiffness of 2 GPa. Therefore, further research was needed. A compression test is done to measure the bending stiffness and the compression strength of the plywood. In Table 25 the results of the compression test for the Okoumé are shown. An average bending stiffness of 1.63 GPa is given, since the supplier mentioned a bending stiffness of 2 GPa, this will value will be used for the calculation for average elasticity modulus.

In the previous paragraphs, a value of 5.5 GPa is taken for the numerical models. Since the main point was to compare the models these values are not adjusted. However in the next paragraphs, the value of 2 GPa is assumed for the plywood.

The calculation includes the estimated average density and elasticity modulus of the composed timber frame. This is of importance since this will be the input value of the computational model. See Appendix B.1 for the calculation and for the new value for the timber frame.

## Compression test

The results of the compression test are given in Table 25 and Figure 50. These results will be used as input values for the numerical model.

Specimen	$f_{c,y}$ (MPa)	$f_{c,u}$ (MPa)	$E_c$ (GPa)
<b>Avg.</b>	<b>12.99</b>	<b>22.66</b>	<b>1.63</b>
<b>St.dev.</b>	<b>0.54</b>	<b>0.37</b>	<b>0.16</b>
<b>C.o.V</b>	<b>0.04</b>	<b>0.02</b>	<b>0.09</b>
<b>Characterisitc value</b>	<b>11.66</b>	<b>21.76</b>	-

Table 25: Compression test results

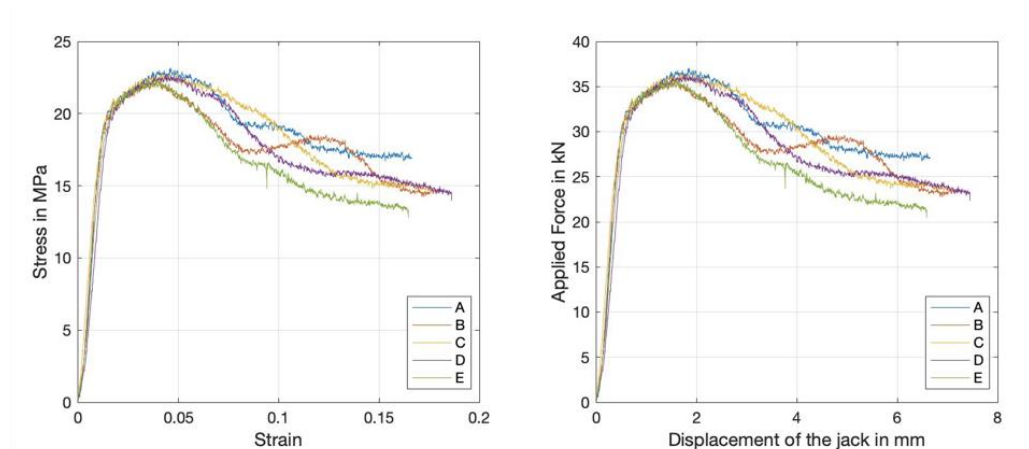


Figure 50: left – stress-strain curve, right- displacement versus applied force

## 4.3 Experimental results

Several experiments have been conducted on the structural window frame. These experiments have been divided into monotonic and cyclic loading and have different measurements based on the type of wall. In this paragraph, the results are discussed.

### 4.3.1 Monotonic loading

In total four experiments are done on the structural glass façade for monotonic loading. The first two experiments are not officially taken into the experimental results. However, these results are still important to discuss.

For the first experiment, the structural façade for the calcium silicate masonry wall is used. During the first experiment, it became clear that the timber frame was not able to withstand the stresses due to the deformation implemented by the jack. Cracking occurred of the multiplex due to pinching of the element. The stresses due to the structural glass panel penetrating the multiplex parallel to grain were too high. The experiment was early stopped around a displacement of 65 mm to prevent further cracking of the multiplex. The displacement curve is shown as the blue dotted line in Figure 52 named experiment 1a. The maximum shear force applied is around 25 kN.

To prevent cracking of the multiplex and thus increase the ductility and stiffness of the timber frame some adjustments were made. Firstly, the old timber frame was repaired by glueing it with wood glue, see Figure 51. To prevent the multiplex from cracking again screws were placed inside the timber frame. The screws were namely placed at the top and lower parts since the stresses were the highest at these locations. See Figure 51 for the exact location of the screws. Screws were also placed in the in-plane direction of the corners to prevent the timber elements from detaching from each other. The repaired façade was tested once more and reacted stiffer and more ductile than in the first experiment. The displacement curve is shown as the red dotted line in Figure 52 named experiment 1b. The maximum shear force is around 40 kN and the experiment was stopped around a displacement of 85 mm. The experiment was not stopped due to cracking, but due to no significant change in structural behaviour. The sudden decline of the shear force at a displacement of approximately 40 and 55 mm is due to stopping the experiment and checking for cracks in the timber frame.

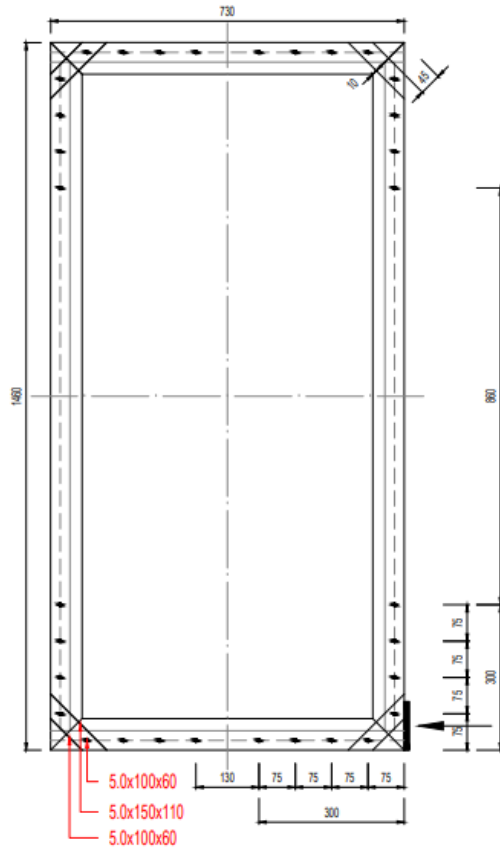


Figure 51: Left: Cracking and repairing of the multiplex  
Right: Location of the screws for the structural window frame

The second façade that was tested is the structural glass façade for the clay brick masonry wall. This façade was strengthened beforehand with screws in the same manner as the first façade. During the experiment, the speed of the displacement was increased slightly if no big changes in structural behaviour was observed for a long period. The original speed for the loading rate is 0.5mm/min. The structural façade reacted similarly to the first strengthened structural façade. The displacement curve is shown as the green line in Figure 52 named experiment 2. The maximum shear stiffness is approximately 37 kN. The experiment was stopped around 100 mm since there was no significant change in the structural behaviour and the limit of the jack was nearly reached. The non-structural glass panel of 4 mm had a small crack before the experimentation and got fully cracked at the end of the experiment. However, in the other experiments the non-structural glass panel showed no damage. In conclusion, the glass panel of 4 mm is not influenced by the displacement of the experiment.

The third façade that was tested is the structural glass façade for the calcium silicate masonry wall. This façade was strengthened beforehand with screws in the same manner as the other façades. During the experiment, the speed of the displacement was changed. The initial speed was 0.5mm/min since the initial displacement has a high structural sensitivity. Around a displacement of 24 mm, the speed got increased until 1 mm/min. This was possible since the structural behaviour became less sensitive to displacement than before. The structural façade reacted similarly to the other strengthened structural façade. The displacement curve is shown as the orange line in Figure 52 named experiment 3. The maximum shear stiffness is a bit higher with approximately 42 kN, however in general it has very similar behaviour. The experiment was stopped around 100 mm since there was no significant change in the structural behaviour and the limit of the jack was nearly reached.

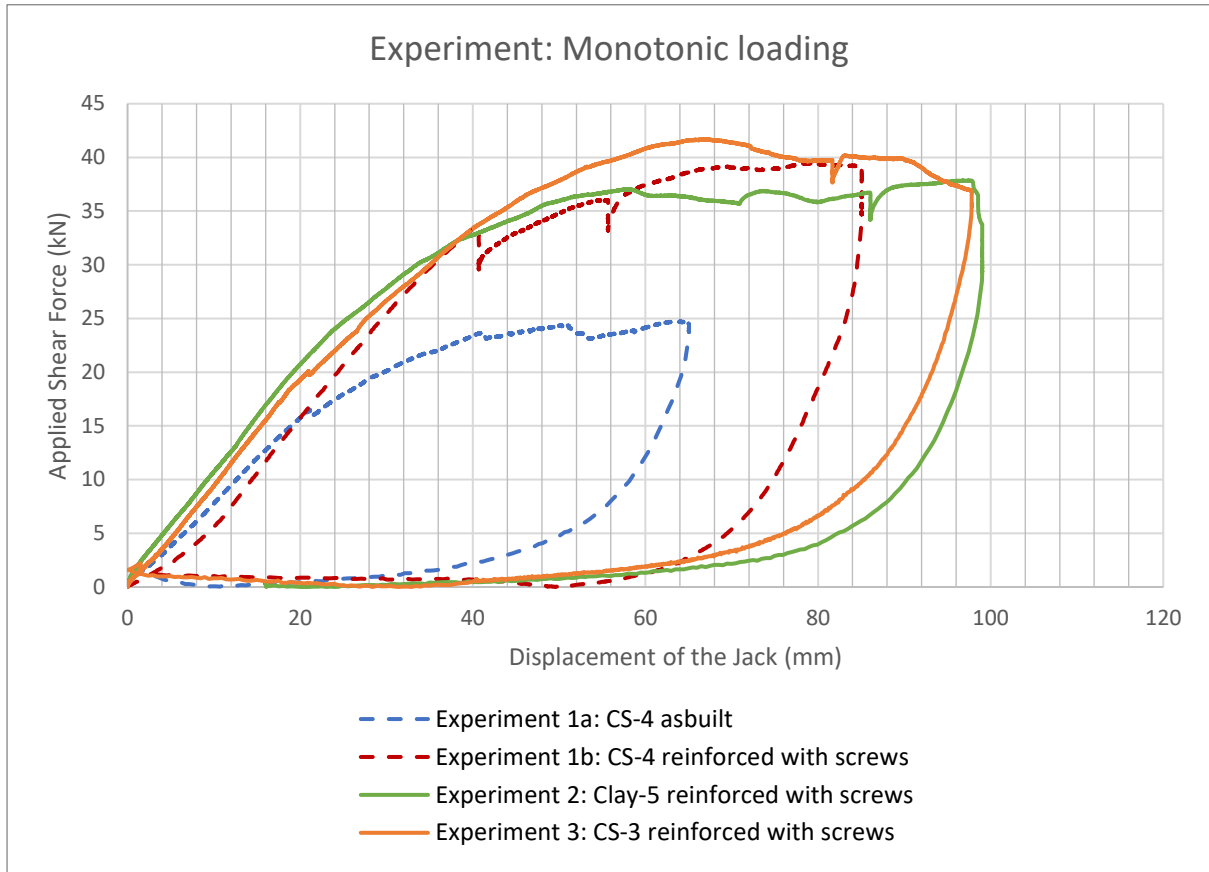


Figure 52: Displacement curve: Monotonic load

## Visual Inspection

After the experimentation, the frame is detached from each other to inspect the structural façade in more detail. To detach the timber frame from the glass panel a hydraulic pump is used, see Figure 53. The hydraulic pump builds up pressure and pushes the timber frames out of each other. Therefore only two bars can be detached, the other two bars are detached using a hammer carefully. These actions need to be done in a controlled environment, to prevent damage to the glass panel.

In case of damage during usage of the structural façade, it would be difficult to replace one element. Since the glass panel could only be replaced by detaching the timber frame from each other. Glueing it back together is practically impossible. Therefore, structural damage to the structural façade should be minimal and maintenance is crucial. In Paragraph 8.3 this topic is more elaborated.

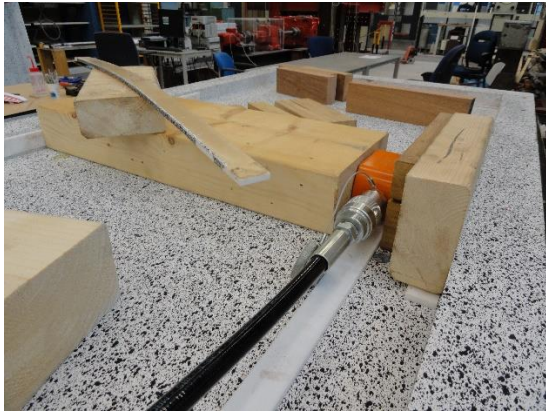


Figure 53: Left: detaching of the timber frame with a hydraulic pump, Right: detaching the timber frame with a hammer

During the experiment, the glass pinches in the timber frame at a certain point. This is because the glass panel is rotating inside the timber frame and the glass has a higher stiffness than the multiplex. From the experiments, it was seen that only the lower and the upper timber bar were pinched, see Figure 54. The glass penetrated approximately 10 mm inside the multiplex. This behaviour is as expected and favourable since peak stresses in the glass are avoided. The penetration of the multiplex also assures the plastic behaviour of the structural system, this is also visible in the graph that is shown in Figure 52. The longer sidebars didn't have any visible damages, this is due geometry of the window frame. The relative interface displacement is less for the sidebars.



Figure 54: Pinching of the timber frame

By detaching the timber frame from the glass panel, the adhesive got spread onto the multiplex and glass panel. This is visible in Figure 54. The hardwood of the timber frame got damaged as well. The upper timber bar for the second façade and the lower timber bar for the third façade had horizontal cracks in the hardwood, see Figure 55. However, it is more likely that these cracks occurred due to detaching of the timber bars. Furthermore, other timber bars didn't show any large cracks.



Figure 55: Left: Crack of the upper timber bar, Right: Cracking of the lower timber bar

### 4.3.2 Cyclic loading

In total four experiments are done on the structural glass façade with cyclic loading. Two with the dimensions that fit the calcium silicate wall and two for the clay brick wall. The monotonic loading was mainly done to observe the initial results. Furthermore, it is a good check to compare the results of the numerical model and the experiments. The cyclic loading experiment is more elaborate and would explain the cyclic behaviour better. For a seismic environment, this is of significant value.

#### Loading protocol

The cyclic experiments are different from the experiments for the monotonic loading. One significant difference is the loading protocol. In Figure 56 an overview of the first horizontal shear load and the repetitions are shown. The loading protocol is divided into a one-way cyclic loading and a two-way cyclic loading. This is done to see the change in structural behaviour for different cyclic loadings. For the first experiment, each displacement has a repetition of 15 cycles. The other experiments had a repetition of 20 cycles. This has to do with the stabilization of the shear force. In each displacement load, the maximum horizontal shear force should stabilize after a certain number of cycles. For the first experiment, it became clear that 15 cycles were not sufficient, therefore from the second experiment 20 cycles for each displacement was used. See Figure 59 for the graph of the reduction of shear force over the number of repetitions.

The displacement rate is faster than the monotonic loading since significantly more cycles needed to be done and to reduce testing time.

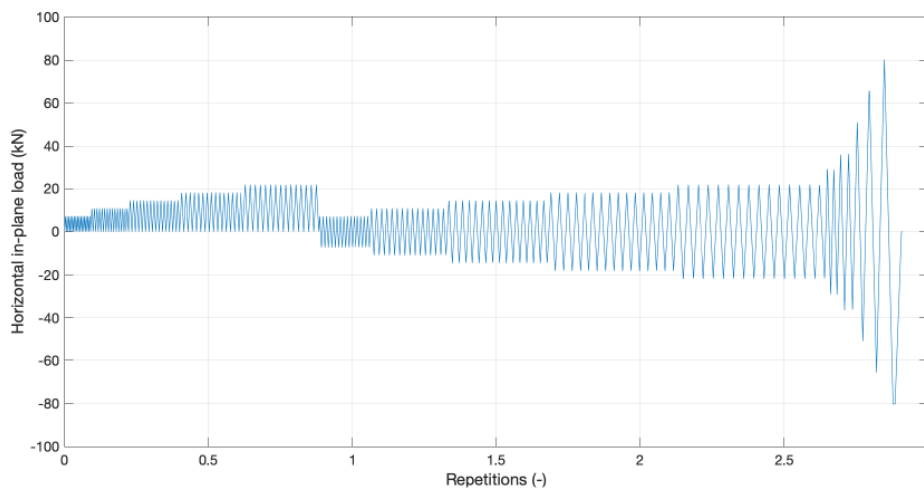


Figure 56: Horizontal load vs the repetitions (Gaggero,2021)

Cycles		Window drift %	Horizontal bottom displacement (mm)		Rate (mm/s)
1	20	0.5*	7.30	-	0.7
21	40	0.75*	10.95	-	0.7
41	60	1.00*	14.60	-	0.7
61	80	1.25*	18.25	-	0.7
81	100	1.50*	21.90	-	0.7
101	120	0.5**	7.30	-7.30	0.7
121	140	0.75**	10.95	-10.95	0.7
141	160	1.00**	14.60	-14.60	0.7
161	180	1.25**	18.25	-18.25	0.7
181	200	1.50**	21.90	-21.90	0.7
201	202	2.00**	29.20	-29.20	1.5
203	204	2.50**	36.50	-36.50	1.5
205		3.50**	51.10	-51.10	1.5
206		4.50**	65.70	-65.70	1.5
207		5.50**	80.30	-80.30	1.5

\* one way cyclic

\*\* two way cyclic

*Figure 57: Cyclic Loading scheme for the second structural window for a clay brick masonry wall*

## Results

In Figure 58 the displacement curve is shown for the experimental results for the horizontal in-plane load versus the drift and the displacement. It is noticeable that with each new displacement step the stiffness decreases as well since the slope of the line decreases. This could be explained due to the pinching of the glass into the timber frame. For small displacements, the stiffness remains nearly constant since the adhesive is still acting linearly.

In Figure 59 the graph of reduction of shear force over the number of repetitions is shown. It is noticeable that for small shear forces and thus small displacements, the shear force remains stable for a small number of repetitions. For large forces and thus large displacements, the shear force is more spread out for a large number of repetitions. This means that the structural window is acting plastically for large displacements and linearly for small displacements, which corresponds to the structural behaviour of the Sikaflex-252.

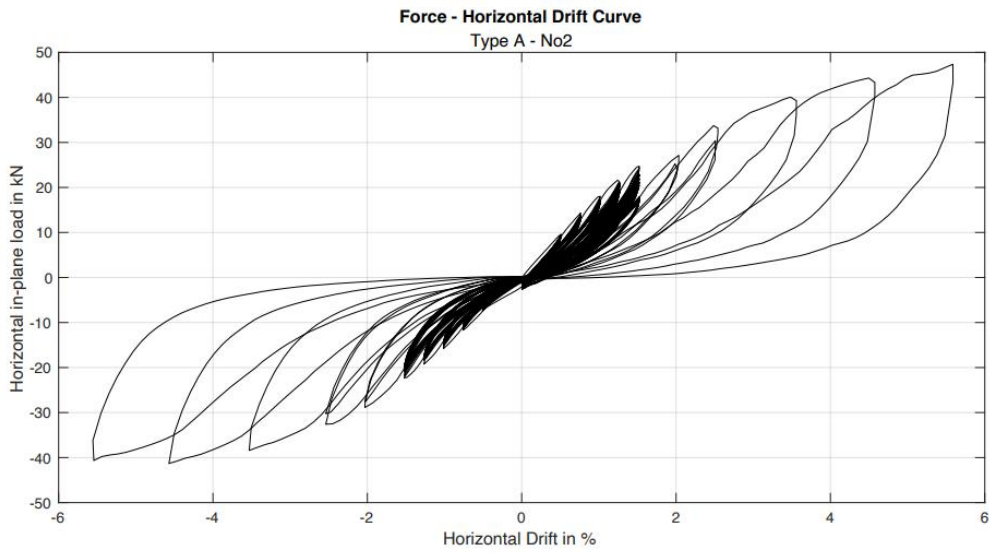
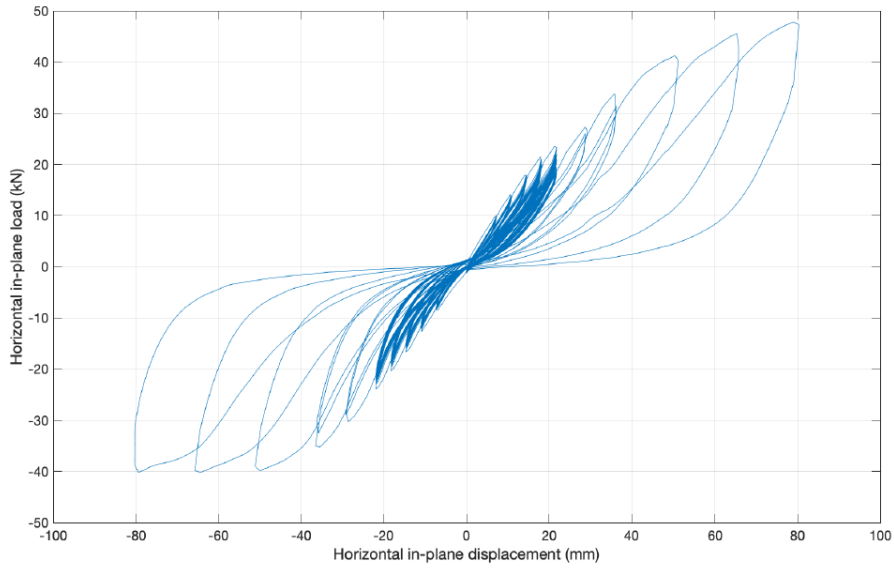


Figure 58: Upper - Displacement curve cyclic loading , Lower - Displacement curve cyclic loading drift (Gaggero, 2021)

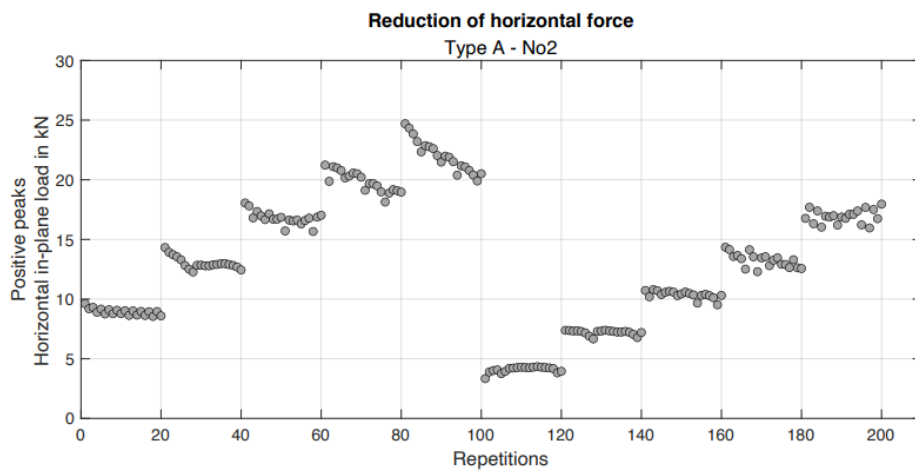


Figure 59: Reduction of the horizontal force for the second structural window for a clay brick masonry wall (Gaggero, 2021)

## Visual inspection

The structural window frame is visually inspected for any structural damages. Therefore, the timber frame is being detached from the glass panel. It is noticeable that no outside cracks are visible on the hardwood, see Figure 60.



*Figure 60: Lower timber bar*

Another noticeable difference is the pinching in the timber bar, see Figure 61. The pinching occurs in both left and right side of the bottom and upper bar, where one side is more deeply pinched than the other. This is due to the experiment, which starts with a one-way cyclic loading and ends with a two-way cyclic loading. Therefore, the left side of the bottom bar is pinched approximately 15 mm deep and has a crack length of 20-25 cm with a gradual transition to no visible damage. The right side is pinched approximately 10 mm deep and has a crack length of 19 cm.

The left side of the upper bar is pinched 10 mm deep with a crack length of 14 cm, although this is difficult to see through the Sikaflex which covers the crack. The right side is pinched 15 mm deep with a crack length of around 30 cm. It is noticeable that both the upper and the lower bar have been damaged similarly. Noticeable is that both the left and right bar of the multiplex are undamaged, just like for the monotonic loading. This is due to the geometry of the structural window frame. The bottom side of the bottom bar and the upper side of the upper bar has shown small cracks however, it is questionable whether these were occurred due to the experiment. Some bars needed to be broken to detach from the glass panel. See Figure 61 for an overview of the damage to the timber bars.



Pinching of the multiplex



No damage to the side bar



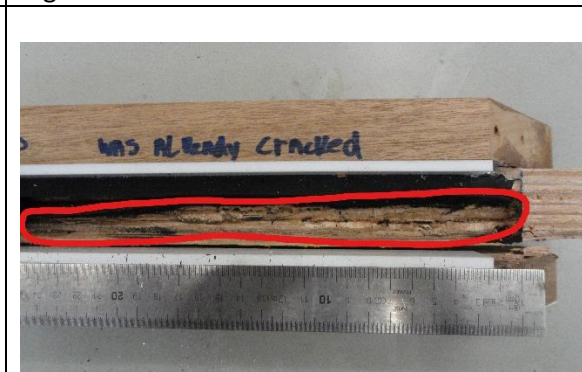
Left side of the lower bar



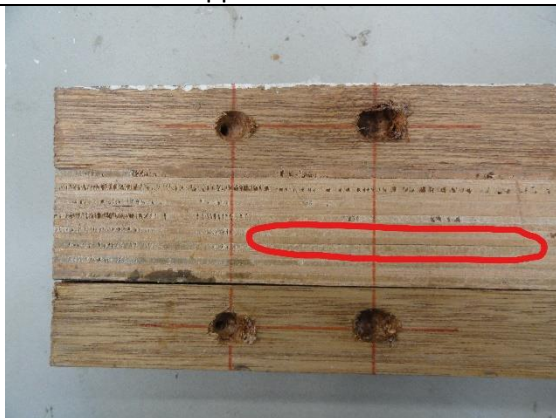
Right side of the lower bar



Left side of the upper bar



Right side of the upper bar



Bottom side of the bottom bar  
Figure 61: Damages of the timber bar



Upper side of the upper bar

The structural and the thin glass panels, remained undamaged during the experiment. These glass panels also remained undamaged for the monotonic loading. One corner was already pre-damaged, but this didn't conclude to any further damages, see Figure 62. The cracks visible in Figure 62 is due to removing of the timber frame and not due to the experiment itself. If it was due to the experiment two opposite edges should be cracked, but this isn't the case.

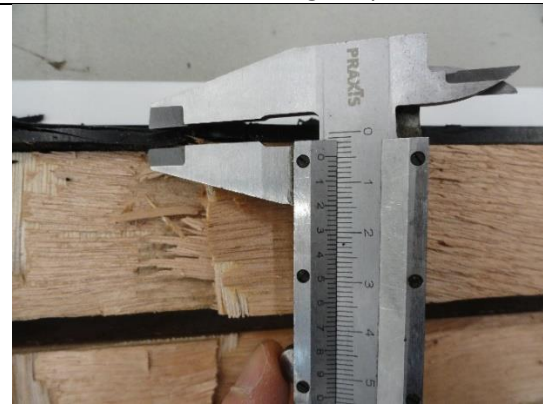
The Sikaflex adhesive was also inspected. Since the left and right bar was relatively undamaged, the thickness of the Sikaflex could be easily measured for the left bar. It was noticeable that one side was thinner than the other side. The left bottom part has a thickness of 6.8 mm thick, the left middle part 5.0 mm and the left upper part 4.8 mm. This means that the Sikaflex is reacting plastically, which is expected behaviour, see Figure 62.

In part 3 all subquestions which are mentioned in paragraph 1.2 for part 3 are answered.



The laminated glass panel after testing

Corner of the laminated glass panel

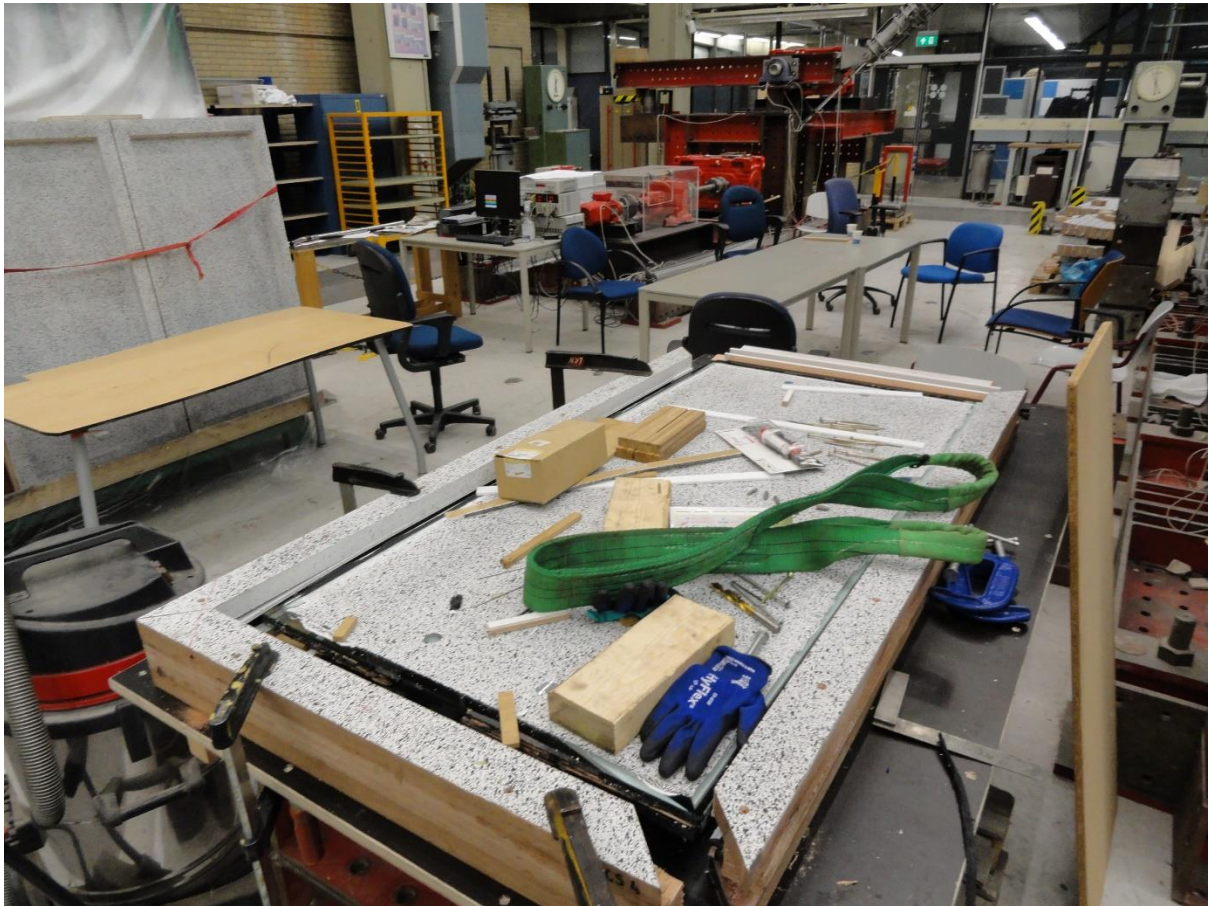


Bottom side of the Sikaflex

Upper side of the Sikaflex

Figure 62: Overview of glass panel and Sikaflex

## PART IV: NUMERICAL STUDY POST-EXPERIMENT



## 5. Numerical model – Structural window frame

Based on the experimental results the numerical model is adjusted. These adjustments will be shown and discussed in this chapter. The numerical model should be made such that it can verify the experimental results.

In the continuation of part IV, the numerical model of the masonry model and the masonry model including the structural window frame is discussed. This is discussed in chapter 6 and 7.

### 5.1 Numerical model after experimental research

#### Initial models

The numerical models don't fully agree with the experimental results. In Chapter 3 several material models are shown and discussed with each their displacement curve. From the experimental results, it is clear that the displacement curve of material model 1 and 2 are the most similar to the experimental results, see Figure 63. However, from the moment of intersection between the glass panel and the timber frame the displacement curves deviate. This intersection also referred to as phase 2, is around 25.8 mm for initial model 1 and 27 mm for initial model 2, see paragraph 3.2. The first two displacement curves of the experiments are not shown, since these values are not in line with the other experiments. After the first experiment screws have been placed which affected the results.

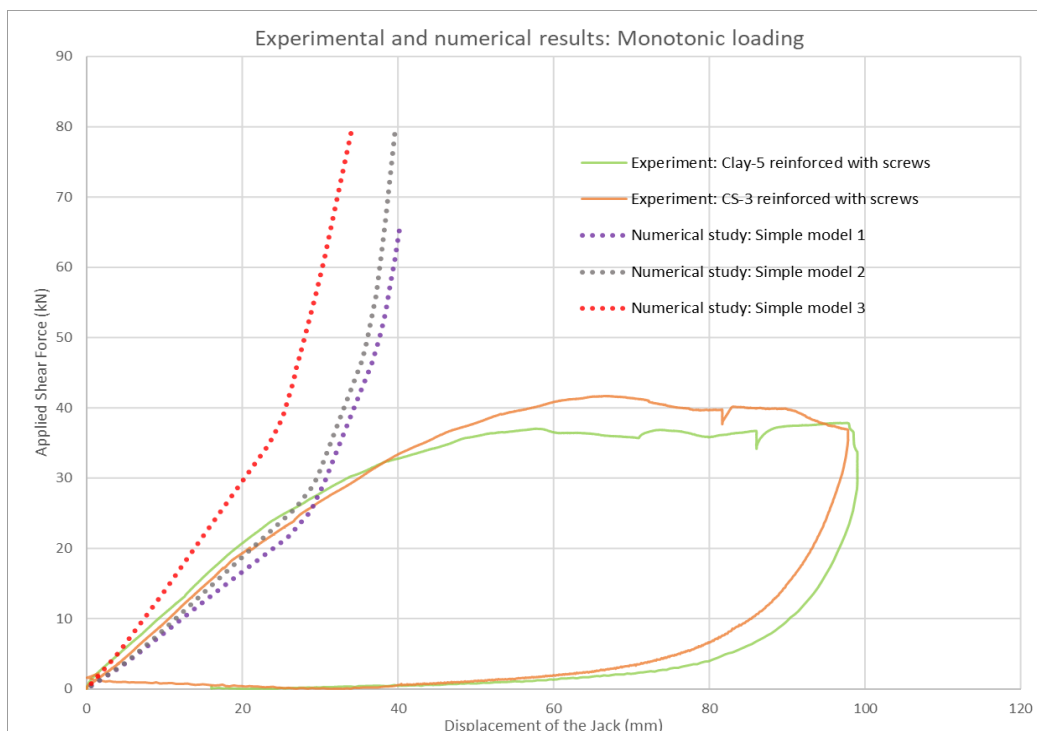


Figure 63: Displacement curve experimental results and computational results

The difference in structural behaviour for the numerical model and the experiment is due to the properties of the multiplex. In the numerical model, the timber frame is modelled as one isotropic material. In the model, the average stiffness and weight are taken as input values. Furthermore, it does not consider that the glass pinches the timber frame and thus the shear force keeps increasing in theory. In reality, the timber frame is a composite structure consisting of multiplex and hardwood. Therefore, the glass will only pinch the multiplex, and the hardwood will only contribute to the overall stiffness of the timber frame. Due to this pinching behaviour, the shear force is increasing less and reaches its maximum peak. This is approximately 40 kN around 60 mm depending on the façade according to Figure 63.

The structural window frame reacts plastically since the deformation could reach 100 mm and possibly even more without any significant strength reduction. The maximum tensile stress is also relatively low inside the glass panel since no cracks occurred in the glass panel.

The maximum compression stress of the multiplex is more significant for the shear force. However, it is also questionable how stiff you prefer the structural façade since a too stiff façade could also be disadvantageous for cracks in a masonry wall.

The numerical model should include pinching behaviour as well. The displacement curve should stabilize after a certain point instead of increasing. This softening behaviour of the timber frame is crucial for the numerical model and should be included. In the numerical model, explained in this paragraph, the properties are adjusted to agree more with the experimental results. These adjustments are not random and are explained in this paragraph.

## New Model - Geometry

The design for the numerical model is the same as for the initial model 2 described in paragraph 3.2 however, the measurements are different and a point load is used instead of a line load. The measurement of the structural façade for the clay brick masonry is taken. A lot of research has been done for clay brick masonry walls which would be helpful for the input values of the numerical model. The glass panel for the numerical model has a dimension of 640 mm x 1370 mm. See Figure 64. For the full dimensions see Appendix E.

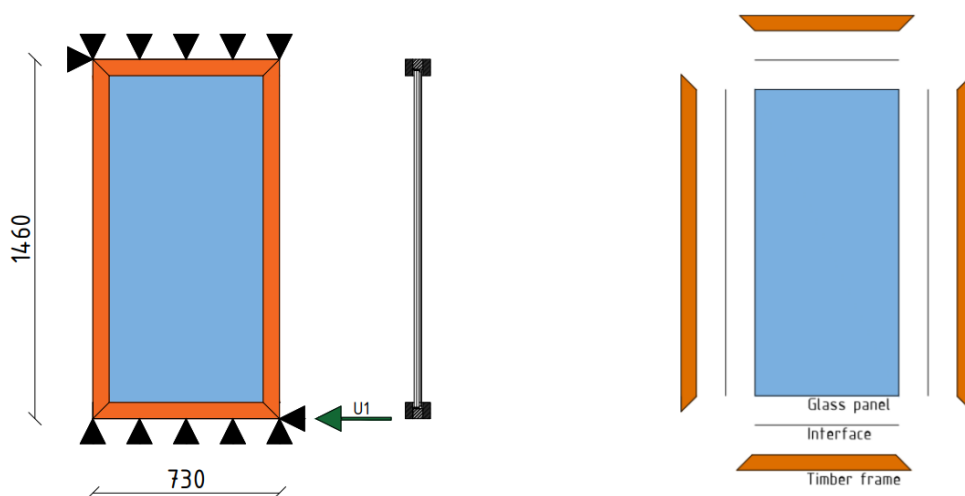


Figure 64: Geometry numerical model

## Discretization

In Table 26 the discretization of the numerical model is shown. The difference of previous models is that for the timber frame a different material model is used, uniaxial nonlinear elasticity. The cross-section is modelled as the actual geometry of the timber frame with the use of the U-shape option.

	Glass pane	Timber frame	PU adhesive
Material model	Linear elastic isotropic	Uniaxial nonlinear elasticity	Nonlinear elasticity
Element class	Regular Plane Stress	Class-III beams 2D	2D line interface
DOFs	$u_x, u_y$	$u_x, u_y, \theta_z$	$u_x, u_y$
Integration scheme	2x2	2-point Gauss	3-point Newton-Cotes
Mesh size (mm)	50	50	50
Thickness (mm)	20	-	5
Cross-section ( $mm^2$ )	-	5500 (U-shape)	-
NLE properties input	-	-	Diagrams

Table 26: Discretization numerical model

To have a more realistic numerical model the adhesive and the timber frame are adjusted. It is relatively complex to model the pinching of the multiplex. It is not possible to model this behaviour inside the timber frame. Therefore, this pinching behaviour is included in the material properties of the adhesive. Both the adhesive and the multiplex have a certain stiffness and thus act like a spring, combined it works as two springs in a serial system. This serial system can be modelled as one spring that has an equivalent spring stiffness. See Figure 65 for a sketch of the serial system and the equivalent spring. However for different displacements, the stiffness varies. To model the behaviour of the timber frame and the adhesive combined, the equivalent stiffness is calculated.

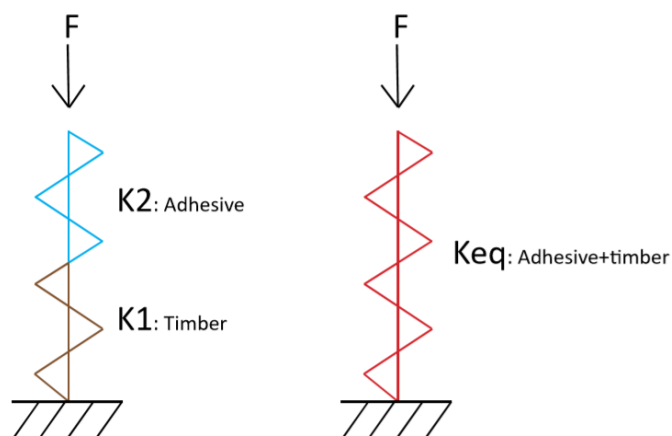


Figure 65: Serial spring system and Equivalent spring

## Stiffness assumptions

In order to calculate the equivalent stiffness, the stiffness of multiplex and the stiffness of the adhesive is calculated. The equivalent stiffness is calculated according to the formulas shown below.

$$k = \frac{F}{u} \rightarrow k_1 = \frac{\sigma_1}{u_1}; k_2 = \frac{\sigma_2}{u_2};$$

$$\frac{1}{k_{eq}} = \frac{1}{k_1} + \frac{1}{k_2}$$

$$\sigma_{eq} = k_{eq} * (u_1 + u_2)$$

The stiffness of a spring is referred to as “k” with unit  $N/mm$ , which is the force divided by the displacement. In DIANA this force is noted as the force per area with unit  $N/mm^2$ , the normal traction. Therefore, the unit for the stiffness of the spring changes from  $N/mm$  to  $N/mm^3$ , but the ratio stays the same. For simplicity reasons the stiffness k in the calculations has the unit  $N/mm^3$ . The normal stiffness of the adhesive and the multiplex are calculated based on the experimental test results of the compression behaviour. These are described in paragraph 3.1 and paragraph 4.2.

In a serial spring system, the same force goes through both springs, but the displacements are different. Therefore, the equivalent stiffness will be calculated on crucial points where the forces of the springs are the same. See Table 27 for the non-linear interface properties for the normal direction, the shear direction stays similar to the properties described in paragraph 3.1. In appendix C.1 the calculation of the equivalent stiffness and the adjusted properties of the adhesive are described and further explained. For tension forces, the same stiffness properties are valid as for the adhesive. After the total displacement of -6.67 mm the stiffness of the multiplex decreases, while the stiffness of the adhesive increases. The equivalent compression force remains the same while the displacement increases. The material properties are shown in Table 28. The Young Modulus for the timber frame here is assumed 12,500 MPa. This is the value based on the compression test of the Multiplex and is the correct value. The Young Modulus of the timber frame assumed in chapter three was based on the non-destructive resonance test.

Normal relative displacement (mm)	Normal traction ( $N/mm^2$ )
-25	-15
-10.25	-15
-6.66	-21.8
-5.5	-18
-0.77	-0.9
0	0
0.75	0.9
2.5	1
25	0.001

Table 27: Adjusted relative displacement-traction diagram

Parameter	Symbol	Unit	Timber frame
Young's Modulus	E	MPa	12,500
Mass density	$\rho$	kg/m <sup>3</sup>	650

Table 28: Material properties timber frame

Strain	Stress (N/mm <sup>2</sup> )
-1	-15
-0.15	-15
-0.1	-15
-0.04	-21.8
-0.015	-20
0	0
0.015	20
0.04	21.8
0.15	15
0.075	20
1	15

Table 29: Stress strain relation for the timber frame

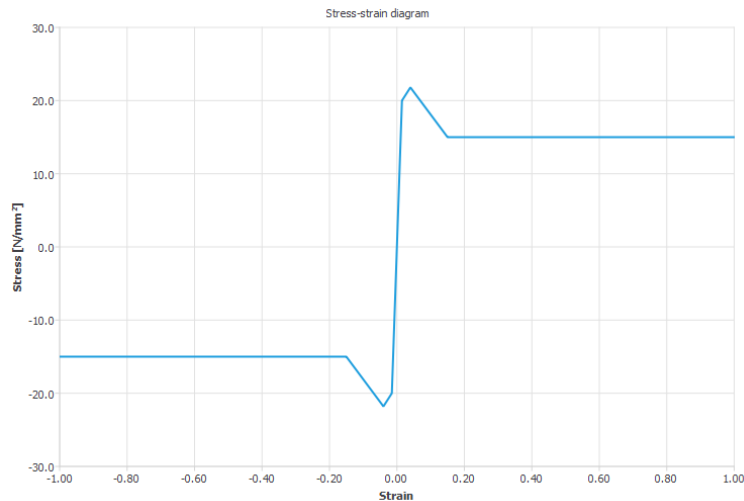


Figure 66: Stress strain relation for the timber frame

The timber frame is modelled with plastic material properties, instead of linear material properties. The material properties and stress-strain diagram of the timber frame are shown in Table 29 and Figure 66. The stiffness of the timber frame is based on the average stiffness of the timber frame calculated in paragraph 4.2.2. The stress-strain diagram is based on the compression test of the multiplex element. This is because the glass panel will only have contact with the multiplex, the outer meranti hardwood elements mainly contribute to the overall stiffness. The compression test is discussed in paragraph 4.2.2. These values are the input material properties of the timber frame for the computational model. For simplification reasons, the same properties are assumed for tension as for compression. This is because of the material properties, for plywood the strength classes have the same values for compression as for tension forces, see Appendix B.2. If linear properties were assumed for the timber frame, the overall shear force capacity and stresses inside the timber frame would be significantly higher.

## Results

The numerical model has a similar structural behaviour as the experimental results, see the blue dotted line in Figure 67. The orange line represents the calcium silicate window and the green line represent the window frame for the solid clay wall. The difference between the green and the yellow line is due to the thickness of the adhesive, and not primarily due to the geometry of the window frame. From post-analysis it concluded that a thicker adhesive is used for the calcium silicate window frame. A thickness of 6,7 mm was measured while for the green line and 5,9 mm for the orange line. In the numerical model, an adhesive thickness of 5 mm is assumed.

Until a displacement of approximately 40 mm the blue dotted line follows the other two lines. After this displacement, the shear force is lower by a significantly small amount. This small difference is

due to the calculated equivalent stiffness of the interface. The traction is increasing in the beginning phase of the displacement. For a displacement of 37 mm, the relative normal displacement of the adhesive is exceeding -6.66 mm, which means that normal traction is decreasing from  $21.8 \text{ N/mm}^2$  to  $15 \text{ N/mm}^2$ . For a displacement of 52 mm, the relative normal displacement of the interface is exceeding 10.25 mm, which means that the normal traction is now continually  $15 \text{ N/mm}^2$ . From the graph, it is clear to see that the curve of the numerical model is decreasing between these points and is rather linear after a displacement of 52 mm. See Appendix C.1 for more detailed information. The numerical model is sensitive to the input values of the interface. The equivalent stiffness of the interface and the multiplex has a high influence on the structural behaviour of the numerical model. This explains that a small difference is likely to happen. Furthermore, the thickness of the interface in the numerical model is less than for the test, this change influences the results as well.

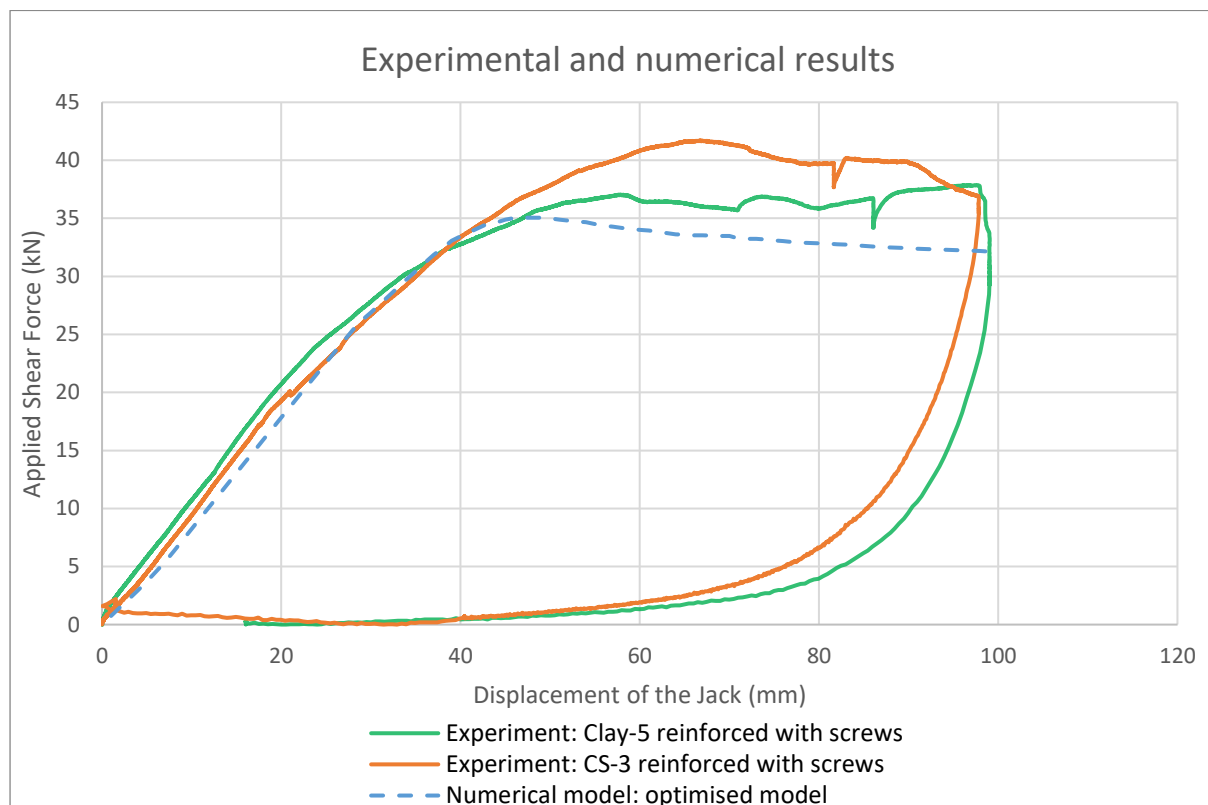


Figure 67: Displacement curve experimental and numerical results

Unfortunately, the unloading behaviour is not included in the numerical model. This behaviour can not be included with non-linear interface elements. Other material models were also not suited to model the complex behaviour of the structural window frame, see paragraph 3.5.

In Appendix C.2 an overview is given of the stresses inside the glass versus the relative interface displacement. What is noticeable is that the stresses inside the glass remained significantly low and did not exceed the 45 MPa for the entire displacement. This seems logical since the glass did not show any cracks whatsoever during the experiment as well. The relative interface exceeded 2.5 mm and thus started tearing at around a displacement of 14 mm. Around a displacement of 31 mm, the glass and timber frame started to have contact with each other. This meant that the relative displacement started exceeding 5.5 mm. This means that the adhesive is 5 mm compressed and the timber is 0.5 mm compressed at the same time. Around a displacement of 100 mm the maximum

tensile stress inside the glass is 5.2 MPa, which is significantly low. The maximum interface displacement is 22 mm.

A maximum shear force capacity is reached around a displacement of 45 mm and has a shear force of around 35 kN. The numerical model behaves similarly to the experimental results however, the unloading behaviour is not modelled due to complications with DIANA. Furthermore, it is complicated to apply the correct thickness of the adhesive in practice. Since the thickness of the adhesive has a large influence on the structural behaviour, this leads to a certain tolerance of the obtained results. As previously mentioned a thicker adhesive is used for the calcium silicate window frame. This resulted in different behaviour of the structural window frames. A thickness of 6,7 mm was measured while for the calcium silicate version and 5,9 mm for clay brick version while the model had only a thickness of 5 mm.

## GOM

The relative interface displacements from GOM software which are made due to the DIC technique are compared with the results of the numerical model. The relative interface displacements results for the vertical normal direction in the corners for the numerical model and the GOM software are relatively similar. This means that the spring stiffness in the normal direction is modelled similarly to the behaviour of the window frame. However, the relative displacement in the horizontal shear direction showed more variation between the numerical model and the GOM software. The numerical model behaves stiffer than the results of the GOM software in the horizontal direction. However, around 45 mm the horizontal relative interface displacement stabilizes due to the stabilization of the shear force around this displacement. Anyhow the horizontal relative interface displacement is similar around the final displacement of 100 mm. See Appendix C.3 and Figure 68.

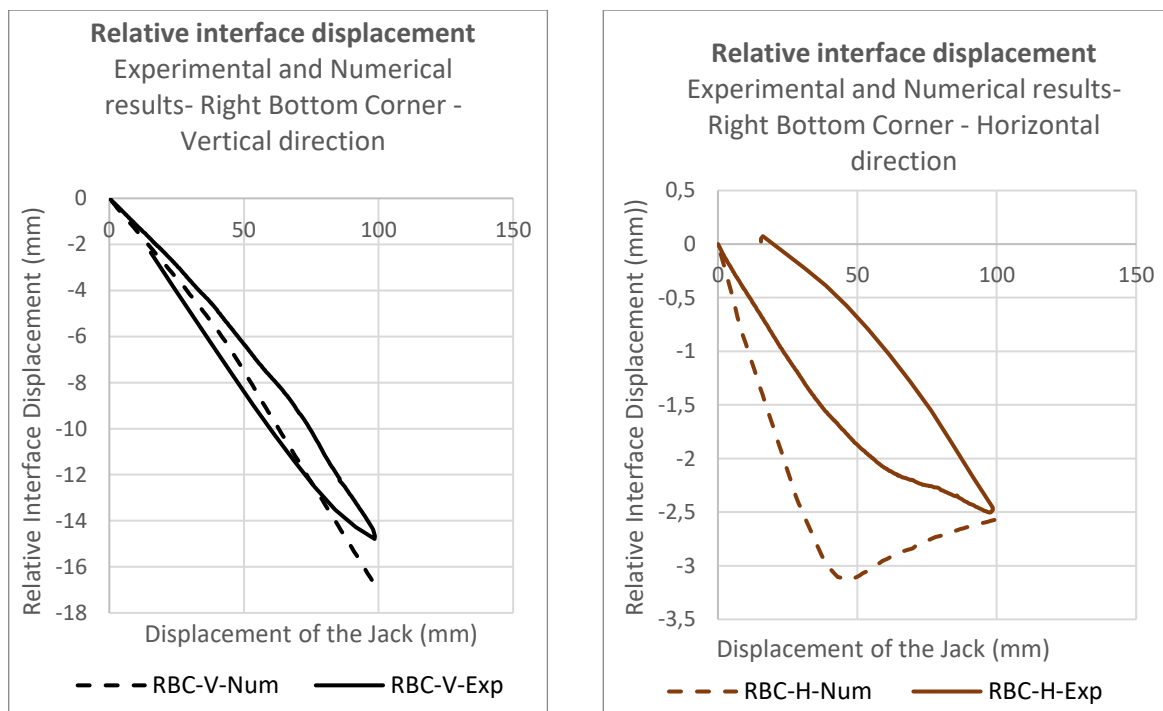


Figure 68: Relative interface displacement in the right bottom corner for the vertical and horizontal direction

## Conclusion

A maximum shear force capacity is reached around a displacement of 45 mm and has a shear force of around 35 kN. The numerical model behaves similarly to the experimental results however, the unloading behaviour is not modelled due to complications with DIANA. Furthermore, it is complicated to apply the correct thickness of the adhesive in practice. Since the thickness of the adhesive has a large influence on the structural behaviour, this leads to a certain tolerance of the obtained results.

In chapter 7 the masonry wall model including the adjusted structural window frame is discussed. In chapter 6 the masonry wall model excluding the window frame is analysed.

## 6. Numerical masonry model

### 6.1 Validation numerical masonry model

A 2D unreinforced masonry wall model is validated with experimental results reported by (Korswagen et al., 2019). In this research of the Delft University of Technology, the cracking mechanism is studied for URM walls subjected to in-plane loading. The aim is to improve knowledge of the underlying physics of crack initiation and propagation in unreinforced masonry typical in the Netherlands. This chapter compared the results of the experimental research with the numerical model made in DIANA FEA.

#### Model Geometry

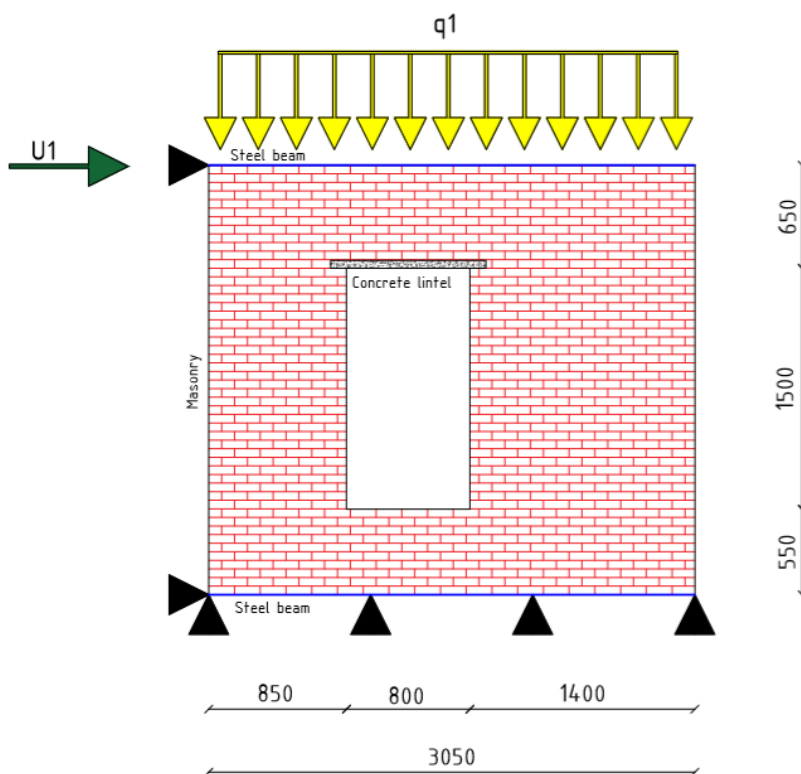


Figure 69: Geometry unreinforced clay brick masonry wall model

In Figure 69 the geometry of the clay brick masonry wall is shown. The masonry wall has a thickness of 100 mm. The masonry is supported by a steel beam on the top and on the bottom, which is an HEB 600 on the top and a HEB300 on the bottom. The wall is being loaded by a precompression of 12 N/mm at the top and a displacement-controlled pushover load of 4 mm at the top left support. The actual geometry of the masonry wall is 3070 mm x 2710 mm, to simplify the mesh the geometry is modelled as a masonry wall of 3050 mm x 2700 mm. The actual geometry of the hole is 780 mm x 1520 mm, this dimension is also simplified to 800 mm x 1500 mm. This is due to the mesh size of 50 mm. These changes do not result in a significant change in the results however, it does create a more accurate mesh. By doing so, the results are more reliable and errors of the calculation are prevented. Furthermore, the numerical model calculated in (Korswagen et al., 2019) made the same assumptions.

## Discretization

In Table 30 an overview of the discretization is shown for the numerical masonry model. Plane stress elements are adopted since out of plane behaviour isn't expected to be significant. The masonry is modelled with nonlinear material properties since failure is expected here. A mesh is used of 50 mm by 50 mm with quadrilateral elements. A mesh size of 50x50 seems reasonable for a masonry wall, it is a standard mesh size that has a good balance between accuracy and calculation time.

	Masonry walls	Concrete lintel	Steel beams
Material model	Engineering Masonry model	Linear elastic isotropic	Linear elastic isotropic
Element class	Plane stress (CQ16M)	Plane stress (CQ16M)	Class-III Beams 2D (CL9BE)
DOFs	$u_x, u_y$	$u_x, u_y$	$u_x, u_y, \theta_z$
Integration scheme	2x2	2x2	1-point Gauss
Mesh size (mm)	50	50	50
Thickness (mm)	100	100	-
Cross-section ( $mm^2$ )	-	-	Top beam: HEB600 Bottom beam: HEB300

Table 30: Discretization into elements for the numerical masonry model

## Material Properties

In Table 31 an overview of the material properties is shown. The concrete and the steel frame are modelled with linear elastic properties.

	Symbol	Unit	Concrete lintel	Steel frame
Young's Modulus	E	MPa	31000	210,000
Poisson's ratio	$\nu$	-	0.2	0.2
Mass density	$\rho$	$kg/m^3$	2450	7800

Table 31: Material properties

An Engineering Masonry Model (EMM) is chosen for the elaboration of the macro model. A macro-modelling approach is an approach where the masonry is modelled as one orthotropic composite continuum, without an explicit definition of the interfaces. This is different from the micro-modelling, where mortar and bricks are connected with interfaces. This approach however is more complex and takes more computational time. The macro-modelling is considered to be the most balanced approach in terms of accuracy and efficiency within the scope of the thesis.

This EEM accounts for the orthotropy from bed and head joints, shear friction, tensile softening, cohesion softening and compression hardening and softening. See Table 32 for the material properties of the masonry wall. These values are based on values used in (Korswagen et al., 2019).

	Parameter	Symbol	Unit	Value
Elasticity	Young's modulus	$E_x$	MPa	2157
		$E_y$	MPa	3087
	Shear modulus	$G_{xy}$	MPa	1354
	Density	$p$	$kg/m^3$	1708
Cracking	Tensile strength	$f_{ty}$	MPa	0.09)
	Tensile fracture energy	$G_{ft}$	N/mm	0.007527
	Diagonal crack orientation	$a$	rad	0.5
Crushing	Compressive strength	$f_c$	MPa	11.35
	Compressive fracture energy	$G_c$	N/mm	26.05
Sliding	Cohesion	$c$	MPa	0.14
	Fracture energy in shear	$G_{fs}$	N/mm	-
	Friction angle	$\varphi$	rad	0.669

Table 32: Material properties masonry wall

## Analysis Method

See Table 33 for an overview of the analysis method. For the analysis, the self-weight + precompression is applied and a pushover load is applied monotonically with 250 load steps. This is done to save computation time and also be accurate.

Self-weight	Load	Load name	Self-weight + precompression
		Load	12 N/mm
		Load steps	1
	Iterative procedure	Procedure	Regular Newton-Raphson
		Max. number of iterations	100
		Line search	Yes
	Convergence criterium	Norm	Force or Displacement
		Tolerance	0.01
		No convergence	Terminate
	Pushover	Load	Load name
Load			4 mm
Load steps			0.004(250)
Iterative procedure		Procedure	Regular Newton-Raphson
		Max. number of iterations	50
		Line search	Yes
Convergence criterium		Norm	Force or Displacement
		Tolerance	0.01
		No convergence	Continue

Table 33: Analysis method masonry wall

## Results

In Figure 70 the displacement curve of the masonry wall is shown. In red the numerical model and in grey the experimental results are shown. It can be seen that the initial stiffness and the force capacity are close to the experimental results shown in (Korswagen et al., 2019). A difference is that the experiments were done for a cyclic load, but the numerical model is done for a monotonic load to save computation time.

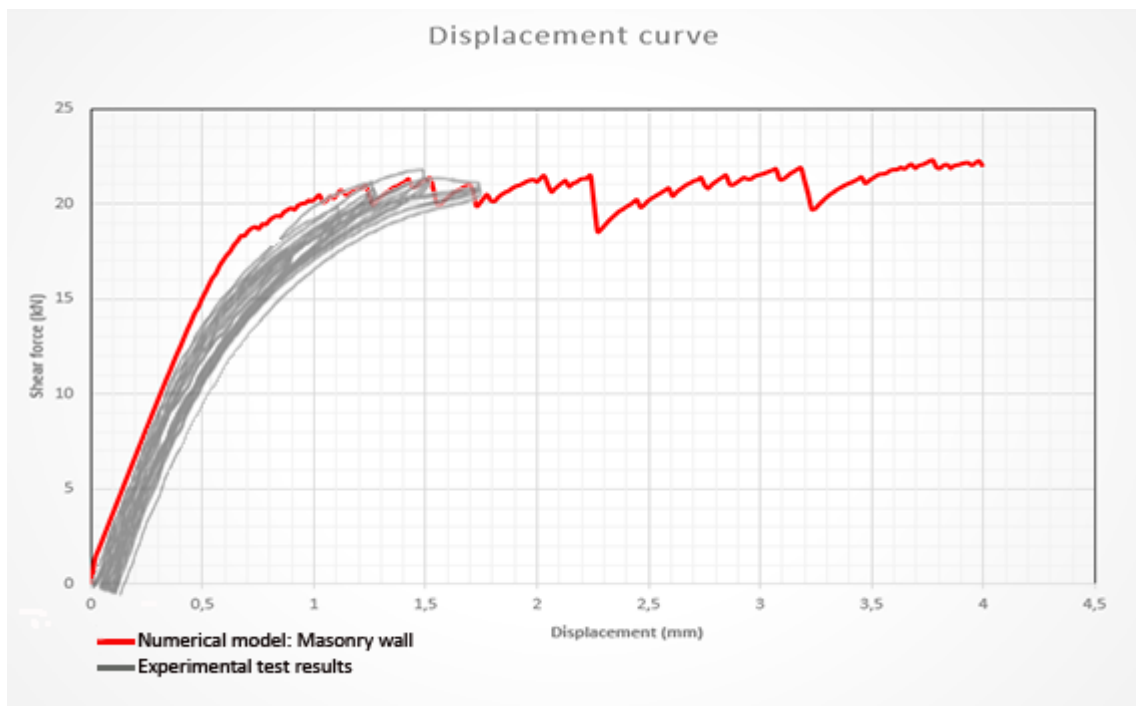
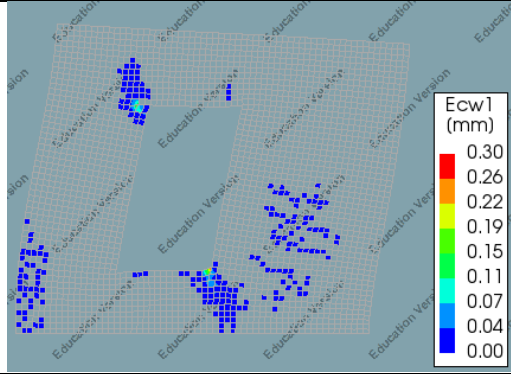


Figure 70: Displacement curve of the numerical model of the masonry wall and the experimental results.

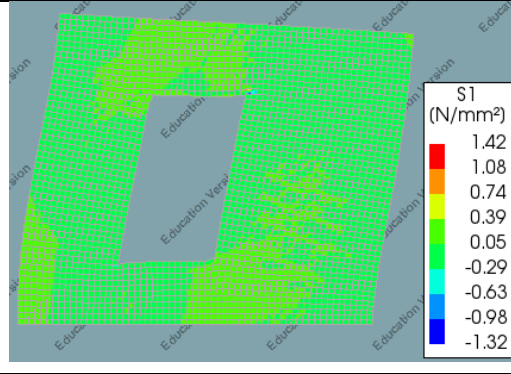
## Crack patterns

Table 34 gives an overview of the results for the numerical model. The crack-width and the total stresses are shown next to each other on specific points. These are the end of the linear elastic stage at 0.69 mm, the end of the experiment at 1.55 mm and the end of the numerical analysis at 4 mm. These values are based on the numerical model and the experimental results. The linear elastic stage ends at the first crack of the masonry.

**Crack-widths**

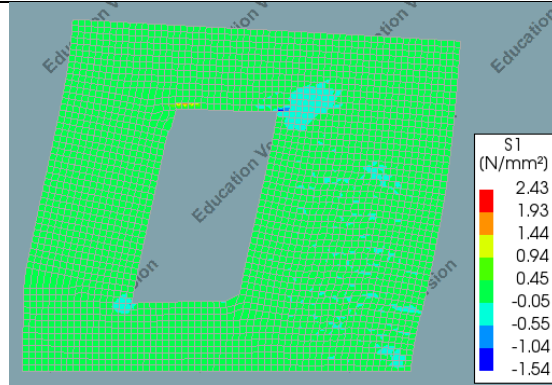
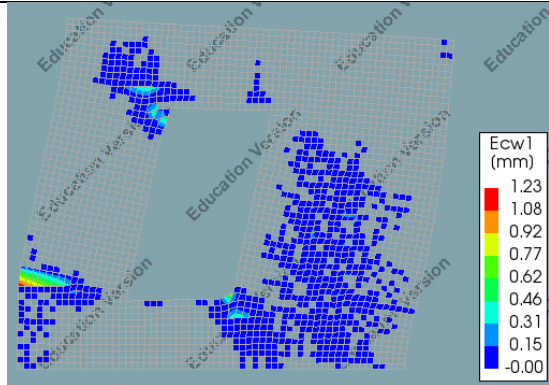


**Cauchy Total stresses**



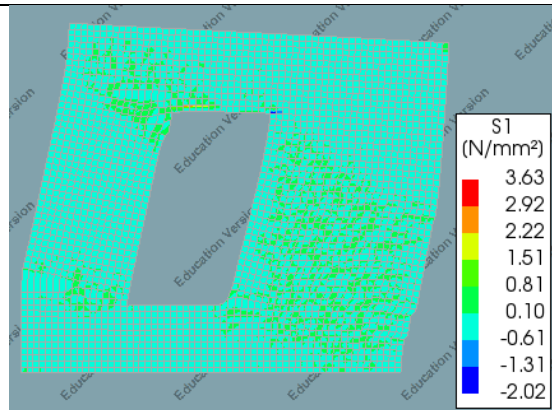
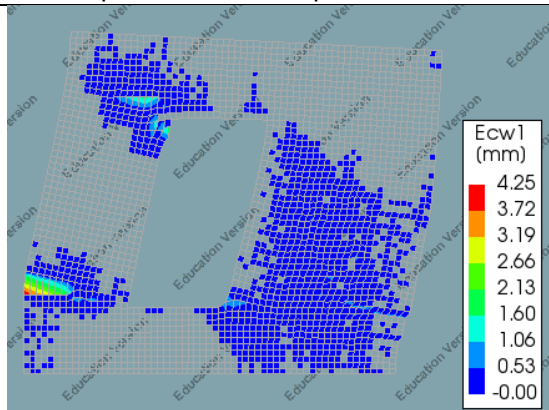
*End of the Linear elastic stage*

Loadstep 44: 0.69 mm displacement



*End of the experiment*

Loadstep 98: 1.55 mm displacement



*End of the numerical model*

Loadstep 250: 4 mm displacement

Table 34: Overview of the crack-width and stresses

The first cracks occur at the edges of the opening. From the end of the experiment, it is seen that the biggest crack occurs on the left side of the masonry. The highest stresses occur also at the corners of the opening. Peak stresses firstly occur at the right top and after also on the left top. The location of the peak stresses remains at similar locations but increase gradually. In Figure 71 the crack patterns of the experimental research and the numerical model are shown. These cracks occurred at the end of the experiment, which is approximately 1.55 mm. The locations of the cracks are at similar locations however, the width of the cracks is different. Cracking seems to occur near the edges of the window opening and the left part of the wall. In the experiments, different crack patterns occurred. These differences could be minimized by using a micro modelling approach, however this is outside the scope of this thesis.

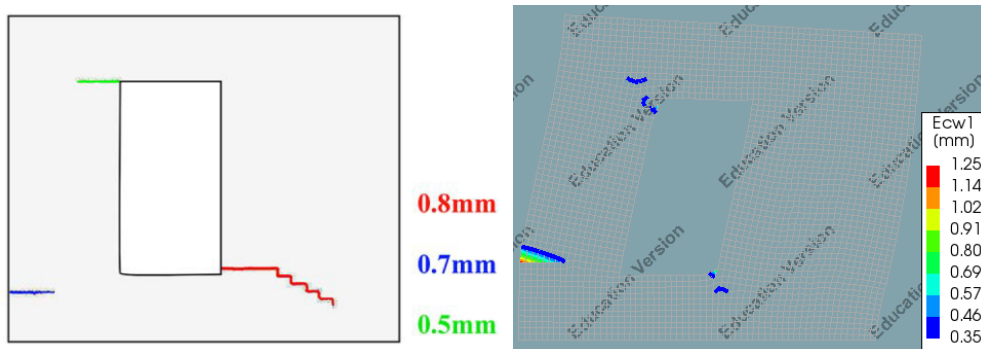
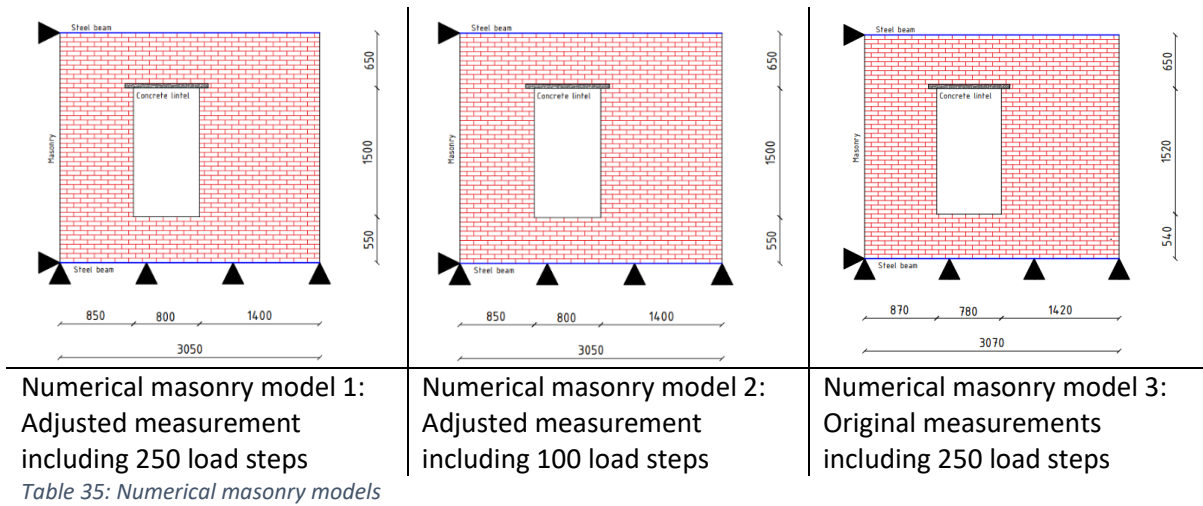


Figure 71: Left: Crack pattern of the experiment, Right: cracks of the numerical result

## Different assumptions

For the numerical model, certain assumptions have been made. The geometry of the wall and the hole in the wall is adjusted to the mesh size. Therefore, the numerical model has fewer problems solving it and will have more realistic values. The geometry of the calculated masonry model is 3050x2700 mm with a hole of 800x1500 mm, referred to as numerical model 1 in Table 35. Two different load steps are used to calculate the model, 250 load steps and 100 load steps. The model where 100 load steps are used is referred to as numerical model 2. The original measurement of the masonry wall is 3070x2710 mm with a hole of 780x1510 mm, referred to as numerical masonry model 3. These minor adjustments shouldn't affect the outcome significantly.



In Figure 72 the displacement curves of the numerical models are compared. The red line represents masonry model 1, the blue line represents masonry model 2 and the grey line represents masonry model 3.

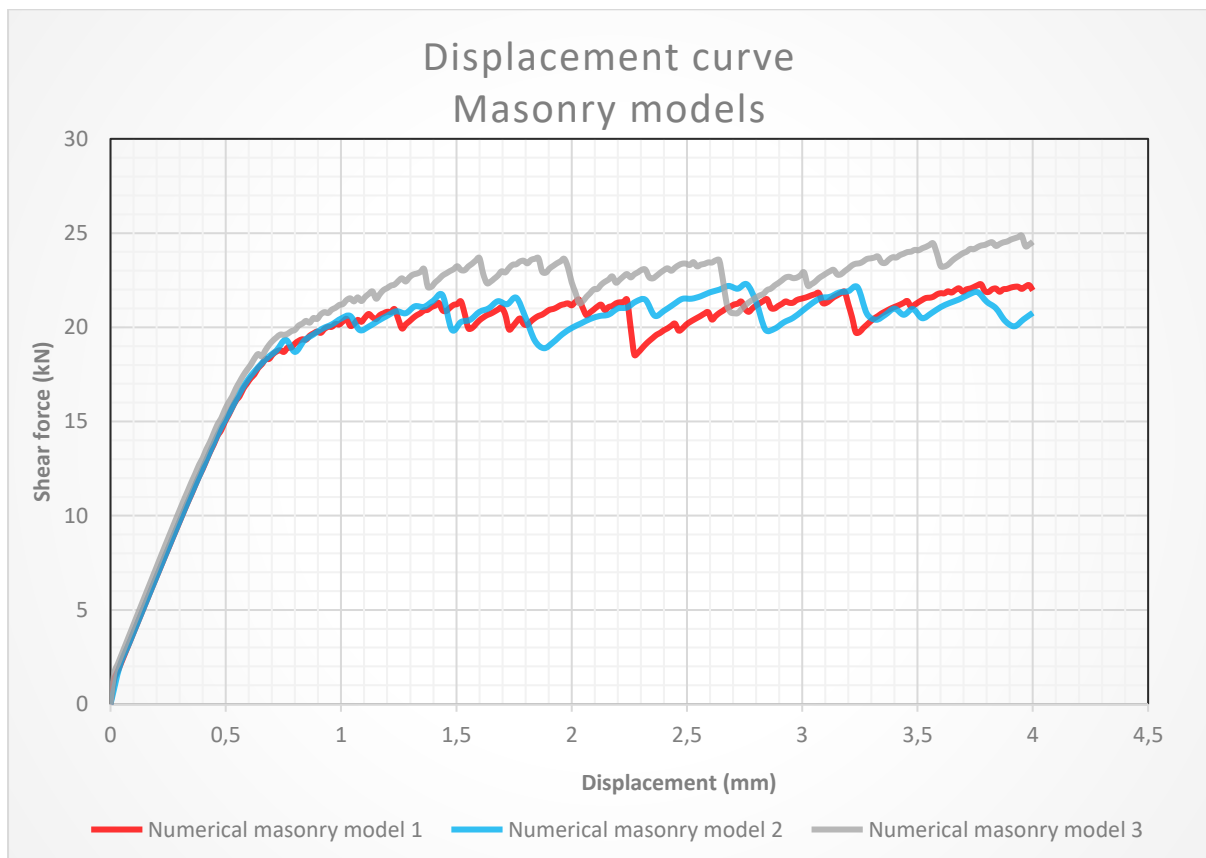


Figure 72: Displacement curve of different assumptions for the numerical masonry wall

In the initial phase, the numerical models behave similarly. It is noticeable that Numerical model 1 and 2 behave on average similar but have different peaks for the shear force. This could be due to the use of more load steps. The advantage of numerical model 1 of model 2 is that it uses less calculation time. However, the crack width and stresses are relatively similar, see Appendix D.1.

Numerical model 3 has a higher shear force on average after the initial phase. This could be explained due to the different geometry. But it is questionable that a small difference in geometry has a significant influence on the shear force. The difference could better be explained that the mesh is probably less stable than the mesh of masonry model 1 and 2. In Appendix D.1 it is shown that the crack width of all models is similar, although the stresses of model 3 for high displacements differ from the other models. Furthermore, the experimental results are closer to numerical model 1 and 2.

## Conclusion

The experimental results are closest to numerical model 1 and 2. Therefore in the next chapter, the principle of the numerical masonry model 2 will be used. The model is accurate and the calculation time is not significantly high. The geometry of the numerical masonry model that will be used for the structural façade will be refined into parts of 50 mm and 100 load steps for the optimal mesh size and computation efficiency

The numerical model of the masonry wall excluding and including the structural window frame is discussed and compared in the next chapter.

## 6.2 Numerical masonry model

The numerical masonry model is validated on behave of experimentation. Since the measurements of the masonry wall which is going to be tested are different, the model needs to be adjusted. All the material properties, discretization and analysis are the same as in the previous paragraph. As mentioned in paragraph 7.1, the basic principles of numerical masonry model 2 are used. Therefore, the geometry is based on a mesh of 50 mm and for the analysis 100 load steps are used. This option has accurate results and saves computation time.

However, there are still some alternatives to reconsider. The structural glass façade should be adjusted to a mesh size of 50 mm to fit the hole in the masonry wall. However, this change should not influence the results significantly. Therefore, the displacement curve of the original measurements and the adjusted measurements should be analysed.

Furthermore, the timber frame of the structural façade is modelled with beam elements. Therefore, the geometry of the modelled structural façade is smaller than the actual hole in the masonry wall. The influence of making the hole of the masonry wall smaller is analysed as well.

### Geometry structural window frame

To begin with, the influence of the geometry on the structural façade will be analysed. The two following geometries will be assumed for the glass panel: 640x1370 mm (original measurement) & 650x1350 mm (adjusted measurement), see Figure 73. The material properties, discretization and analysis are according to Paragraph 5.1.

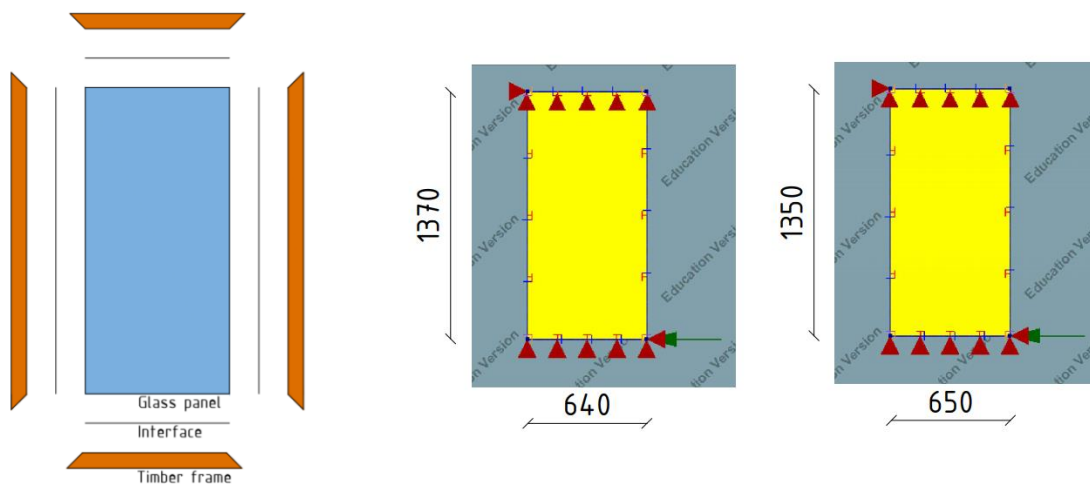


Figure 73: Geometry of the structural façade

### Results window frame

In Figure 74 the displacement curves are shown from the structural façade of the original and the adjusted geometry. The adjusted geometry has a higher shear force however, this difference is insignificant. The maximum difference is 1.5 kN for a shear force of 35 kN, which is lower than 5%. Therefore, the change in geometry is insignificant.

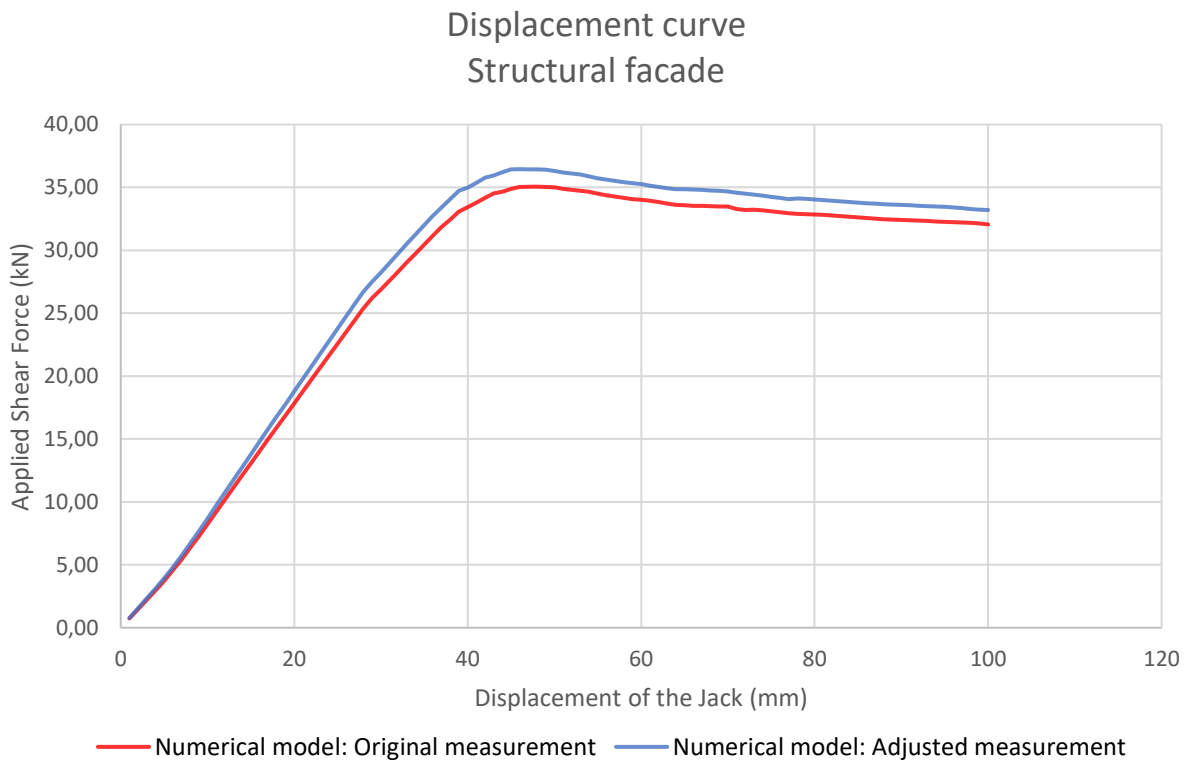


Figure 74: Displacement curve of the structural façade

## Geometry masonry wall

The hole of the masonry wall is different from the geometry of the structural façade, this is because the timber frame is modelled as beam elements. Therefore, it should be analysed if this change in geometry is significant for the results. See Figure 75 for the two different geometries of the numerical masonry models.

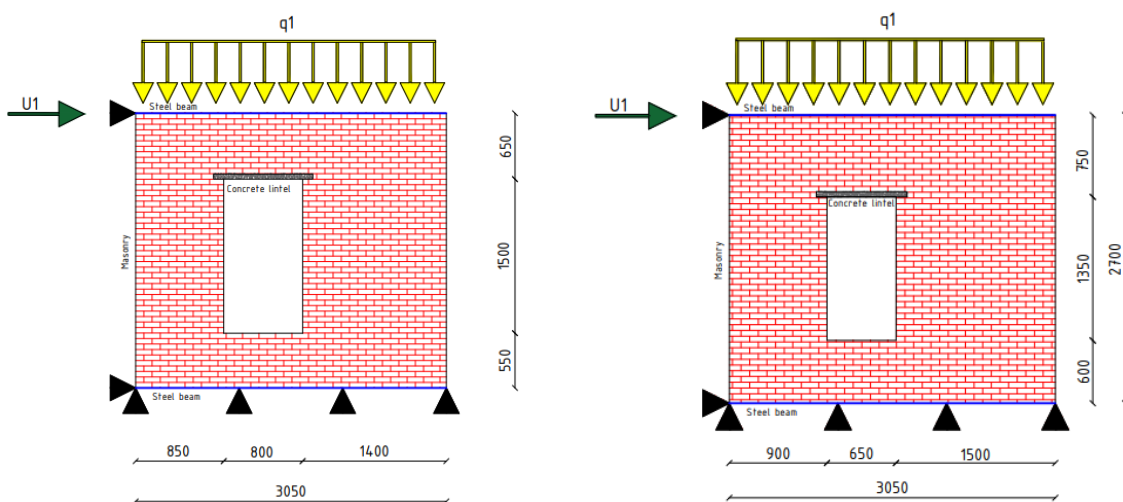


Figure 75: Left: Masonry wall original measurement, Right: masonry wall smaller window size

## Results masonry wall

In Figure 76 the displacement curves of both numerical models are shown. From the graph, it can be seen that the masonry wall with the smaller hole size behaves a bit stiffer. The numerical model of the smaller hole size behaves stiffer in the beginning however, it has some large peaks where the stiffness decreases below the shear force of the numerical masonry model 2.

Appendix D.2 the crack width and the stresses are also compared for the two models. The masonry model with a smaller hole size tends to have larger peak stresses and crack width for larger deformations. However, the difference is rather small.

Furthermore, choosing the masonry model with the bigger opening would lead to changing the model of the structural façade. This would have led to a significant increase in the stiffness of the current model, which isn't realistic. It could also lead to the use of a different material model for the timber frame. A different material model for the timber frame has been researched however, the results were not coherent with the experimental results.



Figure 76: Displacement curve masonry walls

## Conclusion

For the structural window frame, both models behave similarly. Although the adjusted measurement model has a higher shear force. The masonry model with the smaller hole sizes tends to act a little bit stronger as well. However, this slightly positive effect is insignificant and taken into consideration for the numerical model. Furthermore, it is more practical to use the adjusted structural window frame and masonry model with a smaller hole size because the same numerical model for the window frame can be used.

Thus there is chosen to use the adjusted model for the window frame and the masonry model with a smaller opening. This is the most practical model to model the strengthened masonry model in chapter 7.

## 7. Strengthened numerical masonry model

### 7.1 Numerical model

In this paragraph, the numerical model of the masonry wall including the structural window frame is discussed. The numerical model is analysed and compared with the numerical model of the masonry wall excluding the structural façade to analyse the differences.

The aim is to improve knowledge of the underlying physics of crack initiation and propagation in unreinforced masonry and the addition of a structural window frame to the masonry wall.

### Model Geometry

In Figure 77 the geometry of the clay brick masonry wall, the blow-up of the masonry wall and the numerical model of the masonry wall are shown.

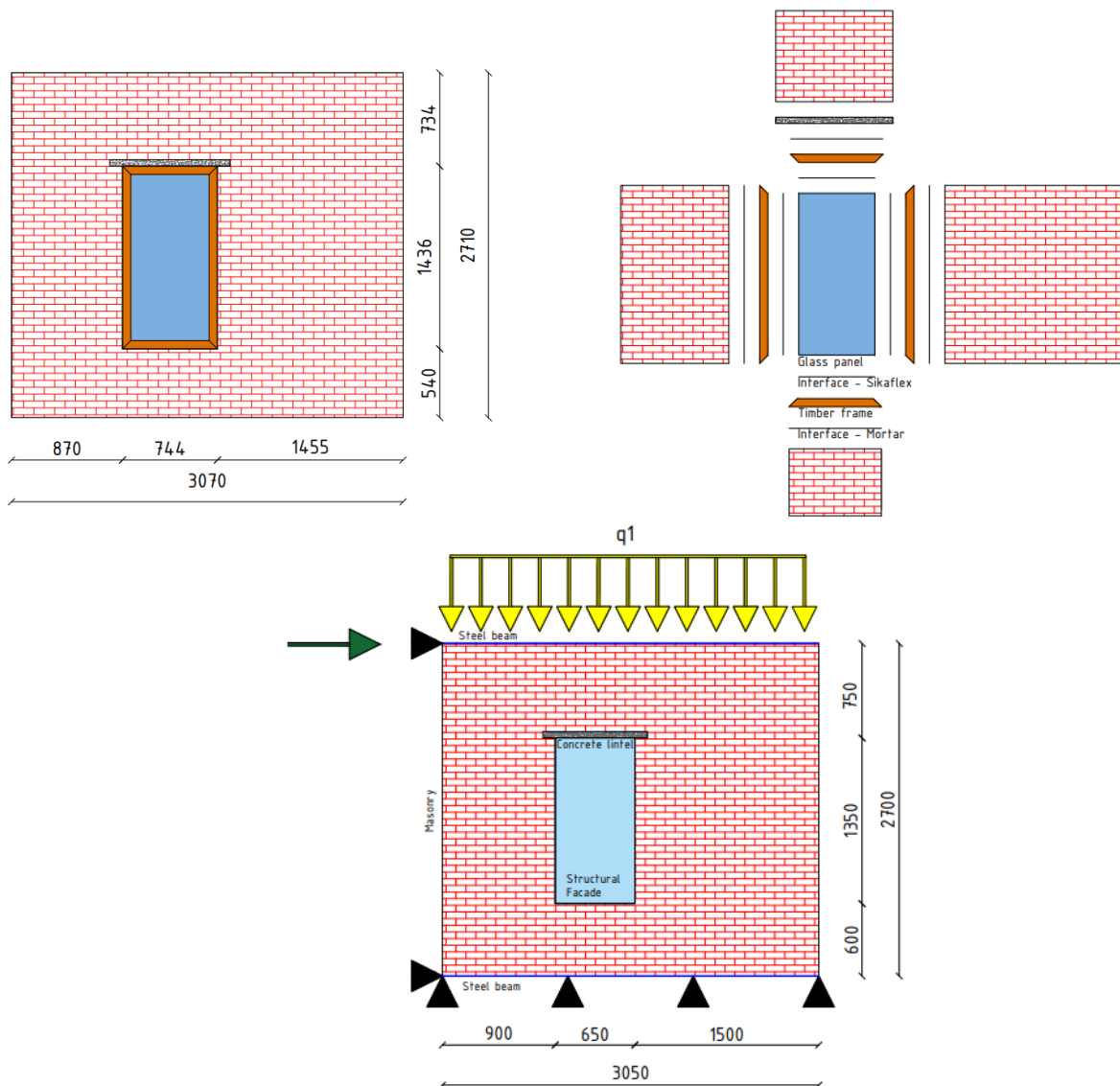


Figure 77: Left top: Geometry of the clay brick masonry wall, right top: blow-up of the masonry wall including the façade, bottom: Geometry of the numerical masonry wall including the façade.

## Discretization

The discretization for the structural façade is the same as in paragraph 5.1 and it is shown in Table 36 as well. The discretization for the masonry wall is the same as in paragraph 6.1 and it is shown in Table 37 as well.

	Glass pane	Timber frame	PU adhesive
Material model	Linear elastic isotropic	Uniaxial nonlinear elasticity	Nonlinear elasticity
Element class	Regular Plane Stress	Class-III beams 2D	2D line interface
DOFs	$u_x, u_y$	$u_x, u_y, \theta_z$	$u_x, u_y$
Integration scheme	2x2	2-point Gauss	3-point Newton-Cotes
Mesh size (mm)	50	50	50
Thickness (mm)	20	-	5
Cross-section ( $mm^2$ )	-	5500 (U-shape)	-
NLE properties input	-	-	Diagrams

Table 36: Discretization into elements for the numerical model of the structural window frame

	Masonry walls	Concrete lintel	Steel beams
Material model	Engineering Masonry model	Linear elastic isotropic	Linear elastic isotropic
Element class	Plane stress (CQ16M)	Plane stress (CQ16M)	Class-III Beams 2D (CL9BE)
DOFs	$u_x, u_y$	$u_x, u_y$	$u_x, u_y, \theta_z$
Integration scheme	2x2	2x2	1-point Gauss
Mesh size (mm)	50	50	50
Thickness (mm)	100	100	-
Cross-section ( $mm^2$ )	-	-	Top beam: HEB600 Bottom beam: HEB300

Table 37: Discretization into elements for the numerical model of the strengthened masonry wall

## Material Properties

The material properties for the structural façade are the same as in paragraph 5.1. The material properties for the structural façade, concrete lintel and steel frame are shown in Table 38. The discretization for the masonry wall is the same as in paragraphs 5.1 and 6.1 and it is shown in Table 39 as well.

	Symbol	Unit	Glass pane	Timber frame	Concrete lintel	Steel frame
Young's Modulus	E	MPa	70,000	15,000	31000	210,000
Poisson's ratio	$\nu$	-	0.23	0.4	0.2	0.2
Mass density	$\rho$	$kg/m^3$	2500	565	2450	7800

Table 38: Material properties for the structural façade, concrete lintel and steel frame

	Parameter	Symbol	Unit	Value
Elasticity	Young's modulus	$E_x$	MPa	2200 (2157)
		$E_y$	MPa	3400 (3087)
	Shear modulus	$G_{xy}$	MPa	1300 (1354)
	Density	$\rho$	$kg/m^3$	1680 (1708)
Cracking	Tensile strength	$f_{ty}$	MPa	0.1 (0.09)
	Tensile fracture energy	$G_{ft}$	N/mm	0.005(0.007527)
	Diagonal crack orientation	$\alpha$	rad	0.792(0.5)
Crushing	Compressive strength	$f_c$	MPa	14 (11.35)
	Compressive fracture energy	$G_c$	N/mm	20 (26.050)
Sliding	Cohesion	$c$	MPa	0.15 (0.14)
	Fracture energy in shear	$G_{fs}$	N/mm	-
	Friction angle	$\varphi$	rad	0.6 (0.669)

Table 39: Material properties of the masonry wall

## Analysis Method

See Table 40 for the analysis method of the numerical model. For the analysis self-weight + precompression is applied and a pushover load. The pushover load has a displacement of 4 mm, which is monitored in 100 load steps. This is the same analysis method used in paragraph 6.1 for numerical masonry model 2. The precompression is based on 0.12 MPa, which is a basic value used during the testing of masonry walls.

Self-weight	Load	Load name	Self-weight + precompression
		Load	12 N/mm
		Load steps	1
	Iterative procedure	Procedure	Regular Newton-Raphson
		Max. number of iterations	100
		Line search	Yes
	Convergence criterium	Norm	Force or Displacement
		Tolerance	0.01
		No convergence	Terminate
Pushover	Load	Load name	Pushover load
		Load	4 mm
		Load steps	0.01(100)
	Iterative procedure	Procedure	Regular Newton-Raphson
		Max. number of iterations	50
		Line search	Yes
	Convergence criterium	Norm	Force or Displacement
		Tolerance	0.01
		No convergence	Continue

Table 40: Analysis method masonry

## Results

In Figure 78 the displacement curve of the masonry wall including and excluding the structural façade is shown. In the initial phase, the shear force of both models behaves similarly. After the cracking of the masonry begins, the stiffness of the masonry wall including the structural window frame is gradually increasing more than the masonry wall excluding the structural window frame. For a displacement of 4 mm, the masonry wall including the structural façade has a shear force of 27,5 kN and the unreinforced wall 23,9 kN. This gives an increase of 15 % of the shear force by using a structural façade for a masonry wall for a displacement of 4 mm. This number can be higher if it is measured for a higher displacement.

The structural window frame also has a large influence on the development of cracks for the masonry wall. In Table 41 the crack propagation is shown, it shows a reduction of the maximum crack width during the pushover load. The maximum displacement of 4 mm gives a maximum crack width of 4,49 mm for the reinforced masonry wall and 5,80 mm for the unreinforced masonry wall. This is a reduction of 23 % of the total crack width. The displacements which are taken from Table 41 are in line with the points of displacement taken in chapter 6.1 and Table 33.

The occurring stress is shown in Table 42 and quite similar to the stresses without the façade. This is due to the maximum stress that occurs in the concrete lintel. The stresses in the masonry wall do have a larger reduction when using the structural window frame.

## Conclusion

In general, using a structural window frame increases the shear capacity of a masonry wall. Dependent on displacement the amount can vary, for a displacement of 4 mm this is 15 %. For the same displacement, the structural window frame reduces the maximum crack width inside the masonry wall by 23 %. Furthermore, the stresses in the masonry wall are lower when using the structural window frame.

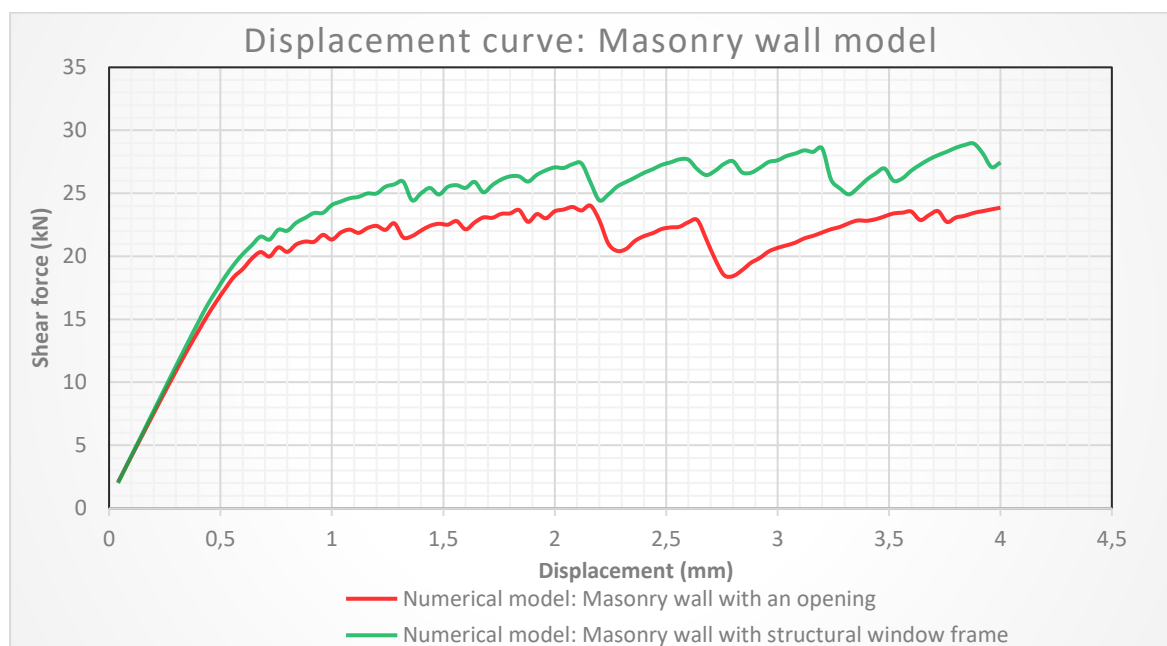
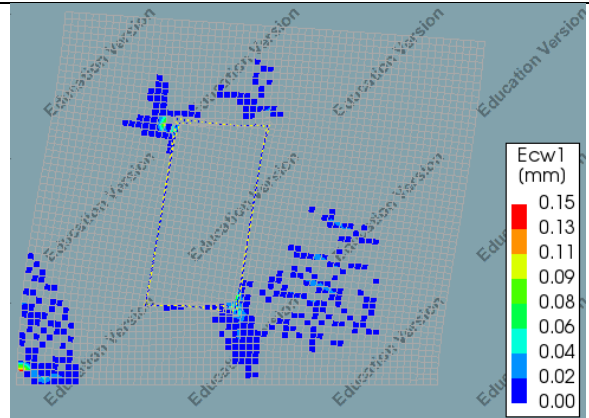
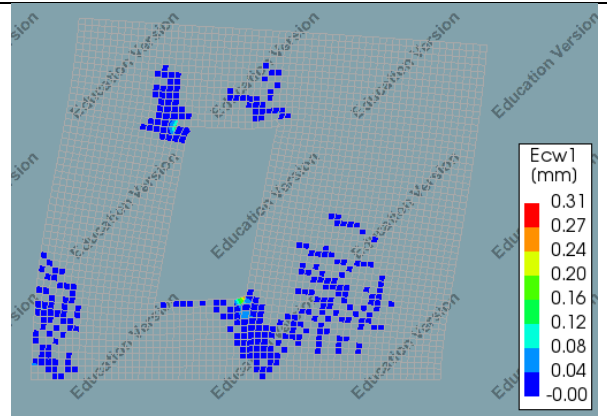


Figure 78: Displacement curve of the masonry wall including and excluding the structural façade

**Numerical masonry model : Structural facade**



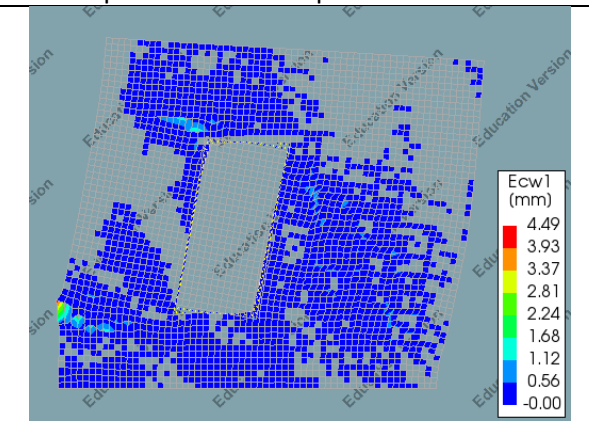
**Numerical masonry model : No facade**



*End of the Linear elastic stage*  
 Loadstep 18: 0.68 mm displacement



*End of the experiment*  
 Loadstep 40: 1.56 mm displacement

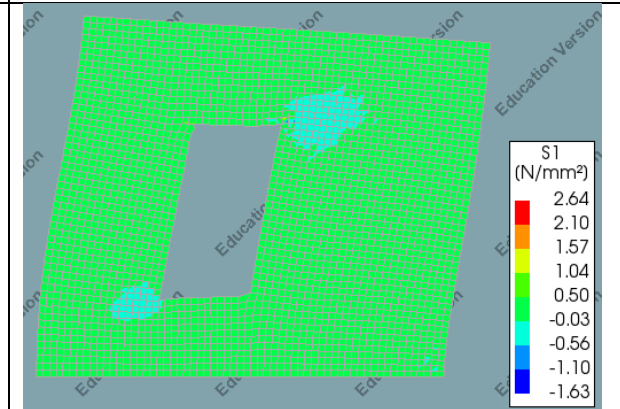
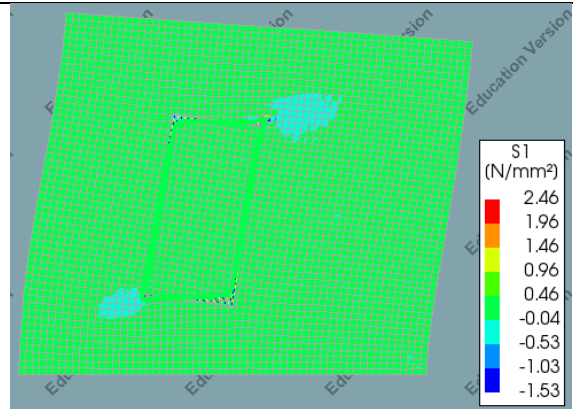


*End of the numerical model*  
 Loadstep 100: 4 mm displacement

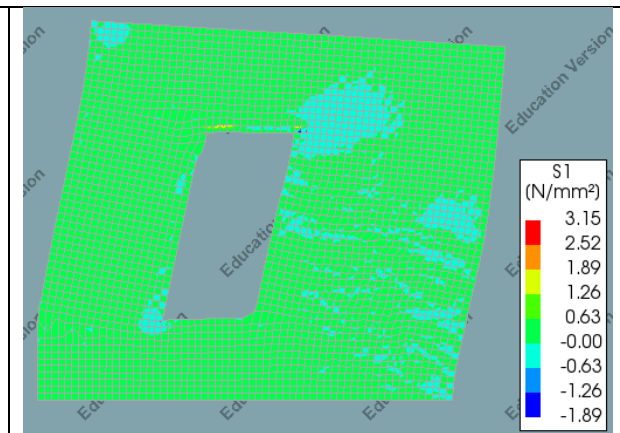
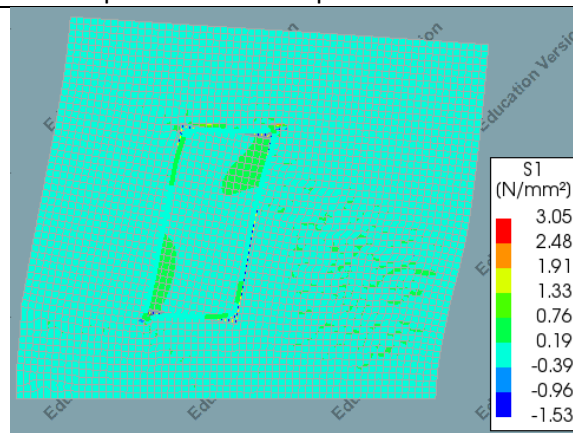
Table 41: Comparison crack width for the masonry wall including and excluding the structural facade

**Numerical masonry model : Structural facade**

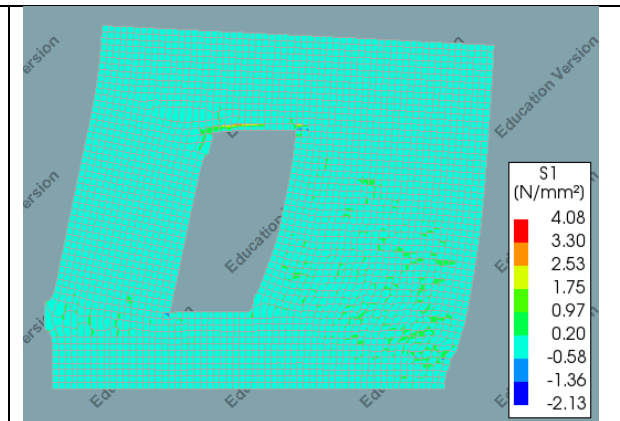
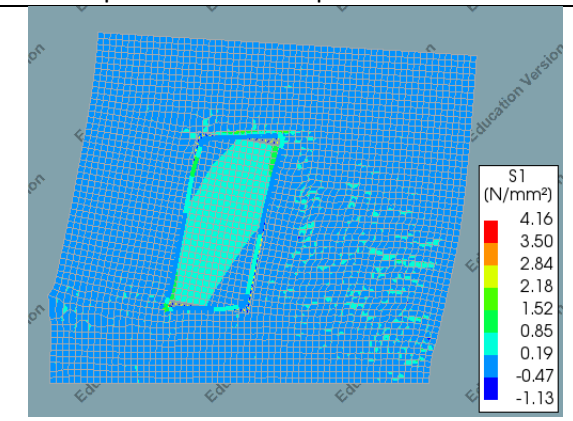
**Numerical masonry model : No facade**



*End of the Linear elastic stage*  
Loadstep 18: 0.68 mm displacement



*End of the experiment*  
Loadstep 40: 1.56 mm displacement



*End of the numerical model*  
Loadstep 100: 4 mm displacement

Table 42: Comparison stresses for the masonry wall including and excluding the structural facade

## 7.2 Pushover calculation

To verify the safety of the strengthened masonry wall a non-linear pushover calculation has been made. Therefore, the pushover curve of the regular and strengthened masonry wall and the ADRS curve is necessary. The ADRS curve, which stands for Acceleration Displacement Response Spectra, depends on the location and the pushover curve depends on the structure. In this paragraph, the calculation and the results are discussed for the regular and strengthened masonry wall.

The pushover curves of the masonry models are made in DIANA and have a maximum displacement of 4 mm. However, for the pushover calculation, the displacement needs to go until the near-collapse of the masonry wall. Unfortunately, in DIANA the convergence for the masonry model is not occurring for “large deformations” . Therefore, experimental results of the near-collapse of a similar masonry wall will be used. It is of importance that this masonry wall has similar geometry and material properties as the numerical model. Furthermore, the results of the numerical model will be used as initial results of the pushover curve, see Figure 78. To include the behaviour of the structural window frame, the displacement curve of the structural window frame is also taken into account, see Figure 67.

### Experiments

The experimental results from (Esposito & Ravenhoorst, 2017) are being discussed in this section. The geometry and material properties of the walls are shown in Table 43, an overview is shown in Figure 79.

Sample name	Material	Length (mm)	Height (mm)	Thickness (mm)	Pre-compression (N/mm <sup>2</sup> )	Boundary condition
TUD_COMP-21	Solid clay brick	3070	2710	100	0.36	Fix-Fix
TUD_COMP-22	Solid clay brick	2960	2710	210	0.36	Cantilever
TUD_COMP-23 (with opening)	Solid clay brick	3070	2710	210	0.36	Cantilever

Table 43: Properties of the masonry walls

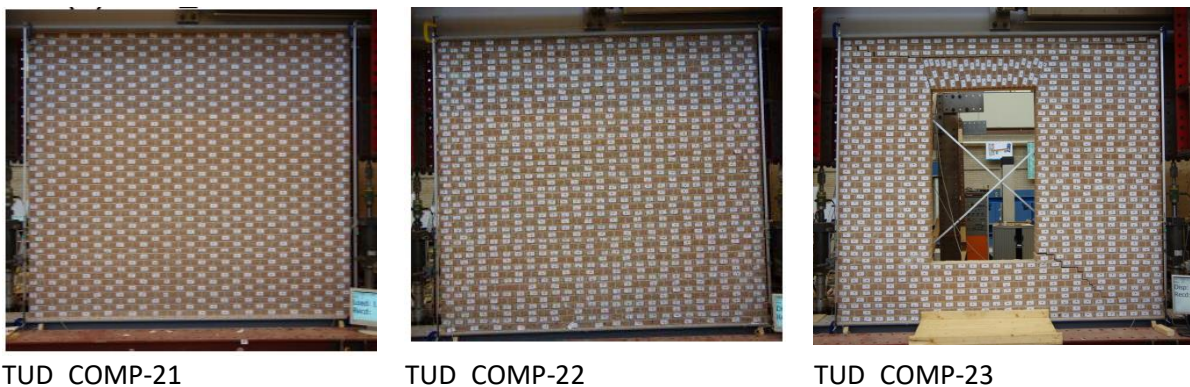


Figure 79: Overview of the masonry walls

The geometry of the masonry wall “TUD\_COMP-23” has a similar geometry to the masonry wall which is being modelled in paragraph 6.2. However, it is twice as thick. Therefore, the shear force capacity is expected to be half of the original value however, it will have a similar post-peak curve behaviour. The maximum shear force is +85.37 and -108.92 kN. The wall was subjected to a

maximum displacement of +23.1 and -33.1 mm, which is a drift of +0.85 and -1.22%. The pre-compression is 0.36 MPa, which is three times higher than the 0.12 MPa assumed for the numerical model (Esposito & Ravenhoorst, 2017). Integrating these values as a comparison for the regular masonry wall would mean the following. The maximum displacement is 33 mm and the maximum shear force is 54.5 kN. This value should not be taken too strictly, since the geometry is not exactly the same and the precompression is different. However, the structural behaviour could say something about the behaviour of the masonry wall in general.

The geometry of the masonry wall “TUD\_COMP-21” is similar to the modelled masonry wall and had the same geometry and thickness however, it doesn’t have an opening. Therefore, the shear force capacity can be assumed as an upper boundary. It should be noted that TUD\_COMP-21 has a different boundary condition. That explains why it has a relatively high shear force and low horizontal displacement. The maximum shear force is +97.29 and -98.95 kN. The wall was subjected to a maximum displacement of 12 mm, which is a drift of 0.47%. Since the maximum shear force is significantly high, it is not expected that this value is reached for the masonry wall.

The masonry wall “TUD\_COMP-22” is twice as thick as “TUD\_COMP-21” furthermore, it has different boundary conditions. Therefore, it behaves differently. The maximum shear force is +116.71 and -117.70 kN. The wall was subjected to a maximum displacement of 50 mm, which is a drift of 1.85%. It is noticeable that the wall behaves more ductile than the other “TUD\_COMP-21”. It is expected that the boundary conditions have the biggest contribution to this behaviour and that the thickness of the masonry wall is of less influence.

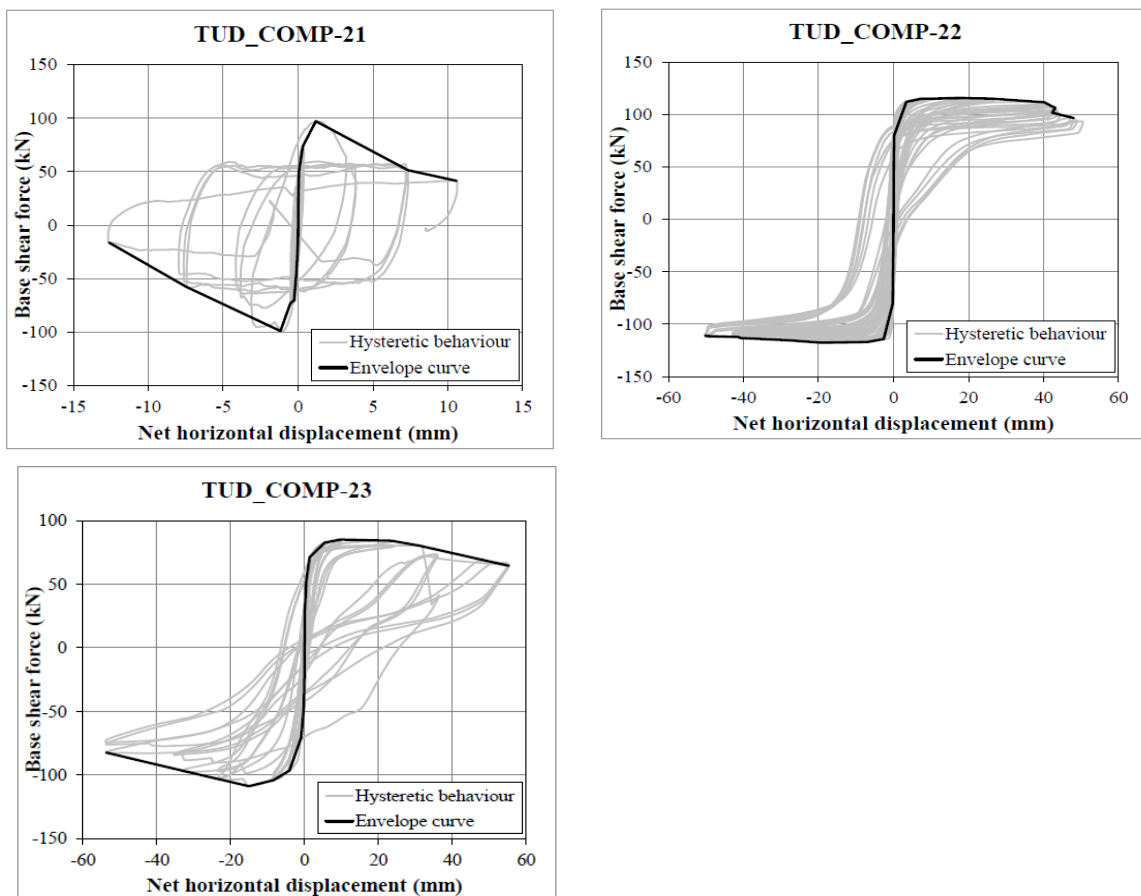


Figure 80: Capacity curves of the masonry walls (Esposito & Ravenhoorst, 2017)

Based on these statements done above. An unreinforced masonry wall of 3070 x 2710 x 100 mm, would have a maximum shear force of  $109/2=54,5$  kN and a maximum displacement of around 33 mm. However, integrating all aspects is a complex task. The results of the experiments of mainly “TUD\_COMP-23” will be used as a rough indication for the total displacement and the structural behaviour. The results of the numerical model are used as the initial results. Based on these initial results and the experimental results an estimated capacity curve is sketched. The difference between the strengthened masonry wall strengthened and the regular masonry wall is increasing with increasing displacement. Around a displacement of 18 mm, it is expected that the shear force will have a kink in the graph. This also happened for the experiments, see Figure 81 for the capacity curves. The displacement is expected to go until 33 mm just as the experiments of “TUD\_COMP-23”.

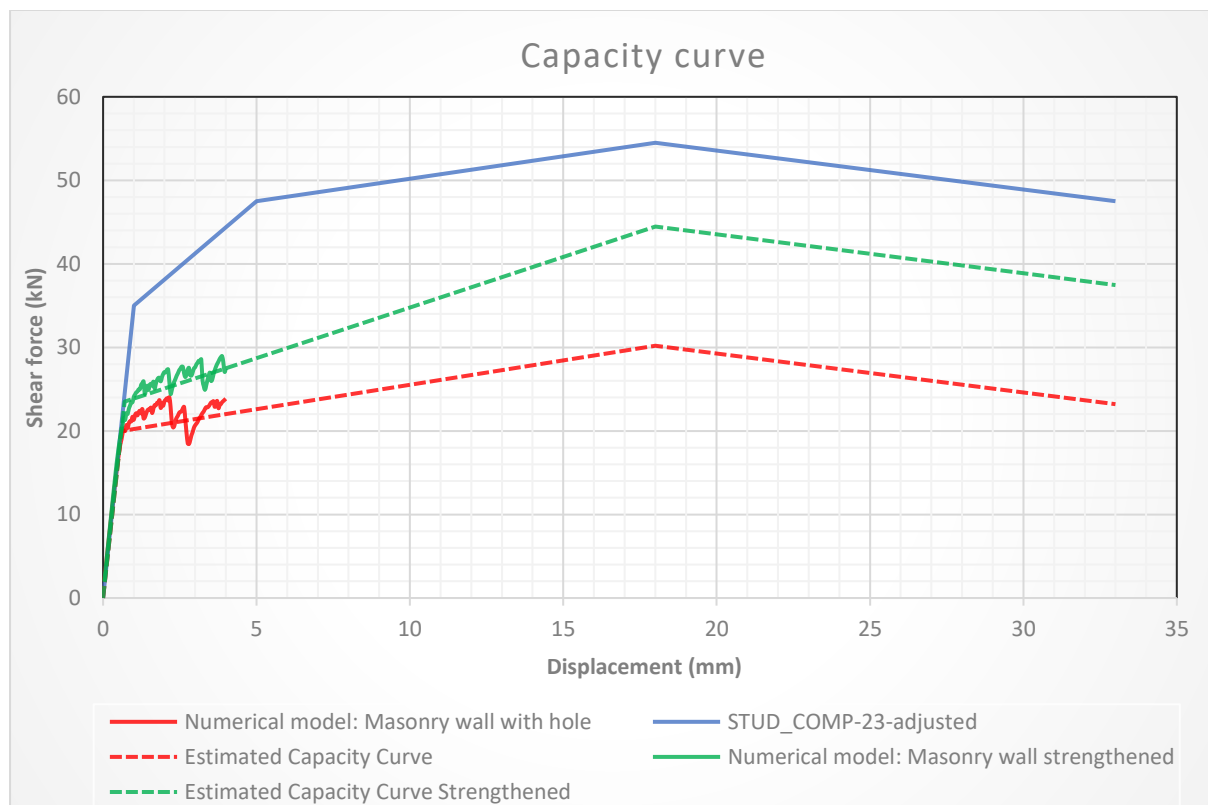


Figure 81: Capacity curves numerical model

## Pushover Calculation

For the pushover calculation the capacity curve of the strengthened masonry wall and the unreinforced masonry wall is used, see Attachment D.3 for the full non-linear pushover calculation. The purpose of the calculation is to calculate whether the seismic resistance of the masonry wall is capable of withstanding an induced earthquake in the Groningen area. To do this the bilinear capacity curve is calculated based on the non-linear capacity curve. The damping factor is calculated to determine the damping of the structure and the reduced ADRS Curve. The ADRS Curve is the seismic response spectrum of the acceleration against the displacement for the Groningen Area. If the bilinear capacity curve is higher than the ADRS curve this means that the structure satisfies to the structural requirements. See Figure 83 for the overview of the capacity curves for the unreinforced and strengthened masonry walls and the original and reduced ADRS curves. Whether it is a practical solution for the Groningen area depends on the experimental results of the masonry wall including the structural window frame. Since these experiments are not included in this thesis and still need to be done.

The ADRS curve, Acceleration Displacement Response Spectra, is taken from the northern part of Groningen. The ADRS curve has the displacement on the horizontal axis and the acceleration on the vertical axis. The ADRS curve allows to evaluate the response for a structure even if they have different ductilities or deformation capacities, and determine the overall capacity of a structure. In the area of Appingedam the peak acceleration of the ground showed to be the highest. Therefore, this location is chosen to compare the capacity curves with, see Figure 82 for the exact location of the data that is taken for the response spectrum.



Figure 82: Screenshot of the response spectrum map of Appingedam (NEN, 2021)

For the near collapse limit state (Ultimate limit state) under seismic design, the safety is considered to have been met if the conditions regarding the capacity of the cross-section, prevention of brittle failure, the stability of the building, the foundation stability, strength of seismic joints and the strength of horizontal diaphragms are met.

The calculations of these topics are not done since it is out of the scope of the thesis. However, it is important that the structural elements and the structure act as a whole and has adequate ductility. The formation of a soft storey plastic mechanism shall be prevented in multistorey buildings.

Two other stages are the limit stage SD and the limit stage DL. For the limit stage SD, the ultimate limit stage has not been exceeded but is on the verge of being exceeded. However, there may be

serious damage resulting in parts falling down. For the limit stage DL, also named the SLS, the ultimate limit stage has not been exceeded. However, there may be slight damage in the form of cracks. For the limit stage NC, the ultimate limit stage with full utilization of the deformation capacity has not been exceeded, but is on the verge of being exceeded. However, there may be serious damage resulting in parts falling down.

According to the NPR9998 the return period for the NC stage for primary seismic elements and for all consequence classes is 2475 years. No return period of existing structures for the DL limit stage have been stated. For the calculation the same return period is assumed as for new buildings for the DL limit stage, which is 95 years. In short, the return period for the ULS is 2475 years and for the SLS is 95 years. This gives different ADRS curves for both stages. See Appendix D.3 for the elaborate calculation.

According to the calculation done in Appendix D.3 the damping factor is 18 % for the ADRS curve. This gives a reduction of the 0,6 to the original ADRS curve. Although this damping is only applicable if the bilinear curve intersects the ADRS curve in the plastic region. The estimated maximum shear force of the bilinear curve for the strengthened masonry wall is 44,5 kN and for the unreinforced masonry wall is 30,2 kN. Both masonry walls suffice for the original ADRS curve and the reduced ADRS Curve. The strengthened masonry wall shows an increase of 47 % for the shear force capacity. However, since this value is based on certain assumptions, the results should not be taken too strictly. More research should be done to verify the exact contribution of the structural window frame to the unreinforced masonry wall.

Due to the displacement and shear force, the structure conducts of a certain ductile behaviour. This ductile behaviour exceeds a certain amount of energy. According to Appendix D.3 the total deformation energy of the reinforced and unreinforced masonry wall is respectively 1211 Nm and 843 Nm.

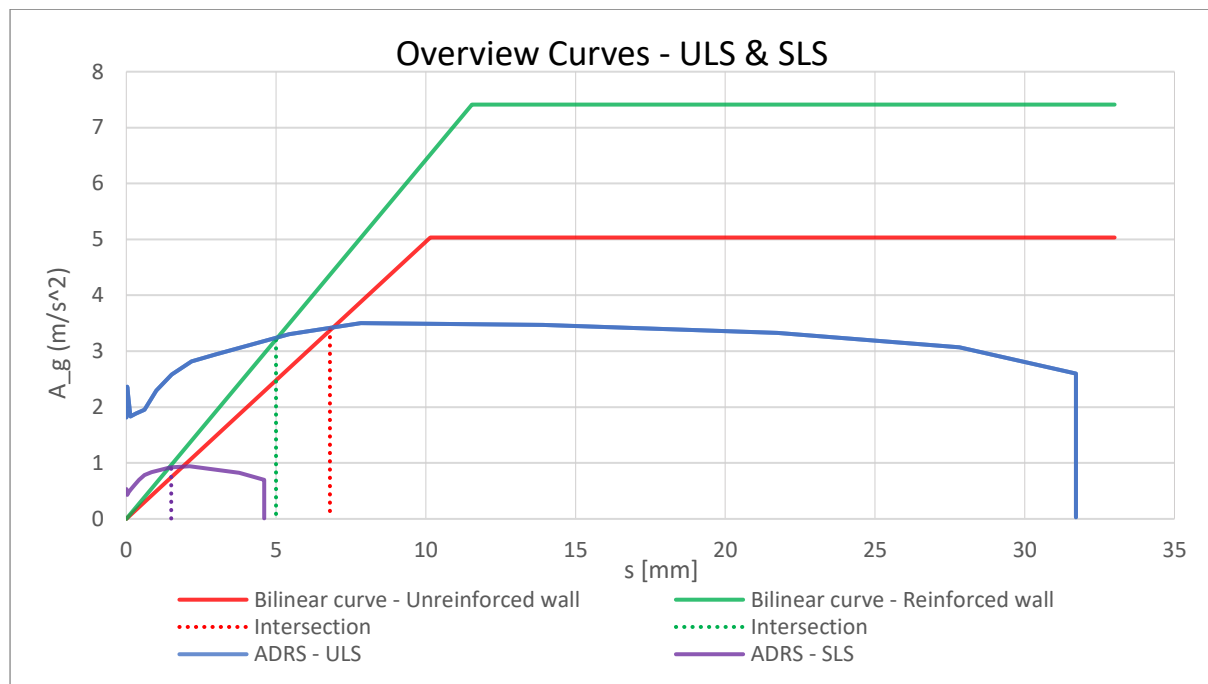


Figure 83: Overview of the Capacity curve and ADRS curves for the pushover calculation in the ULS & SLS

In Figure 83 the ADRS curves for the ULS and SLS stage and the bilinear capacity curves for the strengthened and unstrengthened walls are shown. Both bilinear curves intersect with the ADRS curves in the elastic region, which means there is no hysteretic damping or ductile behaviour of the structure occurring. The intersection of the curves occurs around 1.5, 2, 5 and 6.8 mm, which is the actual displacement, whereas the ultimate displacement is 33 mm. Therefore, for the ULS the ultimate limit displacement is 33 mm and the actual displacement is 5 and 6.8 mm for the strengthened and unstrengthened wall. For the SLS the actual displacement is 1.5 and 2 mm for the strengthened and unstrengthened wall.

In Appendix D.3 the effect of the different effective masses is investigated. An effective mass of 2400 kg and 15000 kg is investigated. The weight of 2400 kg resembles the weight of one masonry wall. The results showed that the masonry wall with 2400 kg had a higher peak acceleration, shorter displacement and still intersected with the ADRS curve in the elastic region. The bilinear curve of the reinforced masonry wall with an effective mass of 15000 kg intersected with the ADRS in the plastic region. Therefore, it had a displacement of 29 mm in the ULS situation. This means that the structure is behaving ductile. Due to the intersection in the plastic region damping of the ADRS curve was included. The bilinear curve of the unreinforced masonry wall intersects with the ADRS as well, however this is at the ultimate limit displacement of 33 mm. For all the curves of the SLS situation the lines intersect in the elastic region and therefore no damping is applicable. To get a clear overview of the behaviour of structure, results of the experiment on the masonry wall including the structural window frame should be used.

## Conclusion

According to the results of the pushover calculation, the increase of the shear force capacity due to the use of a structural window frame for a masonry wall as described in chapter 7.1 can lead up to 47 % for an effective mass of 6000 kg . The displacement of masonry is not high due to the intersection of the bilinear and ADRS curve in the elastic region. The displacement capacity is 5 mm for the strengthened and 6.8 mm for the unstrengthened wall in the elastic region for the ULS. This is around 1.5-2 mm for the SLS. The ultimate displacement capacity is estimated at 33 mm for both walls. The total deformation energy of the reinforced and unreinforced masonry wall is 1211 Nm and 843 Nm for an effective mass of 6000 kg.

By using an effective mass of 15000 kg for the reinforced masonry wall the ADRS curve in the ULS and bilinear curve intersect each other in the plastic region. Therefore, the actual displacement is increased until 29 mm, the ductility of the structure is increased and the hysterical damping is included for the ADRS curve.

However, these results should not be taken too strictly since the calculation is based on estimated values. It still gives a clear overview of the structural behaviour of the unreinforced and strengthened masonry wall. Both masonry walls suffice for the seismic loads according to the original and reduced ADRS curves. The reduced ADRS curve has a reduction of 60% due to the damping of the structure. Whether it is a practical solution for the Groningen area depends on the experimental results of the masonry wall including the structural window frame.

In part 4 all subquestions which are mentioned in paragraph 1.2 for part 4 are answered.

## PART V: DESIGN STUDY



## 8. Improved structural glass façade

The numerical and experimental results of the structural façade are promising. The structural façade behaves plastically and has high stiffness. This structural behaviour is beneficial for seismic loading for masonry walls with large openings. However, there are still some improvement points for the design. In this part and chapter, these improvements will be discussed. These improvements will be based on structural and sustainable aspects.

### 8.1 Structural performance

From the experiments, a few shortcomings came to light. The high stresses in the multiplex caused the splitting of the multiplex. However, the next experiments contained screws to prevent the multiplex of splitting. See Figure 51 for an overview of the screws inside the structural window frame.

From the cyclic experiments, which are discussed in paragraph 4.3.2, it is shown that the stiffness is decreasing for every new cycle. For small displacements, the stiffness remains stable, but for high displacements the stiffness of the structural window frame needs more cycles of the same displacement to stabilize. This is due to the pinching behaviour of the multiplex and tearing of the adhesive for larger displacement. It is unclear whether this can be prevented for large displacements since a too stiff timber frame would lead to peak stresses in the glass panel. It is also not clear whether the masonry wall can take these large displacements in the first place.

The thickness of the adhesive is crucial for the structural behaviour of the structural window frame. In paragraph 5.1 the displacement curve of the structural window frame is shown. It is seen that the structural window frame for the calcium silicate masonry wall has a higher shear force capacity than the structural window frame for the solid clay masonry wall for the monotonic load. This is due to the thickness of the adhesive. For the calcium silicate window, the adhesive thickness is 6.7 mm and for the solid clay window it is 5.9 mm. This means that the thickness, while difficult to control, is crucial for the structural behaviour. Furthermore, the intersection of the glass frame and timber frame, happens relatively late. According to the numerical model, this happens after a displacement of 31 mm and according to the experimental results, this happens after 40,8 mm. This difference is due to the different thicknesses assumed. However, the displacement is around a drift percentage of 3%. Ideally, this drift would smaller, because the masonry wall would not be able to endure large displacements.

Since the timber frame is glued to each other, it is not possible to replace any elements when damage occurs. Since the structural glass panel is glued to the inner part of the timber frame, this cannot be replaced. However, removing the glue would change the structural behaviour dramatically. The thin glass panel however is not glued to the timber frame. By only screwing the meranti hardwood to the plywood, the thin glass panel could still be removed when it is damaged. Furthermore, the production time would be reduced when glueing of the timber frame is neglected.

In short, all the listed topics are shown below:

- Splitting of the multiplex
- Stiffness of the inner part from the timber frame
- The thickness of the adhesive
- Demountable timber frame

The structural window frame should still function as a traditional window frame. However, this is not the scope of the thesis. In Table 44 a list of the functions of a window frame is described.

Safety	Health	Usability	Energy
Structural safety	Daylight	Operation	Thermal insulation
Fire safety	Acoustic performance	Accessibility	Air permeability
Burglary protection	Condensation prevention		
	Water tightness		
	Ventilation possibility		

*Table 44: Functions window frame*

## 8.2 Improvements

In the previous paragraph, the shortcomings of the design are discussed. In this paragraph several solutions to these problems are discussed and whether they are logical to implement or not. The structural effect and practicality will be discussed as well.

### Stiffer frame model

Using screws prevents the splitting of the plywood. However, there can be thought of different solutions to prevent the plywood from splitting. Using a different kind of material can prevent the splitting of the plywood. Using a stiffer material for the plywood can increase the overall stiffness of the structural window frame as well. To investigate the influence of the stiffness for the inner part of the structural frame the material properties have been adjusted. For research purposes, the stiffness properties for the inner part of the frame are taken twice as high as for the material properties for the plywood. By doing so the effect of increasing the stiffness would be clarified.

Similar to the original numerical model, the structural non-linear interface exists of a serial spring. This serial spring exists of one equivalent spring, combining the properties of the Sikaflex adhesive and the stiffness of plywood. In this model, the material properties of the plywood are taken twice as stiff and thus twice as strong. In attachment F.1 an overview of the spring stiffness is given of the interface, timber frame and the combined equivalent spring stiffness properties. The principle behind the calculation is shown in Chapter 5.1 and Attachment C.1. In Table 45 the serial spring stiffness properties are shown of the adhesive, the timber frame and the equivalent stiffness.

Serial spring system

Adhesive stiffness properties			Timber stiffness properties			Equivalent stiffness		
$u_1$ (mm)	$\sigma_1$ (N/mm <sup>2</sup> )	$k_1$ (N/mm <sup>3</sup> )	$u_2$ (mm)	$\sigma_2$ (N/mm <sup>2</sup> )	$k_2$ (N/mm <sup>3</sup> )	$u_{tot}$ (mm)	$k_{eq}$ (N/mm <sup>3</sup> )	$\sigma_{eq}$ (N/mm <sup>2</sup> )
-25	-1200	48	-	-30	-	-25	-	-30
-10	-1200	120.0	-	-30	-	-	-	-30
-5.5	-50	9.1	-6	-30	-	-11.5	-	-30
-5.42	-45	8.3	-1.6	-45	28.1	-7.02	6.41	-45
-5.28	-36	6.8	-0,5	-36	72	-5.78	6.23	-36
-5	-18	3.6	-0.24	-18	75	-5.24	3.44	-18.00
-0.75	-0.9	1.2	-0.012	-0.9	41.7	-0.762	1.18	-0.90
0	0	0.0	0	0	0	0	0	0
0.75	0.9	1.2	-	-	-	0.75	1.2	0.9
2.50	1	0.4	-	-	-	2.5	0.4	1
25	0.001	$4 * 10^{-5}$	-	-	-	25	$4 * 10^{-5}$	0.001

Table 45: Serial spring stiffness properties for the stiffer frame model

In Figure 84 the displacement curves for the numerical model of the original structural window frame model and the stiffer timber frame model. It is seen that in the beginning, both models behave similarly. Around 31 mm the behaviour starts to change, this is when the glass panel and timber frame starts to have contact. This is similar to the original model. The structural interface displacement around this point is 5.3 mm, see Attachment F.1 for more detailed information. After this point, the stiffness of the timber frame is very significant for the structural behaviour. The displacement where the shear force stabilizes is later and higher than the original model. This would be around 55 mm with a maximum shear force of around 58 kN. For the original model, this is around 45 mm and has a maximum shear force of 35 kN. This means that a stiffer inner part for the timber frame results in a higher maximum shear force and stabilizes at a later moment than the original design. However, the structural behaviour before contact of the glass panel and the timber frame is similar for both models. This is because in beginning, in phase 1, the structural behaviour of the adhesive is more leading for the overall structural behaviour. In Attachment F.1 the relation between the relative interface displacement and the stresses inside the glass panel is shown.

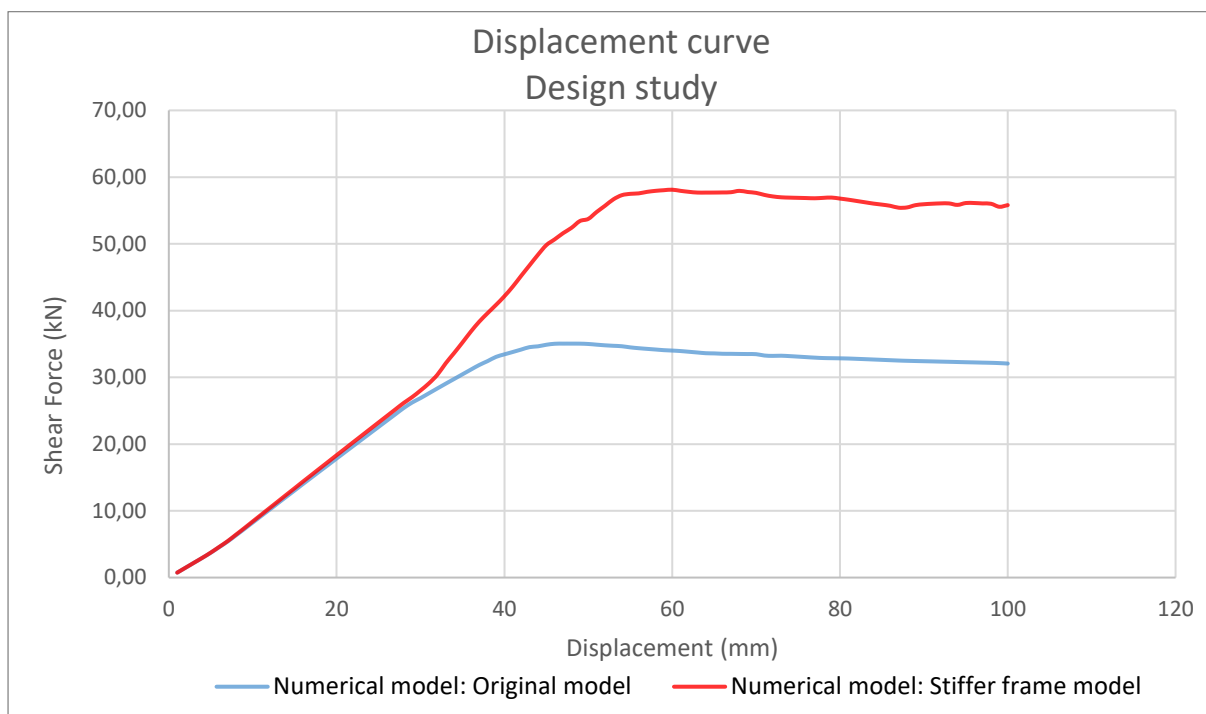


Figure 84: Displacement curve Original model versus the Stiffer frame model

## Thickness adhesive

Studies show that the thicker layer of adhesive gives rise to a larger area of plastic deformation which helps to absorb kinetic energy. Experimental results show that a thicker layer dampens the effect (Zaera et al., 2014). However flexible adhesives are often applied in very thick layers of about 5 mm. The strength is known to decrease as the adhesive thickness increases but on the other hand, under elastic assumptions, the stress concentrations decrease as the adhesive thickness increases.

The thickness of the adhesive is essential for the structural behaviour of the structural window frame. To investigate the thickness of the Sikaflex-252 this has been varied. Previously it is mentioned that the contact of the glass element and timber frame should be shortened. This could be done by making the adhesive thinner than 5 mm. For practical reasons, the adhesive should not be thinner than 3 mm. Therefore, an adhesive thickness of 3 mm is assumed to investigate its influence. For the sake of completeness, there is also looked at the behaviour of no adhesive between the glass panel and timber frame.

Since no research has been done on the properties of Sikaflex-252 for a thickness of 3 mm, linear interpolation is used to estimate the mechanical properties of the adhesive. Therefore, the equivalent spring stiffness of the adhesive and the timber frame is changed. The material properties of the timber frame are assumed to be the same as the original model in Paragraph 5.1. See Table 46 for the spring stiffness properties of the 3 mm adhesive, timber frame and equivalent spring stiffness. What is noticeable is that the glass panel and timber frame should have contact around an interface displacement of 3.5 mm. This is due to when the adhesive of 3 mm is fully compressed, the plywood should be 0.5 mm compressed due to the compression stresses. The tearing of the adhesive is assumed to be at +1.5 mm since this is half of the thickness of the adhesive as well. The Sikaflex adhesive normal and shear properties are matched by the original by linear interpolation. By multiplying the relative interface by 0.6 while remaining the same normal and shear properties, the mechanical properties are adjusted. See Table 46 for an overview of these values.

For the numerical model with no adhesive simply the material properties of the timber are used to model the non-linear interface elements, see Table 46 and Appendix F.2.

### Serial spring system

Adhesive stiffness properties			Timber stiffness properties			Equivalent stiffness		
$u_1$ (mm)	$\sigma_1$ (N/mm <sup>2</sup> )	$k_1$ (N/mm <sup>3</sup> )	$u_2$ (mm)	$\sigma_2$ (N/mm <sup>2</sup> )	$k_2$ (N/mm <sup>3</sup> )	$u_{tot}$ (mm)	$k_{eq}$ (N/mm <sup>3</sup> )	$\sigma_{eq}$ (N/mm <sup>2</sup> )
-25	-15	0.6	-	-15	-	-25	-	-15
-10	-15	2.5	-	-15	-	-	-	-15
-3	-15	5	-6	-15	2.5	-9	-	-15
-3.04	-21.8	7.2	-1.6	-21.8	13,6	-4.6	4.7	-21.8
-3	-18	6	-0.5	-18	36	-3.5	5.14	-18
-0.45	-0.9	2.0	-0.024	-0.9	37.5	-0.47	1.9	-0.90
0	0	0.0	0	0	0	0	0	0
0.45	0.9	2.0	-	-	-	0.45	2.0	0.9
1.5	1	0.7	-	-	-	1.5	0.7	1
25	0.001	$4 * 10^{-5}$	-	-	-	25	$4 * 10^{-5}$	0.001

Table 46: Serial spring properties for an adhesive of 3 mm

In Figure 85 the displacement curve for the original numerical model of the structural window frame is shown in blue, the numerical model with the 3 mm adhesive is shown in orange and the grey line in the numerical model with no adhesive. It is noticeable that a thinner adhesive layer results in a stiffer behaviour for phase 1, just as expected. For the numerical model of 3 mm, the glass panel and timber frame have contact with each other around 20 mm, which is equal to a relative interface displacement of 3.5 mm. For the original model, this is around 31 mm according to the numerical model. The shear force stabilizes earlier than the original model as well, this is around 37 mm with a maximum shear force of 36 kN. For the original model, this is around 45 mm with a maximum shear force of 35 kN. For the numerical model of no adhesive shear force increases very fast, since the timber frame on its own is very stiff. The shear force stabilizes around 20 mm. Around a displacement of 35 mm the shear force increases. However, this behaviour seems not realistic and should be further investigated. Possibly the timber frame could not deform as much since the pinching of the glass inside the timber frame would be very large.

What is also noticeable is that the model with the thinner adhesive has a lower shear force around a displacement of 100 mm, this is because the pinching behaviour happens sooner than the original model. However, the experiments showed that the shear force remained stable after the shear force stabilised. Therefore, it is questionable whether the shear force would decrease as it is shown in Figure 85. This stabilization happens between a displacement of 26 and 45 mm, this is where the peak compression stress of the timber frame of 21.8 MPa is reached and is reduced until 15 MPa. After this point the compression stress remains the same, however the displacement increases, therefor the stiffness decreases.

In attachment F.2 an overview is given of the relative interface displacement versus the stresses inside the glass. It is seen that the stresses inside the glass for phase 1 are higher due to the higher stiffness of the interface. However, the stresses inside the glass don't increase significantly after contact with the timber frame.

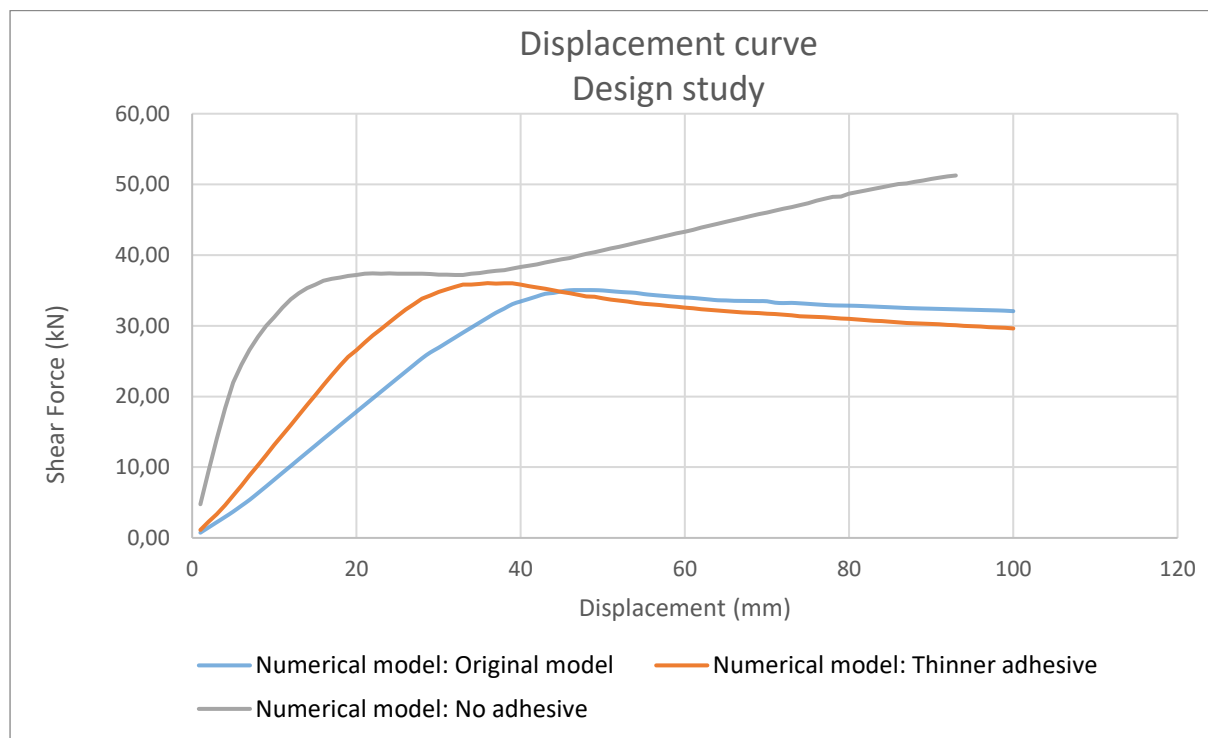


Figure 85: Displacement curve of the original numerical model versus the numerical model of the thinner adhesive

The behaviour of the structural window frame is important. However, the behaviour of the masonry wall is of more importance. In Figure 86 the shear force capacity of these masonry models including the different structural window frames are shown. It is noticeable that the structural behaviour barely changes for a thinner adhesive layer according to the numerical models. This is surprising since a thinner adhesive layer did have a large effect on the structural window frame on its own. In Attachment F.2 an overview is given of the crack widths for these numerical models. It can be concluded that a thinner adhesive layer results in similar or even larger crack widths. Therefore, a thinner adhesive layer would not suggest a more preferable structural behaviour according to the numerical model. However, more research should be needed to verify these findings.

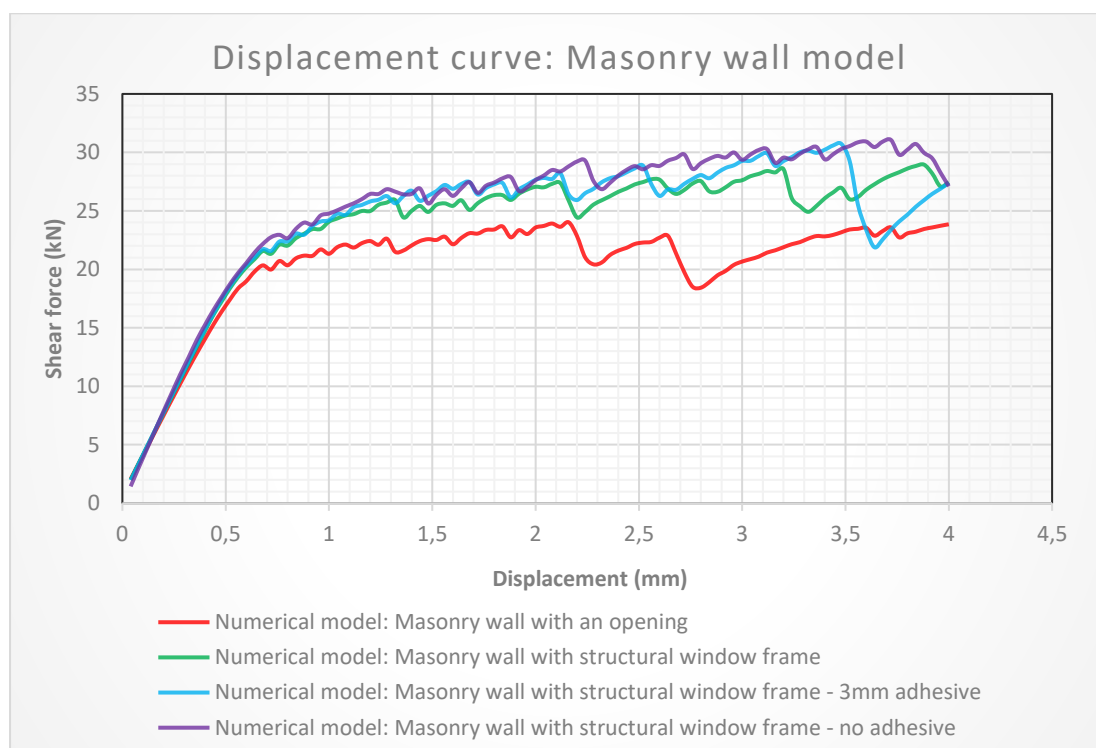


Figure 86: Shear force capacity for alternative masonry wall models

## Demountable timber frame

Currently, the building sector contributes up to 35% of waste generated in the EU and uses more than 40% of all energy. Therefore, there is an urgent need to rethink how we design in the built environment, see Figure 87. The façade of a building represents around 25-30% of its embodied energy. In the Netherlands, a large percentage of construction waste of construction and demolition waste is recycled, but this is not enough for a sustainable future (Michael, 2016).

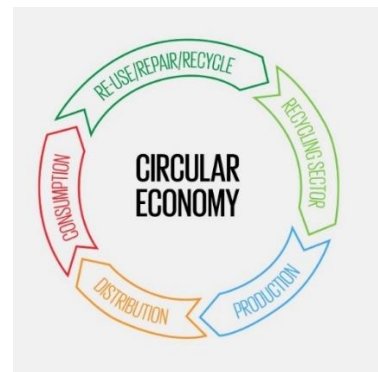


Figure 88: Circle of the Circular economy

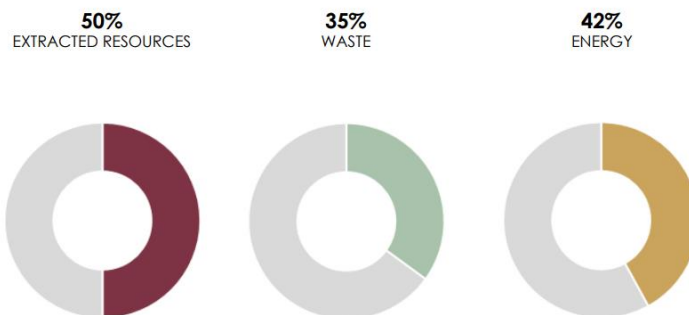


Figure 87: Impact of construction industry within the EU (European Commission, 2011)

To design a more sustainable façade the essential steps of the circular economy are being implemented. Circular economy focuses on reducing the amount of waste and consumed energy, by enabling the users to reuse components or materials (Michael, 2016).

The first step of a circular design is to maintain the façade. Ensure that the window frame is cleaned and checked for cracks regularly. Regular varnishing of the wood keeps the meranti hardwood in good shape.

The second step is to reuse the window frame in its complete form in a different building. This would mean that the mortar that is being used to connect the masonry wall to the window frame should not be stronger than the masonry or the timber frame. This would lead to damage when the window frame would be removed.

The third step is to repair elements of the window frame. Since the timber frame is glued to the laminated glass panel, the glass panel cannot easily be replaced when damage occurs. However, when a screwed connection is being used instead of glue, there are more options available. By doing so, the hardwood elements and the thin glass panel could be easily replaced when damage occurs. This would prevent replacing the whole window frame when damage occurs. It is important to note that the thin glass panel is located on the outside. See Figure 89 for a sketch of the positioning of the screws. The technical drawing is shown in Attachment F.3.

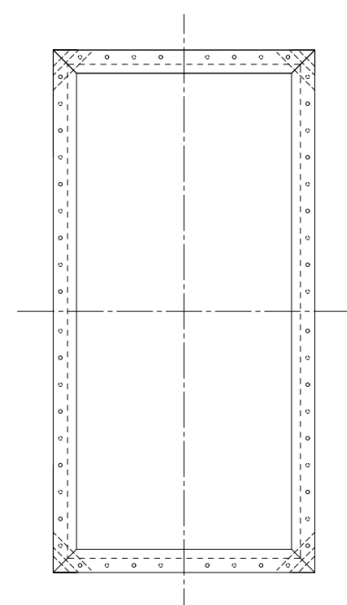


Figure 89: Positioning of the screws

Furthermore, during testing of the window frame, it was discussed that the corner connection of the plywood is too weak in the horizontal direction. To strengthen the corner a different corner design is made. The corner now has a similar edge, see Attachment F.3.

The fourth principle is remanufacturing. This principle is mostly skipped by the building industry, because of the complications. The process includes quality insurance and possibly making changes. However, using reusable parts could prevent making new elements and thus reducing materials and CO2 pollution. In the design of the structural window frame, this is possible. If the window frame cannot be reused as a whole, the timber bars of the frame and the glass panels could still be reused. The timber frame can be demounted into the hardwood bars and the plywood bars, since no glue will be used. By only making screwed connections this would be possible.

If nothing is reusable anymore the final step would be the recycling of the materials. The recovered materials would come back into the production and thus less construction waste is made and fewer new materials are being used.

A few basic principles which are implemented in the design are: minimizing the number of materials and ensuring separation of materials. The connections are preferred to be mechanical since separation would be easier. Providing information about disassembly is also important.

## Conclusion

Using a stiffer inner part with a higher compression strength for the timber frame results in a higher maximum shear force. Furthermore, the shear force stabilizes at a later moment than the original design. However, the structural behaviour before and at the moment of contact of the glass panel and the timber frame is similar for both the stiffer and the original model.

Using a thinner adhesive layer leads to a stiffer behaviour of the structural window frame. The moment of contact between the glass panel and timber frame is being reduced from around 31 mm to 20 mm, by using an adhesive layer of 3 mm instead of 5 mm according to the numerical model. The maximum shear force of both models is similar to each other. However, for the numerical masonry wall models, it is not preferable to use a window frame with a thinner adhesive layer. Since this would not increase the shear force capacity or decrease the crack width significantly. However, more research should be needed to verify these findings.

The design of the structural window is adjusted to fit into the circle of circular economy. Maintenance to the window frame is one of the first step. Screwed connections are preferred instead of glued connections to facilitate repairment and reusing of elements.

In part 5 all subquestions which are mentioned in paragraph 1.2 for part 5 are answered.

## Discussion

The design of the structural window frame is promising. The shear force capacity showed an increase of 15 % for the numerical model of an unreinforced masonry wall for a displacement of 4 mm, see Paragraph 7.1. This increase of shear force could be higher if the displacement increases. According to the assumed properties the increase of shear force capacity could lead up to 47%, see Paragraph 7.2. However, these results need to be validated by experimental results. Unfortunately, the testing campaign of the structural window frame was delayed due to the pandemic and this also affected the master thesis. Initially, the experiments for the masonry walls including the structural window frame were included in the thesis. However, due to delay this could not be included anymore. Therefore, it is important to compare the numerical results of the masonry wall including the structural window frame with the experimental results.

The geometry of the structural window frame is of big influence for the effectivity. In the research of (Groot, 2019) it was concluded that a structural window improved the in-plane seismic performance of the masonry and reduces the expected damage. The seismic force capacity of the strengthened masonry walls reaches 137%, 300% and 367% compared to an unstrengthened wall, depending on the window size. The larger the window size, the more effect it has. This indicates that a larger window size would also have a larger influence for the current numerical model and thus has more potential. There are some differences of the current model, which has increase of 15% of the force capacity, compared to the older model, which has an increase of 37%. These are the geometry of the structural window, which are 780 x 1510 mm for the older model and 650 x 1350 mm for the current model. The displacement load is 8 mm for the older model and 4 mm for the current model, since the shear force is increasing with the displacement this has a significant influence. Furthermore, the material properties of the structural window frame are more up to date for the current model than the older model. Other parameters for the effectivity of the structural window frame are the: type of wall which it is used, the geometry of the wall, the seismic response and several other factors. Due to the former research done by (Groot, 2019) it would suggest that modelling the current structural frame model for larger geometries would have a larger increase of shear force as well. By having a complete overview of the influence of smaller and larger window frames it would be more clear if the structural window frame is a relevant solution the situation in the northern part of the Netherlands. This is not further investigated, since it is not the essence of the thesis.

### Numerical model

The numerical model showed a similar behaviour compared to the experimental results for a monotonic loading. This was due to including the material properties of the adhesive and plywood as a serial spring into one equivalent spring. However, the unloading behaviour is not included in the numerical models. In the numerical models, non-linear interface elements were used. For this material model, the unloading behaviour is the same as the loading behaviour, thus there is no strength reduction. Other material models were also investigated such as Coulomb friction and Mooney-Rivlin however, these models didn't show the preferred loading and unloading behaviour. Contact was made with the professionals within the company of DIANA and several other DIANA experts to discuss the possibility of modelling the unloading behaviour of the model. However, it was concluded that no existing material model was able to model the loading and unloading behaviour for the structural window frame. The strength reduction of the adhesive due to tearing and the timber due to pinching was too complicated. It was a possibility to make a new material model all by myself in DIANA, that would match these properties. However, this would have been

too much work since it is not the essence of the thesis. Therefore, the focus of the numerical model remained for only the monotonic loading behaviour. Another possibility would be to model the structural window frame with a different finite element program to include this unloading behaviour. During the thesis, a lot of time was put into making a model that included the cyclic behaviour of the structural window frame. It would have been better if I or the professionals from DIANA could come to this conclusion sooner so I could focus on other aspects. However, it was still a learning full experience.

According to the estimates done in paragraph 7.2 the strengthened masonry behaves ductile for an effective mass of 15000 kg in the ULS. This ductile behaviour creates certain deformation energy. The plastic behaviour is highly dependent on the effective mass since the ADRS curve and bilinear curve need to intersect in the plastic region to create ductile behaviour and for the occurrence of hysteric damping. It would be interesting to have experiments and to do numerical modelling that can verify this behaviour for the masonry wall for different effective masses. Furthermore, the calculations that were done were based on assumptions and not on identical experiments. The results of experiments with similar properties should be used as input values of the calculation. This will provide a more accurate calculation. Therefore, a final numerical model and experiment are essential.

## Design

The design of the structural window frame is a prototype that can still be improved if necessary. In chapter 8 a few possible improvements are discussed such as: increasing the stiffness of the timber frame, decreasing the thickness of the adhesive and making the window frame more sustainable. It would be interesting to compare the results of the numerical model for a thinner adhesive with the experimental results. It is preferred to have the contact between glass and timber frame in a sooner stage and decreasing the adhesive thickness could provide this. However, it would be difficult to precisely put a thickness of 3 mm for the adhesive. From the testing campaign, it became clear that a small difference in thickness of the adhesive is easily obtained and that this results in a significant difference in the structural behaviour. Therefore, attention should also lay to the application of the adhesive.

The design of the structural window frame is made for a masonry wall located in the area of Groningen where induced earthquakes could happen. However, the use of this design could be implemented in a broader sense. Areas where they have similar seismic activity, similar material properties for the masonry wall and similar geometries, could make use of the structural window frame. This means that it also could be useful to use for a small tectonic earthquake however, the usage of the structural window frame should always be investigated for the location and purpose. For example, the masonry walls in Italy tend to be thicker than the masonry walls in Groningen. Therefore, the period is larger and increasing the stiffness would not be beneficial in this example.

The use of the structural window frame could also be to increase the stability of a façade for non-seismic purposes. Stabilizing buildings with glass facades could be promising since they are seen as weak points. Think about extensions to a building where a timber-glass façade could contribute to the overall stability. Normally a steel structure would take this function, but by using a timber-glass façade this will not be necessary. With the rise of more transparent facades, it could function as secondary stability elements. It could be combined with transparent solar panels or just used as a structural element. There are a lot of possibilities where it could be useful. All these applications need to be further investigated to prove their efficiency.

Changing the design of the window frame to make it more sustainable and circular could increase the added value of the design. However, it is important to note that the structural behaviour should not be affected negatively by making these sustainable changes. The structural behaviour should be leading in this purpose.

## Conclusion

This master thesis is aimed at modelling the numerical model for the structural window frame in order to assess the seismic performance for unreinforced masonry structures. Based on the numerical analysis and calculations the seismic performance for unreinforced and reinforced masonry structures is made. The focus of the thesis is on the validation of the numerical model based on the experimental testing campaign. Based on these results the structural façade is improved and further suggestions and usages are explored.

The results of this research are slightly different from former research done by (Groot, 2019). The former research showed an increase of 37% while the current research showed an increase of 15 % for the shear force capacity. However, these differences are due to: slightly different geometries, different displacement loads and different material properties. The former research assumed a window frame of 780 x 1510 mm and a displacement load of 8 mm. While the current research assumed a geometry of 650 x 1350 mm, a displacement load of 4 mm and has more updated material properties. Due to the former research done by (Groot, 2019) it suggests that modelling the current structural frame model for larger geometries would have a larger increase of shear force as well. By having a complete overview of the influence of smaller and larger window frames it would be more clear if the structural window frame is a relevant solution the situation in the northern part of the Netherlands. However, this is not further investigated, since it is not the essence of the thesis.

## Numerical model

The structural window frame is modelled according to Paragraph 5.1. to agree with the experimental results. Beam elements and non-linear interface elements have been used to model the timber frame and the adhesive layer. The adhesive is modelled as one spring in DIANA with an equivalent stiffness combining both the properties of Sikaflex-252 and the Okoumé plywood. The adhesive and the plywood act like a serial spring system. Around a displacement of 31 mm, the timber frame and the glass panel have contact with each other. A maximum shear force capacity is reached around a displacement of 45 mm and has a shear force of around 35 kN. The numerical model behaves similarly to the experimental results however, the unloading behaviour is not modelled due to complications with the material model. Furthermore, it is complicated to apply the correct thickness of the adhesive in practice. Since the thickness of the adhesive has a large influence on the structural behaviour, this leads to a certain tolerance of the obtained results.

The numerical results of the masonry model including the structural window frame are promising. An increase of the shear force capacity is shown of 15 % for a displacement of 4 mm by using the structural window frame for an unreinforced masonry wall. According to the assumptions and calculations, the shear force could increase up to 47 % for a displacement of 18 mm. However, this needs to be verified with experimental results. Whether it is a practical solution for the Groningen area depends on the experimental results of the masonry wall including the structural window frame.

According to the numerical model, the structural window frame reduces the maximum crack width inside the masonry wall by 23 % for a displacement of 4 mm. The reinforced wall gives a crack width of 4,49 mm and 5,80 mm for the unreinforced masonry wall. Furthermore, the stresses in the masonry wall are lower when using the structural window frame. The peak stresses inside the glass panel are relatively low according to the numerical model of the structural window frame. According to the post-numerical model the peak stresses don't exceed 5 MPa for a displacement of 100 mm. This would correspond with the experimental results, since there was no cracking of the glass obtained. While in older the calculations the peak stresses rose above 45 MPa, which would mean

cracking of the glass. However, in these models the pinching behaviour of the timber frame was not included.

The pushover calculation showed that both the unstrengthened and strengthened masonry wall are able to withstand the seismic loads in Appingedam. However, the displacement capacity or ductility of the masonry is not high due to the intersection of the bilinear and ADRS curve in the elastic region. Furthermore, there is no hysterical damping of the ADRS curve due to the intersection of the curves in the elastic region. Both masonry walls suffice for the seismic loads according to the original and reduced ADRS curves. By increasing the effective mass to 15000 kg the ductility of the structure is increased since the intersection of the bilinear curve and the ADRS curve will intersect in the plastic region. Furthermore, hysteric damping will take place due to the intersection of the curves in the plastic region. The total deformation energy of the reinforced and unreinforced masonry wall is 1211 Nm and 843 Nm. The reduced ADRS curve has a reduction of 60% due to the damping of the structure. Since the calculation is only valid for the assumed values, these results should not be taken too strictly

## Design

The design of the structural window frame could be improved structurally and sustainably. A thinner adhesive layer would result in a stiffer behaviour of the structural window frame. No adhesive layer at all would increase stiffness even more. The maximum structural shear force capacity remains similar. However based on the masonry model, making the adhesive thinner doesn't increase the stiffness or the shear force capacity. The crack width for a masonry wall remains similar or increases with thinner adhesive. In addition, it is difficult to precisely apply the correct thickness of the adhesive. Therefore, using a thinner adhesive than 5 mm does not result in more beneficial results. Using a frame that is twice as stiff and strong has resulted in a significant change in the structural behaviour. The initial behaviour is the same since the behaviour of the adhesive is more dominant in the beginning. The maximum shear force is higher since the stiffer timber frame is able to withstand higher loads. Furthermore, the stabilisation of the in-plane shear force occurs later. For sustainable adjustments to the design, taking care of maintenance and making only screwed connections instead of glued connections can increase the sustainability of the structural window frame.

## Recommendations

The results from the master thesis are promising. However scientific research is not a sprint but a marathon. More research needs to be done to continue the research. In this paragraph, the recommendations for new research are discussed.

### Experimental research

Due to the pandemic, the experimental research got delayed frequently. Therefore, the experimental research on the masonry walls could not be included in the master thesis. It would be recommended to do experimental research on the masonry walls including the structural window frames and to compare the experimental results with the numerical results of the masonry wall.

Since the experimental research is based on the one geometry of the structural window frame it is recommended to do experiments with different measurements. When the window measurements have increased, the effectivity of the window frame in the masonry wall will increase as well according to (Groot, 2019). By doing experimental research on larger structural window frames the full potential of the structural window frame will be made clear.

It is recommended to experiment with the thickness of the adhesive for the structural window frame. According to the numerical results a thinner adhesive layer results in stiffer structural behaviour of the structural window frame. However, for the numerical masonry model it does not have a largely beneficial influence. Furthermore, the crack width increased or stayed the same for a thinner adhesive layer. It is recommended to verify these findings with experimental research or further numerical research.

It is recommended to reconsider the design of the structural window frame. Using screwed connections instead of glued connections can increase the sustainability of the window frame. In addition, it is recommended to investigate its influence of using only screwed connections for the window frame.

### Numerical modelling

It is recommended to investigate how the unloading behaviour could be modelled of the structural window frame. This could be done by coding an original material model or making use of a different finite element program to include the unloading and pinching behaviour of the structure. This should also be done for the numerical masonry model including the structural window frame.

Since the most potential was shown for large window sizes in previous research, it is recommended to model the structural window frame with larger measurements. Modelling the structural window frame in a masonry wall with different window sizes and two floors would give more insight into the behaviour of a strengthened residential building.

Modelling with different effective masses would be interesting to understand whether the strengthened masonry wall would behave more ductile as is assumed in the calculations.

## Design

It is recommended to further investigate whether the structural window frame has potential abroad for strengthening of masonry walls. Abroad there are different parameters like the type of earthquake, the intensity of the earthquake and the building style.

It is recommended to further investigate whether the structural window frame has potential for other functions. With the rise of more transparent facades, stabilizing buildings with glass facades could be promising since they are seen as weak points. An example of this is an extension of a building. There are a lot of possibilities where it could be useful however it should be further investigated to prove its efficiency.

## References

- Amadio, C., & Bedon, C. (2015). Effect of circumferential sealant joints and metal supporting frames on the buckling behavior of glass panels subjected to in-plane shear loads. *Glass Structures and Engineering*, 1(2), 353–373. <https://doi.org/10.1007/s40940-015-0001-2>
- Amstutz, C., Bürgi, M., & Jousset, P. (2018). Characterisation and FE simulation of polyurethane elastic bonded joints under multiaxial loading conditions. *International Journal of Adhesion and Adhesives*, 83(March), 103–115. <https://doi.org/10.1016/j.ijadhadh.2018.02.029>
- Bachman, H. (2003). Seismic conceptual design of buildings -Basic principles for engineers, architects, building owners and authorities. In *Resonance* (Vol. 12, Issue 8). <https://doi.org/10.1007/s12045-007-0085-3>
- Bal, İ. E., Dais, D., & Smyrou, E. (2018). “Differences” Between Induced and Natural Seismic Events. *“Proceedings of the 16th European Conference on Earthquake Engineering”?*, 1–12.
- Castori, G., & Speranzini, E. (2017). Structural analysis of failure behavior of laminated glass. *Composites Part B: Engineering*, 125, 89–99. <https://doi.org/10.1016/j.compositesb.2017.05.062>
- Cruz, P. J. S., Pequeno, J., Lebet, J. P., & Mocibob, D. (2010). Mechanical modelling of in-plane loaded glass panes. *Challenging Glass 2 - Conference on Architectural and Structural Applications of Glass, CGC 2010, May*, 309–318.
- DIANA. (2017). *DIANA Finite Element Analysis Theory Manual*. <https://dianafea.com/manuals/d102/Diana.html>
- Esposito, R., & Ravenhoorst, G. (2017). *Quasi-static cyclic in-plane tests on masonry components 2016/2017*.
- Groot, A. De. (2019). *Structural window design for in-plane seismic strengthening*.
- Huveners, E. M. P. (2009). *Circumferentially Adhesive Bonded Glass Panes for Bracing Steel Frames in Façades* (Issue 2009). <https://doi.org/10.6100/IR657800>
- KNMI. (2019). *Aardbevingen door gaswinning*. <https://www.knmi.nl/kennis-en-datacentrum/uitleg/aardbevingen-door-gaswinning>
- Korswagen, P. A., Longo, M., Meulman, E., & Rots, J. G. (2019). Crack initiation and propagation in unreinforced masonry specimens subjected to repeated in-plane loading during light damage. In *Bulletin of Earthquake Engineering* (Vol. 17, Issue 8). Springer Netherlands. <https://doi.org/10.1007/s10518-018-00553-5>
- M.B.Gaggero. (2020). *Wood properties* (Vol. 1, Issue 1).
- M.B.Gaggero, & P.Korswagen. (2020). *Structural Glass window design for in-plane seismic strengthening*.
- Michael, C. (2016). Design for disassembly. In *Appliance*.
- Modena, C., Casarin, F., Porto, F., Garbin, E., Mazzon, N., Munari, M., Panizza, M., & Valluzzi, M. R. (2009). *Structural Interventions on Historical Masonry Buildings : Review of Eurocode 8 Provisions in the Light of the Italian Experience*. 225–236.
- NEN. (2021). [www.seismischekrachten.nen.nl](http://www.seismischekrachten.nen.nl). <https://seismischekrachten.nen.nl/map.php>

- Noteboom, C., Rombouts, I., Thiel, E. Van Der, & Lenk, P. (2020). *Complex Curved Storefront : The Looking Glass*. June.
- Rijksoverheid. (2018). *Schade door gaswinning*.  
<https://www.rijksoverheid.nl/onderwerpen/gaswinning-in-groningen/schade-door-gaswinning>
- Rijksoverheid. (2019). *Gaswinning Groningen komend jaar onder 12 miljard Nm3*.  
<https://www.rijksoverheid.nl/onderwerpen/gaswinning-in-groningen/nieuws/2019/09/10/gaswinning-groningen-komend-jaar-onder-12-miljard-nm3>
- Roijackers, R.H.G., Schaveling J., & S. M. M. J. (2017). Op zoek naar de versnelling. *Bouwen Met Staal*, 255, 10–14.
- Rosliakova, V. (2014). Architectural application and Ecological Impact Studies of Timber-Glass Composites Structures. *Engineered Transparency. International Conference at Glasstec, OCTOBER 2014*, 1–8. <https://doi.org/10.13140/RG.2.1.1772.1766>
- Schittich, C., Staib, G., Balkow, D., Schuler, M., & Sobek, W. (2007). *Glass Construction Manual*.
- Sika Nederland B.V. (2012). *Sikaflex® -252* (Vol. 4).
- Stepinac, M., Rajčić, V., & Žarnić, R. (2016). Timber-structural glass composite systems in earthquake environment. *Gradjevinar*, 68(3), 211–219. <https://doi.org/10.14256/JCE.1505.2015>
- TC 13 'Aardbevingsbestendig Ontwerpen' van Bouwen met Staal Typologie gebouwen in Groningen. (2014). *Bouwen Met Staal*, 1, 1–15.
- Zaera, R., Navarro, C., Sanchez-Saez, S., Sanchez-de la Sierra, M., & Pérez-Castellanos, J. . (2014). *Influence of the Adhesive in the Ballistic Performance of Ceramic Faced Plate Armours*. June 2014, 9.